CATALYSIS BY TRANSITION METAL MODIFIED CERIA AND CERIA-ZIRCONIA MIXED OXIDES PREPARED VIA SOL-GEL ROUTE

Thesis submitted to the

Cochin University of Science and Technology

By

Maya G.

In partial fulfillment of the
requirements for the award of the degree of

DOCTOR OF PHILOSOPHY

Under the Faculty of Science

Department of Applied Chemistry
Cochin University of Science and Technology
Cochin-682 022, Kerala, India.

December 2006

CERTIFICATE

This is to certify that the thesis entitled **"Catalysis by Transition Metal Modified Ceria and Ceria-Zirconia Mixed Oxides Prepared via Sol-Gel Route"** is an authentic record of research work carried out by Ms. Maya G. under my supervision in the Department of Applied Chemistry, Cochin University of Science and Technology, and it has not been included in any other thesis previously for the award of any other degree.
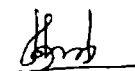
Cochin-22

21-12-2006

Dr. S. Sugunan

(Supervising Guide)

Professor,

Department of Applied Chemistry,

CUSAT

DECLARATION

I hereby declare that the thesis entitled **"Catalysis by Transition Metal Modified Ceria and Ceria-Zirconia Mixed Oxides Prepared via Sol-Gel Route"** is the bonafide report of the original work carried out by me under the supervision of Dr. S. Sugunan in the Department of Applied Chemistry, Cochin University of Science and Technology, and no part of this has been included in any other thesis submitted previously for the award of any degree.

Cochin-22
21-12-2006

Maya G.

Acknowledgements

Preface

Catalysis is one of the fundamental pillars of green chemistry, the design of chemical products and processes that reduce or eliminate the use and generation of hazardous substances. The design and application of new catalysts and catalytic systems are simultaneously achieving the dual goals of environmental protection and economic benefit. No subject so pervades modern chemistry as that of catalysis. Catalysis offers numerous green chemistry benefits including lower energy requirements, catalytic versus stoichiometric amounts of materials, increased selectivity, and decreased use of processing and separation agents, and allows for the use of less toxic materials. Heterogeneous catalysis, in particular, addresses the goals of green chemistry by providing the ease of separation of product and catalyst, thereby eliminating the need for separation through distillation or extraction.

Rare earth oxides have been widely investigated as structural and electronic promoters to improve the activity, selectivity and thermal stability of the catalysts. The most significant of the oxides of rare-earth elements in industrial catalysis is certainly ceria. Its use in catalysis has attracted considerable attention in recent years, especially for those applications, such as treatment of emissions, where ceria shown great potential. In the present study, the modification of ceria using zirconia and transition metals were carried out. Major part of the work is oriented to evaluate the catalytic activity of transition metal modified ceria and ceria-zirconia catalysts.

The thesis is organized into seven chapters. The first chapter deals with the brief introduction and literature survey on modified ceria catalysts. Second chapter expounds the materials and methods employed in the work. Results and discussion regarding the characterization and activity studies are described in subsequent chapters. Last chapter includes the summary of the investigation and the conclusions drawn from the work.

CONTENTS

Chapter 2 Materials and Experimental Methods

Chapter 4 Oxidation of Ethylbenzene

Chapter 5 Friedel Crafts Benzylation of Toluene and *o*-xylene

CHAPTER 1

GENERAL INTRODUCTION AND LITERATURE SURVEY

Abstract

Catalysis research is central to the science of modern chemical processing, fuel technologies and environmental control. It controls more than 90% of the world's chemical manufacturing process and is one of the most important technologies in national economies. Modern society as we know it would be impossible without catalysis. Catalysis is a multidisciplinary science. It is a combination of fundamental and applied science with major contribution from chemistry, physics and material science. Its technological importance lies in the tremendous achievements of this science to give humanity some cheap, highly convenient and outstanding material. The most significant of the oxides of rare-earth elements in industrial catalysis is certainly CeO_2. Its use in catalysis has attracted considerable attention in recent years. This chapter deals with the general introduction and literature review of different components of the newly developed system and the various reactions undertaken for the present investigation.

1.1 Catalysis

A *catalyst* was defined by J. J. Berzelius in 1836 as a compound, which increases the rate of a chemical reaction, but which is not consumed by the reaction. This definition allows for the possibility that small amounts of the catalyst are lost in the reaction or that the catalytic activity is slowly lost. However, the catalyst affects only the rate of the reaction, it changes neither the thermodynamics of the reaction nor the equilibrium composition. The principal theme in catalysis is the desire to control the rate of chemical reactions and the secondary theme is to understand the mechanism of the control. Catalysis is of crucial importance for the chemical industry, the number of catalysts applied in industry is very large and catalysts come in many different forms, from heterogeneous catalysts in the form of porous solids over homogeneous catalysts dissolved in the liquid reaction mixture to biological catalysts in the form of enzymes.

Catalysis plays a prominent role in our society. The majority of all chemicals and fuels produced in chemical industry have been in contact with one or more catalysts. Catalysis becomes also progressively more important in environmental pollution control. Stoichiometric processes which generate waste problems are more and more replaced by selective catalytic routes. The three-way catalyst effectively reduces pollution from car engines. Catalytic processes to clean industrial exhaust gases are currently developed and installed. In short, catalysis is vitally important for our economies now and it will be even more important in future.

1.1.1 Heterogeneous Catalysis

Catalysts which operate on reactions taking place on surfaces, heterogeneous catalysts, are of great importance in chemical industry and in living organisms. In heterogeneous catalysis, the reacting species are held on the surface of the catalyst by a physical attraction called adsorption while the reaction takes place. Adsorption may

be relatively weak (physical adsorption) or may have a strength comparable to the strengths of chemical bonds (chemisorption). In either case adsorption is generally not uniform across a solid surface. Adsorption, and therefore catalysis, occurs primarily at certain favorable locations called active sites. The function of the catalyst is to provide an energetically favorable pathway for the desired reaction, in which the activation barriers of all intermediate steps are low compared to the activation energy of the uncatalyzed reaction.

1.2 Oxide Catalysts

Historically, oxide catalysts have been used primarily for vapor phase reaction in the petroleum and petrochemical industries. Recent work, however, has shown that these catalysts can also be effective in promoting a number of synthetically useful reactions. While simple oxides show activity for some oxidations they are more commonly used as solid acids or bases. Complex oxides can act as acids or bases as well as oxidation catalysts. Complex oxide can range in composition from the simple, amorphous, binary oxides to the more complex ternary and quaternary systems. The use of zeolites and clays can impart shape selectivity to a number of reactions, a feature that makes these systems particularly appealing for use in synthesis[1].

Oxide catalysts fall into two general categories. They are either electrical insulators or they can act as semiconductors. Insulator oxides are those in which the cationic material has a single valence so they have stoichiometric M:O ratios. The simple oxides, MgO, Al_2O_3 and SiO_2 and the more complex zeolites, which are aluminosilicates, fall into this category. These materials are not effective as oxidation catalysts and find more use as solid acids[2] or bases[3,4].

Semiconductor oxides are most commonly used in oxidations. They are materials in which the metallic species is relatively easily cycled between two valence states. This can be two different positive oxidation states as in Fe_2O_3, V_2O_5, TiO_2,

CuO or NiO, or the interconversion between the positive ion and neutral metal as with the more easily reduced oxides such as ZnO and CdO[5,6].

Basically, some oxides are semiconductors because they can have either a slight excess or deficiency of electrons. In the former case there is a net negative charge so the material is referred to as an n-type semiconductor. A net positive charge gives a p-type semiconductor. These two types are appreciably different in their adsorption and reaction characteristics.

1.2.1 Simple Oxides

A simple oxide catalyst can be used in either the bulk state or supported on an inert oxide support material. In general, the simple semiconductor oxides are not very good catalysts for synthetic reactions. The insulator oxides like Al_2O_3 can be used as acid catalysts[7,8] and MgO and BaO for base catalyzed reactions[3,4].

1.2.2 Supported Oxides

Supported oxides have several advantages over unsupported materials[9]. Supports can be used to improve the mechanical strength, the thermal stability and the lifetime of the catalyst. They can also provide the means for increasing the surface area of the active species. In addition, data have shown that supported oxides frequently have structural features and chemical compositions different from those on the surface of the support material. There are several general ways in which the active oxide can be found on the surface of the support material[10].

The active component and the support can be intimately mixed throughout the catalyst particle. This arrangement provides the maximum interaction between the support and the catalyst so it maximizes the catalyst support interaction. Unfortunately, it also leaves a large portion of the active material buried in the bulk of the particle. The active component can be molecularly dispersed on the support with

respect to maximizing the catalyst support interaction. Here individual molecules of the catalytically active species are bound to the support surface as a localized binary oxide. The nature of the support can then have a significant influence on the reaction characteristics of the catalyst.

The catalyst component can form an active molecular monolayer on the support. Here, too, catalyst support interactions can be strong because of the large contact area between the support and oxide relative to the surface area of the support. It is this monolayer coverage that is considered the best for a number of supported oxides but, realistically, it is recognized that it is improbable that the entire surface of a high surface area porous support material will be uniformly covered by the catalytic species. Instead, there will be areas of monolayer coverage accompanied by some larger supported oxide particles and some uncovered support surface.

1.3 Ceria, Zirconia and Ceria-Zirconia

1.3.1 Ceria

Cerium is the most abundant member of the series of elements known as lanthanides or rare earths, the elements in the periodic table in which the inner 4f electron shell is being filled. Cerium is characterized chemically by having two stable valence states, Ce^{4+}, ceric and Ce^{3+}, cerous and this property underlies several technological uses. The ceric ion is a powerful oxidizing agent but when associated with the strongly coordinating ligand, oxygen, is completely stabilized and indeed cerium oxide, $Ce^{4+}O_2$, (also called ceria) is the form of cerium most widely used. Ceria has the fluorite, CaF_2, structure, space group Fm3m, with 8-coordinate cations with oxygens filling all the tetrahedral holes; the structure-determining OCe_4 coordination tetrahedral thereby share all edges in three dimensions[11].

Ceria is now the focus of constant and varied research due to its industrial applications in areas such as high temperature ceramics, catalysis and solid oxide fuel cell applications[12]. This is because of its oxygen storage capacity which is based on a unique ability to undergo reversible redox transitions to form a series of non-stoichiometric phases of composition $CeO_2 \rightarrow CeO_{2-x}$ and this underpins the current interest[13]. As a vital component in the so-called three-way catalysts (TWC) for automotive exhaust emission control, ceria has proven useful in several ways; it aids the stabilization the alumina washcoat, prevents the inward diffusion of noble metals such as rhodium into the washcoat and prevents those metals being deactivated by being held in high oxidation states. However, it is its oxygen storage capacity (OSC) that gives ceria-based catalysts the unique ability to oxidize unburnt hydrocarbons or reduce nitrous oxides under fuel rich and lean conditions respectively[14].

1.3.2 Zirconia

Zirconium oxide (ZrO_2) known as zirconia is also a relevant material in adsorption and catalysis. Zirconium dioxide is found in nature in small quantities as the mineral baddeleyite (monoclinic zirconia). It can also exist in tetragonal and cubic forms, both stable at higher temperature but stabilized by doping down to room temperature[15]. The most significant difference between monoclinic, tetragonal and cubic structures is the change in the coordination of Zr atoms which is seven in the monoclinic phase and eight in the other two. The presence of seven fold coordination in the m-ZrO_2 is consistent with the strong covalent character of Zr-O bonding.

Zirconia is a special transition metal oxide that possesses bifunctional characteristics of weak acid and base properties[16,17]. The p-type semiconductivity exhibits abundant oxygen vacancies on its surface. The high ion-exchange capacity and redox activities make it possible to be used in many catalytic processes as the catalyst, the supporter, and the promoter. In addition, the superior chemical stability,

mechanical strength, and ion-exchange capacity are favorable for applications in ceramic toughening, thermal-barrier coating, electronics, and oxygen sensors[18-22].

1.3.3 Ceria-Zirconia

In recent studies it has been shown that the redox behavior of cerium oxide can be severely modified by incorporation of zirconium and the formation of mixed Ce-Zr oxides. Among the possible compositions and phases forming Zr-Ce mixed oxides, it has been shown that the greatest promoting effect on cerium reduction is produced for compositions with Ce/ Zr (atomic ratio) close to one and in the presence of pseudo cubic phase t" (with Zr and Ce cations occupying the corresponding positions in the cubic fluorite-type lattice, but with overall tetragonal symmetry due to oxygen displacement from the ideal fluorite sites[23]. CeO_2-ZrO_2 mixed oxides are extensively used as promoters for three way catalysts. Due to their high thermal stability and enhanced redox properties compared to traditionally employed ceria, these systems are now employed as a so-called oxygen storage device. Oxygen storage and release capacity is the ability of a TWC to store oxygen under net oxidizing conditions and release it under net reducing conditions, thereby maintaining the air to fuel ratio at close to stoichiometric conditions, where the highest conversions are attained. For highly sintered CeO_2-ZrO_2 mixed oxides, a remarkable property is that insertion of ZrO_2 into the CeO_2 lattice distorts the oxygen sublattice, making mobile lattice oxygen available for redox processes[24].

1.4 Methods of Preparation of Metal Oxides

A heterogeneous catalyst is a composite material, recognized by: (a) the relative amounts of different components (active species, physical and/or chemical promoters, and supports); (b) shape; (c) size; (d) pore volume and distribution; (e) surface area. The optimum catalyst is the one that provides the necessary combination

of properties (activity, selectivity, lifetime, ease of regeneration and toxicity) at an acceptable cost. These requirements are in many cases in conflict and catalyst design mainly consists of the achievement of a suitable compromise.

1.4.1 Precipitation and Co-precipitation

Precipitation is one of the most widely employed preparation methods and may be used to prepare either single component catalyst and supports or mixed catalysts. In the latter case intimate mixing of the catalyst components can be achieved by either the formation of very small crystallites or the formation of mixed crystallites containing the constituents. During coprecipitation the pH has to be adjusted and kept constant[25-27]. Hydroxides and carbonates are the preferred precipitates because of their low solubility, easy decomposition and minimal toxicity and environmental problems[28].

1.4.2 Impregnation

Impregnation is the procedure whereby a certain volume of solution containing the precursor of the active phase is contacted with the solid support, which, in a subsequent step, is dried to remove the imbibed solvent[29,30]. Two methods of contacting may be distinguished, depending on the volume of solution: wet impregnation and incipient wetness impregnation. In wet impregnation an excess of solution is used. After a certain time the solid is separated and the excess solvent is removed by drying. The composition of the batch solution will change and the release of debris can form a mud which makes it difficult to completely use the solution. The heat of adsorption is released in a short time. In incipient wetness impregnation the volume of the solution of appropriate concentration is equal or slightly less than the pore volume of the support. Control of the operation must be rather precise and repeated applications of the solution may be necessary.

1.4.3 Adsorption

Adsorption allows the controlled anchorage of a precursor (in an aqueous solution) on the support[30,31]. The term adsorption is used to describe all processes where ionic species from aqueous solutions are attracted electrostatically by charged sites on a solid surface. Often consideration is not given to the difference between true ion exchange processes and electrostatic adsorption at the charged surface of oxides. Catalyst systems, which need charge compensating ions, are ideal materials for ion exchange (zeolites, cationic clays or layered double hydroxides). Instead most oxide supports, when placed in an aqueous solution, develop a pH-dependent surface charge. These oxides may show a tendency for adsorption of cations (SiO_2–Al_2O_3, SiO_2), or anions (ZnO, MgO) or both, cations in basic solutions and anions in acid solutions (TiO_2, Al_2O_3). The surface charge of an oxide depends on its isoelectric point as well as on the pH and ionic strength of the solution.

1.4.4 Deposition-Precipitation

In deposition–precipitation two processes are involved: (1) precipitation from bulk solutions or from pore fluids; (2) interaction with the support surface[32-34]. Slurries are formed using powders or particles of the required salt in amounts sufficient to give the desired loading, and then enough alkali solution is added to cause precipitation. However, precipitation in the bulk solution must be avoided, since it gives rise to deposition outside the pores of the support. A well-dispersed and homogeneous active phase is reached when the OH- groups of the support (for example, the silanols of silica) interact directly with the ions present in the solution, thereby also determining the nature of the phase formed[34,35]. The nucleation rate must be higher at the surface than in the bulk solution and the homogeneity of the solution must be preserved. A method to obtain uniform precipitation is to use the hydrolysis of urea as a source of OH- instead of conventional alkali. Urea dissolves in water and

decomposes slowly at 90°C, giving a uniform concentration of OH- in both the bulk and pore solutions.

1.4.5 Sol-gel Method

The sol-gel method is a homogeneous process which results in a continuous transformation of a solution into a hydrated solid precursor (hydrogel). Sol-gel methods have several promising advantages over precipitation. In general, sol-gel syntheses have been recognized for their versatility which allows better control of the texture, composition, homogeneity and structural properties of the final solids. The nanoscale chemistry involved in sol-gel method is a more direct way to prepare highly divided materials. Four main steps may be identified in taking a precursor to a particular product via sol-gel preparation: formation of a hydrogel, its ageing, removal of solvent and heat treatment. The versatility of this preparation method lies in the number of parameters that can be manipulated in each of these steps[36].

In the sol preparation, the precursors (either organic or inorganic) undergo two chemical reactions: hydrolysis and condensation or polymerization, typically with acid or base as catalysts, to form small solid particles or clusters in a liquid (either organic or aqueous solvent). The solid particles or clusters are so small (1~1,000 nm) that gravitational forces are negligible and interactions are dominated by van der Waals, coulombic and steric forces. Sols are stabilized by an electric double layer, or steric repulsion, or their combination. Sol-gel processing is a simple technology in principle but has required considerable effort to become of practical use. Sol-gel enables materials to be mixed on an atomic level and thus crystallization and densification to be accomplished at a much low temperature. However, a true atomic level homogeneity in a multiple component system is an endeavor; the difficulty arises from the fact that the chemical reactivity varies greatly from precursor to

precursor. Precursor modification and step-wise partial hydrolysis are the common approaches to homogeneity in multiple component systems.

The advantages of the sol-gel process in general are high purity, homogeneity, and low temperature. For a lower temperature process, there is a reduced loss of volatile components and thus the process is more environmental friendly. In addition, some materials that cannot be made by conventional means because of thermal and thermodynamical instability can be made by this process. The sol-gel process has many applications in synthesis of novel materials. Examples include aerogels used in space crafts to capture stellar dust, xerogels as matrix in biosensors, and high power laser materials. It is well known that the properties of materials show a huge change when particle size is reduced to submicrometric or nanometric scale[37].

1.5 Preparation of Ceria, Zirconia and Ceria-Zirconia

Ceria based catalysts were prepared by a large variety of techniques such as mechanochemical processing[38], hydrothermal hydrolysis[39], atomic layer deposition[40], ultrasonic aerosol decomposition[41], homogeneous precipitation route[42], hybrid organic/inorganic route[43], inert gas condensation[44] solid state decomposition technique[45], homogeneous precipitation with microemulsion[46] etc. Thermally stable ordered Mesoporous ceria has been synthesized with the use of neutral surfactants by Lyons et.al.[47].

A few research groups prepared ceria sols by using the commercial 20 wt.% CeO_2 aqueous colloidal dispersions[48] or peptizing CeO_2 precipitation by addition of an equimolar quantity of HNO_3[49]. Zou et al.[50] synthesized high surface area cerium oxide and high concentration ceria sols by a new method based on homogeneous precipitation method in an acidic environment using cerium (IV) nitrate as the precursor. Li et al.[51] reported synthesis of ceria nano particles by solid phase

mechanochemical reaction of hydrate cerium chloride with hydrate sodium carbonate. Khalil et al.[52] carried out a two step sol-gel process for the preparation of cerium oxide in which Cerium (IV) isopropoxide was dispersed in isopropanol by the aid of ultrasonic radiation to overcome the solubility problem. Zhou et al.[53] were successful to synthesize ceria nanorods with well-defined reactive planes as a result of the recent development of controlled synthesis of nanostructured materials. Rane et al.[54] used three ceria sols prepared from different precursors (commercial sol, cerous sol and ceric sol) to prepare unsupported ceria membranes. They confirmed fluorite type phase for ceria derived from all these sols. Ozer[55] showed that crystalline ceria films can be prepared by the sol-gel process using cerium ammonium nitrate as precursor. Orel et al.[56, 57] and his coworkers used aqueous based sol-gel process for the preparation of ceria. Transparent colloidal solution containing 2 nm ceria particles were synthesized by Inoue et al.[58]. Atkinson et al.[59] prepared ceria sol by peptizing a slurry of cerium hydroxide with nitric acid. They could obtain de-aggregated primary particles about 8 nm in size.

Extensive methods have been explored to synthesize zirconia, including precipitation[60], sol-gel[61], thermal decomposition[62] and hydrothermal treatment[63]. Among these, the sol-gel process is considered to be a promising way to produce homogeneous sols with modified physico-chemical properties. Zhao et al.[64] found out that highly stable, homogeneous zirconia sols could be prepared from zirconium n-propoxide modified by diglycol. Zirconium n-propoxide was used as the precursor because of its high reactivity with water and it being typically representative of metallic alkoxides. Ferino et al.[65] prepared zirconia catalysts from xero- and aerogels obtained using zirconium n-propoxide.

Many preparation methods have been applied for the preparation of CeO_2-ZrO_2 solid solutions for catalytic applications. These include microemulsion method[66,67], hydrothermal synthesis[68], sol-gel route[69-72], Co-precipitation route[73-75],

high energy ball milling[76], glycine-nitrate process[77,78], sonochemical processing[79], flame spray synthesis[80], spray drying technique[81], pechini process[82], solution combustion synthesis[83] etc .

1.6 Transition Metal Modified Ceria and Ceria-Zirconia as Catalyst

Among the rare earth metal oxides that have been widely investigated in ceramics and industrial catalysis, cerium dioxide (CeO_2) certainly stands apart[14,84]. The redox property of ceria plays a prominent role in catalyzed reactions. The number of effective redox sites and their ability to exchange oxygen can be manipulated by incorporating transition metal ions into the ceria lattice and promoted by noble metals dispersed on ceria[68,85,86]. Replacing cerium ions by cations of different size or charge modifies ion mobility inside the modified lattice, resulting in the formation of a defective fluorite-structured solid solution. Such modifications in the defect structure of ceria confer new properties to the catalyst such as better resistance to sintering at high temperatures and high catalytic activity for various reactions[87]. The mixing of two different oxides could result in the formation of new stable compounds that may lead to totally different physico-chemical properties and catalytic behaviour[88].

Supported chromium oxide catalysts have been of significant industrial importance for many decades and are now vital for the polymerization of ethylene (in the manufacture of high-density polymers) as well as the generation of valuable alkenes via the dehydrogenation of low-cost alkane feedstocks[89-91]. More recently cerium oxide supported chromia catalysts have been used for the oxidative dehydrogenation of isobutane where the activity of these materials was attributed to dispersed $Cr^{6+}O_x$ species[92, 93]. Harisson et al.[94] studied chromium promoted cerium catalysts towards oxidation of CO and propane. The thermal decomposition behavior

of ceria supported chromia phase and the effect of support in various chemical and molecular states of chromia with the temperature was reported by Viswanath et al.[95].

Rossi et al.[96] has examined structural and catalytic properties of numerous chromia/zirconia, chromia/alumina and chromia/silica catalysts, covering a wide range of Cr concentration. Dehydrogenation activity per total Cr atom is substantially higher for zirconia-based catalysts. This higher activity was related to the higher concentration on zirocnia of mononuclear Cr^V species, which reduce to the active mononuclear Cr^{III} species under reaction conditions. Effect of preparation route and thermal treatment on the nature of copper and chromium doubly promoted ceria catalysts was reported [97].

Interestingly, MnO_x-CeO_2 mixed oxides have been developed as environmental friendly catalysts for the abatement of contaminants in both liquid phase and gas phase, such as oxidation of ammonia[98], pyridine[99], phenol[100] and acrylic acid[101]. It was further showed that the MnO_x-CeO_2 mixed oxides had much higher catalytic activity than those of pure MnO_x and CeO_2 owing to the formation of the solid solution between manganese and cerium oxides. Incorporation of manganese ions into ceria lattice greatly improved the oxygen storage capacity of cerium oxides as well as the oxygen mobility on the surface of the mixed oxides. Qi et al.[102] reported that MnO_x-CeO_2 is a superior catalyst for NO reduction by NH_3. The high activity is attributed to the highly dispersed Mn species and the more active oxygen species that is formed. Mn/Ce composite catalysts are found to be effective for the wet oxidation of phenol[103,104], ammonia[105] and poly (ethylene glycol)[106].

The vapor-phase synthesis of 3-pentanone from 1-propanol was investigated over CeO_2-Fe_2O_3 catalysts by Kamimura et al.[107]. The addition of Fe_2O_3 to CeO_2 enhances the ability of CeO_2 for the catalytic dehydrogenation of 1-propanol to propanone without losing the ability for the dimerization of propanol, whereas the

stability of catalyst is related to the catalyst composition. Nagashima et al.[108] investigated ketonization of different carboxylic acids over CeO_2 based catalysts. CeO_2 catalysts modified with Mg, Al, Fe, Ni, Cu and Zr are effective for the ketonization of propnaoic acid form 3-propanone. CeO_2-Mn_2O_3 is the most efficient catalyst. The degree of mixing in a solid solution affects the catalytic activity for the ketonization. Nascente et al.[109] found out using X-ray photoelectron spectroscopy that the addition of iron oxide to CeO_2-ZrO_2 mixed oxide helped the stabilization of tetragonal phase. Mitchell et al.[110] examined the decomposition of dimethyl methylphosphonate (DMMP) on supported cerium and iron co-impregnated oxides at room temperature. They suggested that the active component for DMMP decomposition is a two dimensional ceria network on the alumina support and the effect of iron is to increase the number of ceria defect sites in the crystallites that do form by disrupting the crystal structure and/of facilitating the formation of smaller particles.

Cobalt based catalysts are currently the best systems for obtaining paraffins of high molecular weight with little CO_2 or alcohol formation. Ernst et al. reported the effects of highly dispersed ceria addition on reducibility, activity and hydrocarbon chain growth of a Co/SiO_2 Fischer-Tropsch catalyst[111]. CoO_x/CeO_2 composite catalysts of various cobalt loading have been prepared and tested for carbon monoxide oxidation by Kang et al.[112]. These catalysts showed good resistance to water vapor poisoning, due to the strong interaction of the two materials. The study of the cinnamaldehyde hydrogenation over supported cobalt catalysts showed that the addition of cerium to cobalt increases selectivity to unsaturated alcohol without decrease of the activity[113].

Nickel has been explored as a possible substitute for precious metals since nickel-based catalysts are relatively inexpensive and have been known to possess high

activities for the synthesis gas-forming reaction[114-117]. Upadhya et al.[118] reported that Ni-stabilized zirocnia can be used for the chemoselective transfer hydrogenation of nitroarenes, aldehydes and ketones with propan-2-ol. Incorporation of Ni into the bulk structure of ZrO_2, not only stabilized ZrO_2 in its cubic form but also moderated the reactivity of Ni in the stabilized zirconia enabling chemoselective functional group reduction. $CeNi_xO_y$ mixed oxides were used in oxidative dehydrogenation of propane[119].

CuO-CeO$_2$ mixed-metal oxides have important applications as electrolytes in fuel cells[120], gas sensors[121] and efficient catalysts for various reactions such as the combustion of CO and methane[122,123], the water-gas shift reaction[85] the reduction of SO_2 by CO[124], methanol synthesis[125] and wet oxidation of phenol[126]. Cu-Ceria-Yttria stabilized zirconia anodes for solid oxide fuel cells were used by Krishnan et al.[127]. Rao et al.[128] investigated the surface and catalytic properties of Cu-Ce-O composite materials prepared by solution combustion method. CO oxidation using copper oxide supported on cerium-zirconium mixed oxide has been studied by Martinez-Arias et al.[129]. They concluded that the two main factors governing the catalytic activity of this kind of system are the facility for the partial prereduction of the copper oxide component at the interface zone and the redox properties of the interface between that partially reduced copper oxide component and the underlying ceria based support. Catalytic production for hydrogen by steam reforming of methanol reaction over Cu/Al$_2$O$_3$ promoted with CeO$_2$ was reported. The results showed that CeO$_2$ could enhance the surface dispersion of copper on catalysts, and prevent copper crystallites from sintering. It is suggested that high activity, selectivity and stability of CeO$_2$ promoted catalysts have been resulted from higher copper dispersion and smaller copper crystallites and the synergetic effect of ceria[130]. CO oxidation of nonstoichiometric nanostructured CuO$_x$/CeO$_2$ composite particles prepared by inert gas condensation was studied by Skarman et al.[131]. The interaction between a metal

oxide catalyst such as copper oxide and the ceria support is complicated since a variety of metal-support interaction can lead to synergetic effects and enhanced catalytic properties. Further more of chemical factors, such as crystal structure, oxidation state, crystallinity, morphology and dispersion effect influence the activity of Cu_x/CeO_2 during catalysis for CO oxidation[132,133].

Ceria based catalysts are very effective for the synthesis of cyclic carbonate such as ethylene carbonate and propylene carbonate by the reaction of CO_2 with ethylene glycol and propylene glycol. The addition of Zr to CeO_2 was very effective at maintaining the high surface area of the catalysts calcined at high temperature and this is related to the calcinaton temperature dependence. On the basis of the catalyst characterization it is suggested that the active sites could be weak acid-base sites which are present on the plain surface of the catalyst calcined at high temperature[134]. The redox cycle of $Ce^{4+} \rightarrow Ce^{3+}$ on the surface of ceria is found to play a role for the dehydration of diols [135,59]. Sugunan et al.[136] investigated structural and catalytic investigation of vanadia supported on ceria promoted with high surface area rice husk silica.

Banwenda et al.[137] demonstrated that cerium dioxide is a potential photocatalyst that can be used to decompose water to produce oxygen in aqueous suspension containing an electron acceptor. Ceria is abundant, nontoxic and inexpensive. Furthermore, ceria is an n-type semiconductor with a band gap of 2.9 eV and consequently it can be phtoactivated by irradiation with light in the near UV-vis range[138]. These characteristics suggest that CeO_2 could be potentially used as a photocatalyst for the oxidation of pollutants. Coronado et al.[139] carried out EPR study of radicals formed upon irradiation of ceria-based photocatalysts (CeO_2, TiO_2, CeO_2/TiO_2). The photocatalytic activity was tested for toluene oxidation. They concluded that the main effect of ceria incorporation to the titania sample is the partial

blockage of the surface sites available for photodegradation. It is proposed that the main effect of UV photoactivation of CeO_2 could be to favor the formation of surface oxygen vacancies.

1.7 Surface Acidity Measurements

Supported metal oxides often show acidic properties and form an important "class" of solid acids. Thus, many such systems have been thoroughly investigated. However, the origin of the acidity, the development of the acid sites, and their relations with the surface species are not, to date, fully understood. Ceria-based composite oxides have been increasingly studied for their role as acid-base catalyst/promoter for various reactions. The promoting/catalyzing effect of ceria in pure or in the form of composite oxide is attributed to the combination of acid-base and redox properties of ceria. Incorporation of zirconia into ceria lattice modifies the surface acid-base properties. The Zr^{4+} radius (0.84 Å) is smaller than that of the Ce^{4+} (0.97 Å) and is likely to exhibit acidic nature in solid solution. Generation of acid sites is due to the exposed Ce^{4+} and Zr^{4+} ions which are accompanied by exposed O^{2-} ions which are the basic sites[140]. Sato et al.[141,142] examined CeO_2-MgO catalysts towards alkylation of phenol and concluded that the generation of weak basic sites at low ceria content is effective for the reaction.

The acidic and basic properties of solid catalysts are usually measured by a method utilizing the temperature-programmed desorption spectra of ammonia (NH_3-TPD)[143-147] and carbon dioxide (CO_2-TPD)[148-149], respectively. Tago et al.[150] proposed a new TPD method for simultaneously characterizing the acidic and basic properties of solid catalysts by utilizing the co-adsorption of NH_3 and CO_2 on catalysts.

Dealing with catalytic systems that involve at least one acid/base catalytic step, it is quite important to be able to evaluate nature and amount of surface acidic centers. This need becomes particularly important in the case of systems in which

both protonic Brønsted acidity (B acid sites) and aprotic Lewis acidity (L acid sites) are simultaneously present in variable proportion[151]. It is long time now that the identification of the type of acidity present at the surface of oxidic systems of catalytic interest is carried out routinely by the IR spectroscopic study of the adsorption/desorption of pyridine (py) at temperatures ranging between ambient temperature (RT) and some 423 K. This is so because it has been long recognized that, in the complex mid-IR spectrum of adsorbed pyridine, there are two bands, centered at ~1540 cm^{-1} (broad, and of m-intensity) and at ~1445 cm^{-1} (sharp, and of s-intensity) that are analytical of B-bound py species ([py-B]) and of L-bound py species ([py-L]), respectively[152]. Zaki et al.[153] reported in situ FTIR spectra of pyridine adsorbed on SiO_2-Al_2O_3, TiO_2, ZrO_2 and CeO_2. Granados et al.[154] used infrared spectrum of chemisorbed pyridine to characterize phosphated ceria samples. They could observe only one band due to molecularly adsorbed pyridine and no infrared bands of pyridine chemisorbed on Bronsted acid sites were visible. They concluded that Ce(IV) ions show similar acid strength on the surfaces or pure ceria and of phosphated samples. The integrated molar absorption coefficients of the infrared bands characteristic of adsorbed lutidine (2,6-dimethylpyridine) were determined for the purpose of quantifying the acid sites of solid catalysts by Onfroy et al.[155].

1.8 Test Reactions for Acidity

The conversion of cumene is a model reaction for identifying the Lewis/Bronsted acid site ratio of a catalyst: cumene is cracked to benzene and propene over Bronsted acid sites, whereas dehydrogenation to α-methylstyrene occurs over Lewis acid sites. The relative amounts of benzene and α-methylstyrene in the product mixture can therefore be a good indication of the types of acidities possessed by catalyst [156].

Kooli et al.[157] used cumene cracking to compare titania pillared clays using montmorillonite, saponite and rectorite hosts. High cumene conversion and significant activity of saponite sample reflected the higher Bronsted acidity seen for these materials. Various rare earth phosphates were characterized by catalytic activities on cracking/dehydrogenation reaction of cumene[158]. Lanthanum and samarium polyphosphates gave low selectivity of cumene to benzene and propene which showed that these catalysts had poor Bronsted acid sites. High selectivity of cumene cracking products, benzene and propene over Ce, Pr, Nd, Yb and Y polyphosphates showed that there are rich Bronsted acid sites over these catalysts. Nanosized sulfated TiO_2 obtained by sol-gel hydrothermal route showed high activity for cumene cracking indicating the presence of medium and strong Lewis acid sites[159]. Gedeon et al.[160] reported that AlSBA materials showed a high and durable activity in cumene cracking. The cracking products were only benzene and propene, indicating that the active sites are of Bronsted type.

Alcohol decomposition reaction has been widely studied because it is a simple model reaction to determine the functionality of an oxide catalyst. Dehydration activity is linked to the acidic property and dehydrogenation activity to the combined effect of both acidic and basic properties of the catalyst. Cyclohexanol decomposition reaction is considered as universal test reaction for acid-base properties of solid catalysts. Besides, in the dehydration reaction, cyclohexene is produced, a liquid compound easier to handle, instead of gaseous alkene obtained in the reaction of several aliphatic alcohols alternatively used in this respect[161]. Furthermore stronger acid sites may also be detected in this probe reaction, by the formation of methyl cyclopentenes through the consecutive (or secondary) reaction of cyclohexene[162].

Jothiramalingam et al.[163] found that cerium incorporated OMS-2 catalysts favor the dehydrogenation of cyclohexanol due to the presence of basic sites in the

cerium incorporated OMS-2 catalysts. Bautista et al.[164] studied the influence of acid-base properties of catalysts in the gas-phase dehydration-dehydrogenation of cyclohexanol on amorphous $AlPO_4$ and several inorganic solids. They concluded that this reaction can be used as a reaction model for the characterization of solid acid-base catalysts, but taking into account that dehydration reaction is carried out not only in acid sites but also in basic ones, and that cyclohexanone obtained throughout dehydrogenation reaction requires an additional redox ability not necessarily associated to basic sites. Sugunan et al.[165] correlated cyclohexanol conversion to total acidity for vanadia supported ceria promoted with rise husk silica. Mishra et al.[166] reported that addition of ceria into ZnO matrix generates new acidic sites along with increased number of basic sites which correlates with the catalytic activity obtained for cyclohexanol dehydrogenation.

1.9 Reactions Selected for the Present Study

1.9.1 Ethylbenzene Oxidation

Oxidation is a fundamental transformation in organic synthesis. The selective oxidation of hydrocarbons is one of the main processes since the reaction products are either vital themselves or intermediates in numerous industrial organic chemicals. The oxidation products of ethylbenzene are widely employed as intermediates in organic, steroid, and resin synthesis. However selective oxidation of hydrocarbons is still a challenge to scientific community as they are currently oxidized by environmentally detrimental chromates and permanganates in stoichiometric amounts[167-169]. These processes also lead several problems like difficulty separation, recovery and recycling of catalysts after reaction as well as the disposal of wastes, deactivation complications etc., which makes them highly unattractive. Owing to the limitations of stoichiometric reagents/homogeneous catalysts, and in the wake of increasingly stringent environmental legislation, attention is being focused towards

the design and development of greener processes such as heterogeneous catalytic oxidation[170].

Silicate xerogels containing cobalt is found to be especially active for the oxidation of alkyl aromatic compounds[171]. Sivasanker et al.[172] reported oxidation of ethylbenzene over zeolite Y-encapsulated copper tri- and tetraaza macrocyclic complexes. Al_2O_3 supported V_2O_5 catalysts have been effectively used for acetophenone synthesis from ethylbenzene[173]. Using H_2O_2 oxidant Ti, V- and Sn-containing silicalites with MFI structure found to catalyze ethylbenzene oxidation[174]. The major products were 1-phenyl ethanol and acetophenone arising from the oxidation of side chain. Aromatic ring hydroxylation leads to the formation of ortho- and para-hydroxy ethylbenzene as a minor side reaction. The differences in the product selectivities could be explained on the basis of the reaction intermediates. Vetrivel et al.[175] examined the catalytic activity of manganese containing MCM-41 molecular sieves for the liquid phase oxidation of ethylbenzene using t-butyl hydroperoxide as oxidant. Both primary and secondary carbons of the side chain of ethylbenzene are observed to be acted upon by activated t-butyl hydroperoxide giving α-phenylethanol as the major product and acetophenone, benzaldehyde and phenylacetaldehyde other products.

1.9.2 Benzylation of Toluene and *o*-xylene

Alkylation of aromatic compounds is an important area of industrial research. Benzylated aromatics, a class of alkyl aromatics are very useful intermediates in petrochemicals, cosmetics, dyes, pharmaceuticals and may other chemical industries[176]. Liquid phase alkylation of aromatic compounds, using homogeneous acid catalysts such as $AlCl_3$, BF_3, H_2SO_4 pose several problems, such as difficulty in separation and recovery, disposal of spent catalysts, corrosion, high toxicity, etc. Development of reusable solid acid catalysts is, therefore, of great practical

importance. Choudhary et al.[177] reported highly active, reusable and moisture sensitive catalyst obtained from basic Ga-Mg-hydrotalcite anionic clay for Friedel-Crafts type benzylation and acylation reactions. Sugunan et al.[178,179] investigated liquid phase benzylation of toluene and *o*-xylene over different catalysts.

Bhaskaran et al.[180,181] reported that rare earth oxides like CeO_2 and Pr_2O_3 are effective for benzylation and benzoylation of *o*-xylene. They stated that the presence of strong as well as weak acid sites on the catalyst surface appears to be very important for the feasibility of the reaction. Sugunan et al.[182] studied benzylation of toluene over tungsten incorporated pure and sulfated ceria systems producing monoalkylated products.

1.9.3 Methylation of Phenol and *o*-cresol

Among alkylation reactions, methylation of phenol has attracted considerable attention due to industrial importance of methyl phenols as chemical intermediates in the manufacture of pharmaceuticals, agrochemicals, resins, various additives, polymerization inhibitors, antioxidants and various other chemicals[183]. In particular, ortho-alkylated phenols such as *o*-cresol, 2,6-xylenol and trialkyl substituted phenol are more important alkyl phenols. The alkylation of phenol with methanol being an acid-base catalyzed reaction the product selectivity depends upon the acidity as well as the basicity of the catalyst[184].

Sato et al.[185] investigated the alkylation of phenol over various oxides of rare earth metals and they found that only CeO_2 had sufficient activity and selectivity for the reaction. They have also reported the ortho-selective methylation and propylation of phenol catalyzed by CeO_2-MgO[141,142]. They proposed that the ortho-position of phenol adsorbed perpendicularly on the weak basic site on CeO_2 species is selectively alkylated by the alkylating agent which is possibly activated in the form of hydroxyl

alkyl radical. A new ternary system based on SnO_2 with the addition of cerium dioxide and rhodium oxide (Sn-Ce-Rh-O) was applied for the ortho-selective methylation of phenol with methanol by Klimkiewicz et al.[186] and they concluded that the presence of weak acid sites and comparatively strong basic sites facilitates the reaction.

2.0 Main Objectives of the Present Work

Looking into the future, one can see many exciting challenges and opportunities for developing totally new catalytic technologies. Knowledge of the local structure of the catalyst surface and of factors that determine the surface structure has played an important role in developing and optimizing supported metal oxide systems in heterogeneous catalysis. Characterization of the surface structure of supported metal oxides however is complicated since several different structures as well as chemical states might coexist in the supported metal oxide systems.

From the literature sited, it is clear that the surface properties and catalytic activity of ceria can be improved by synthesizing appropriate ceria-based composite oxides. The thesis is based on the sol-gel preparation, characterization and catalytic activity studies of transition metal incorporated (Cr, Mn, Fe, Co, Ni. Cu) ceria and ceria-zirconia mixed oxides. The main objectives of the present work are,

> To prepare transition metal (Cr, Mn, Fe, Co, Ni and Cu) incorporated ceria and ceria-zirconia mixed oxide catalysts through sol-gel route.

> To investigate the surface properties of the prepared systems by techniques such as XRD, EDX, SEM, BET surface area-Pore volume measurements, FT-IR, FT-Raman, DRS UV-vis, TGADTA and EPR.

> To examine the surface acidic properties of the catalytic systems using various independent techniques such as TPD of ammonia, TGA of adsorbed

2,6-DMP and test reaction like cumene cracking and cyclohexanol decomposition.

➤ To explore the catalytic activity of the systems towards oxidation of ethylbenzene.

➤ To test the catalytic activity of the system towards liquid phase benzylation of *o*-xylene and toluene.

➤ To evaluate catalytic performance of the prepared systems in methylation of phenol and *o*-cresol.

References

[1]   R. L. Augustine, Heterogeneous Catalysis for the Synthetic Chemist, Marcel Dekker, Inc. (1996).

[2]   J. M. Thomas, Sci. Am. 266 (1992) 112.

[3]   H. Hattori, Mater. Chem. Phys. 18 (1988) 533.

[4]   H. Hattori, Stud. Surf. Sci. Catal. 78 (Heterog. Catal. Fine Chem.; III) (1993) 35.

[5]   G. C. Bond, Heterogeneous Catalysis, Principles and Applications, Clarendon Press, Oxford (1987).

[6]   A. Holden, The Nature of Solids, Columbia Univ. Press, New York, (1965).

[7]   T. Curtin, J. B. McMonagle, B. K. Hodnett, Catal. Lett. 17 (1993) 143.

[8]   T. Curtin, J. B. McMonagle, M. Ruwet, B. K. Hodnett, J. Catal. 142 (1993) 172.

[9]   G. C. Bond, Appl. Catal. 1 (1991) 71.

[10]   T. Fransen, P. C. van Berge, P. Mars, Stud. Surf. Sci. Catal. 1 (1976) 405.

[11]   Cerium: A Guide to its Role in Chemical Technology, Molycorp, Inc. Mountain Pass, CA U.S.A (1992).

[12]   A. Trovarelli, C. de Leitenburg, M. Boaro, G. Dolcetti, Catal. Today 50

(1999) 353.

[13]   Non-Stoichiometric Oxides, O. T. Sorensen (Ed), Academic Press, New York (1981).

[14]   A. Trovarelli, Catal. Rev. Sci. Eng. 38 (1996) 439.

[15]   E. F. Lopez, V. S. Escribano, M. Panizza, M. M. Carnascialli, G. Busca, J. Mater. Chem. 11 (2001) 1891.

[16]   C. L. Su, J. R. Li, D. H. He, Appl. Catal. A 202 (2000) 81.

[17]   M. S. Wong, D. M. Antonelli, J. Y. Ying, Nanostruct. Mater. 9 (1997) 165.

[18]   Z. G. Wu, Y. X. Zhao, D. S. Liu, Microporous Mesoporous Mater. 68 (2004) 127.

[19]   M. Mamak, N. Coombs, G. Ozin, J. Am. Chem. Soc. 122 (2000) 8932.

[20]   H. Verveij, Adv. Mater. 10 (1998) 1483.

[21]   A. Ziehfreund, U. Simon, W. F. Maier, Adv. Mater. 8 (1996) 424.

[22]   F. P. F. van Berkel, F. H. van Heuveln, J. P. P. Huijsmans, Solid State Ionics 72 (1994) 240.

[23]   A. Martinez-Arias, M. Fernandez-Garcia, O. Galvez, J. M. Coronado, J. A. Anderson J. C. Conesa, J. Soria, G. Munuera, J. Catal. 195 (2000) 207.

[24]   P. Fornasiero, E. Fonda, R. D. Monte, G. Vlaic, J. Kaspar, M. Graziani, J. Catal. 187 (1999) 177.

[25]   Ph. Courty, Ch. Marcilly, in: G. Poncelet, P. Grange, P.A. Jacobs (Eds.), Preparation of Catalysts III, Studies in Surface Science and Catalysis, vol.16, Elsevier, Amsterdam (1983).

[26]   C. Perego, P.L. Villa, Catal. Today 34 (1997) 281.

[27]   F. Schüth, K. Unger, in: G. Ertl, H. Knozinger, J. Weitkamp (Eds.), Handbook of Heterogeneous Catalysis, Vol. 1, Wiley/VCH, New York/Weinheim (1997).

[28]   M. V. Twigg (Ed.), Catalyst Handbook, 2nd ed., Wolfe, London (1989).

[29]   J. F. Le Page, J. Cosyns, P. Courty, E. Freund, J.-P. Franck, Y. Jacquin, B. Juguin, C. Marcilly, G. Martino, J. Miquel, R. Montarnal, A. Sugier, H. Van Landeghem, Applied Heterogeneous Catalysis: Design, Manufacture, Use of Solid Catalysts, Technip, Paris (1987).

[30]   M. Che, O. Clause, Ch. Marcilly, in: G. Ertl, H. Knözinger, J. Weitkamp (Eds.), Handbook of Heterogeneous Catalysis, Vol. 1, Wiley/VCH, New York/Weinheim (1997) 191.

[31]   H. Knözinger, E. Taglauer, in: G. Ertl, H. Knözinger, J. Weitkamp (Eds.), Handbook of Heterogeneous Catalysis, Vol. 1, Wiley/VCH, New York/Weinheim (1997) 216.

[32]   J. W. Geus, in: G. Poncelet, P. Grange, P. A. Jacobs (Eds.), Preparation of Catalysts III, Studies in Surface Science and Catalysis, vol. 16, Elsevier, Amsterdam (1983) 1.

[33]   P.T. Cardew, R.J. Davey, P. Ellitt, A.W. Nienow, J.P. Winterbottom, in: B. Delmon, P. Grange, P.A. Jacobs, G. Poncelet (Eds.), Preparation of Catalysts IV, Studies in Surface Science and Catalysis, vol. 31, Elsevier, Amsterdam (1987) 15.

[34]   J. W. Geus, J. Van Dillen, in: G. Ertl, H. Knözinger, J. Weitkamp (Eds.), Handbook of Heterogeneous Catalysis, vol.1, Wiley/VCH, New York/Weinheim (1997) 240.

[35]   L. A. M. Hermans, J. W. Geus, in: B. Delmon, P. Grange, P. A. Jacobs, G. Poncelet (Eds.), Preparation of Catalysts II, Studies in Surface Science and Catalysis, vol. 3, Elsevier, Amsterdam (1979) 113.

[36]   E. I. Ko, in: G. Ertl, H. Knözinger, J. Weitkamp (Eds.), Handbook of Heterogeneous Catalysis, Vol. 1, Wiley/VCH, New York/Weinheim (1997) 86.

[37]   C. J. Brinker, G. W. Scherer, Sol Gel Science The Physics and Chemistry

of Sol-gel Processing, Academic Press (1989).

[38]   Y. X. Li, W. F. Chen, X. Z. Zhou, Z. Y. Gu, C. M. Chen, Mater. Lett. 59 (2005) 48.

[39]   S.-H. Yu, H. Colfen, A. Fischer, Colloids Surf. A 243 (2004) 49.

[40]   J. Paivasaari, M. Putkonen, L. Niinisto, J. Mater. Chem. 12 (2002) 1828.

[41]   B. Xia, I. W. Lenggoro, K. Okuyama, J. Mater. Chem. 11 (2001) 2925.

[42]   P. L. Chen, I-Wei Chen, J. Am. Ceram. Soc. 76 (1993) 1577.

[43]   D. Terribile, A. Troverelli, J. Llorca, C. de Leitenburg, G. Dolcetti, J. Catal. 178 (1998) 299.

[44]   A. Tschope, J. Y. Ying, Nanostruct. Mater. 6 (1995) 1005.

[45]   H. K. Varma, P. Mukundan, K. G. K. Warrier, A. D. Damodaran, J. Mater. Sci. Lett. 10 (1999) 666.

[46]   Y. He, B. Yang, G. Cheng, Mater. Lett. 57 (2003) 1880.

[47]   D. M. Lyons, K. M. Ryan, M. A. Morris, J. Mater. Chem. 12 (2002) 1207.

[48]   F. Czerwinski, J. A. Szpunar, J. Sol-Gel Sci. Technol. 9 (1997) 103.

[49]   F. Czerwinski, J. A. Szpunar, Thin Solid Films 289 (1999) 213.

[50]   H. Zou, Y. S. Lin, N. Rane, T. He, Ind. Eng. Chem. Res. 43 (2004) 3019.

[51]   Y. X. Li, W. F. Chen, X. Z. Zhou, Z. Y. Gu, C. M. Chen, Mater. Lett. 59 (2005) 48.

[52]   K. M. S. Khalil, L. A. Elkabee, B. Murphy, Microporous Mesoporous Mater. 78 (2005) 83.

[53]   K. Zhou, X. Wang, X. Sun, Q. Peng, Y. Li, J. Catal. 229 (2005) 206.

[54]   N. Rane, H. Zou, G. Buelna, Jerry Y. S. Lin, J. Membr. Sci. 256 (2005) 89.

[55]   N. Ozer, Sol. Energy Mater. Sol. Cells. 68 (2001) 391.

[56]   Z. C. Orel, Appl. Spectrosc. 53 (1999) 241.

[57]   Z. C. Orel, I. Musevic, B. Orel, Nanoparticles in Solids and Solutions, J. H. Fendler, I. Dekany (eds.) (1998) 519.

[58]   M. Inoue, M. Kimura, T. Inui, Chem. Commun. (1999) 957.

[59]   A. Atkinson, R. M. Guppy, J. Mater. Sci. 26 (1999) 3869.

[60]   M. Z. C. Hu, M. T. Harris, C.H. Byers, J. Colloid Interf. Sci. 198 (1998) 87.

[61]   B. Ben-Nissan, D. Martin, J. Sol-Gel Sci. Technol. 6 (1996) 187.

[62]   M. Minoru, M. Atsushi, N. Tomoyuki, I. Shinji, T. Tadayoshi, T. Akimasa, K. Kenji, Solid State Ionics 104 (1997) 303.

[63]   B. Mottet, M. Pichavant, J. M. Beny, J. A. Alary, J. Am. Ceram. Soc. 79 (1992) 2515.

[64]   J. Zhao, W. Fan, D. Wu, Y. Sun, J. Non-Cryst. Solids 261 (2000) 15.

[65]   I. Ferino, M. F. Casula, A. Corrias, M. G. Cutrufello, R. Monaci, G. Paschina, Phys. Chem. Chem. Phys. 2 (2000) 1847.

[66]   M. Fernandez-Garcia, A. Martinez-Arias, A. Iglesias-Juez, C. Belver, A. B. Hungria, J. C. Conesa, J. Soria, J. Catal. 194 (2000) 385.

[67]   A. Martinez-Arias, M. Fernandez-Garcia, V. Ballesteros, L. N. Salamanca, J. C. Conesa, C. Otero, J. Soria, Langmuir 15 (1999) 4796.

[68]   D. Srinivas, C. V. V. Satyanarayana, H. S. Potdar, P. Ratnasamy, Appl. Catal. A 246 (2003) 323.

[69]   V. Solinas, E. Rombi, I. Ferino, M. G. Cutrufello, G. Colon, J. A. Navio, J. Mol. Catal. A: Chem. 204-205 (2003) 629.

[70]   S. Rossignol, F. Gerard, D. Duprez, J. Mater. Chem. 9 (1999) 1615.

[71]   M. Thammachart, V. Meeyoo, T. Risksomboon, S. Osuwan, Catal. Today. 68 (2001) 53.

[72]   C. K. Narula, L. P. Haack, J. Phys. Chem. B 130 (1999) 3634.

[73]   V. S. Escribano, E. F. Lopez, M. Panizza, C. Resini, J. Manuel, G. Amores, G. Busca, Solid State Sciences 5 (2003) 1369.

[74]   A. Trovarelli, C. de Leitenburg, A. Primavera, G. Dolcetti, Catal. Today. 47 (1999) 133.

[75]   D. Terribile, Y. Nagai, T. Yamamoto, T. Tanaka, S. Yoshida, T. Nonaka, T. Okamoto, A. Suda, M. Sugiura, Catal. Today 74 (2002) 225.

[76]   M. G. Cutrufello, I. Feirno, V. Solinas, A. Primavera, A. Trovarelli, A. Auroux, C. Picciau, Phys. Chem. Chem. Phys. 1 (1999) 3369.

[77]   D. G. Lamas, G. E. Lascalea, R. E. Juarez, E. Djurado, L. Perez, N. E. W. de Reca, J. Mater. Chem. 13 (2003) 904.

[78]   H. S. Potdar, S. B. Deshpande, Y. B. Khollam, A. S. Deshpande, S. K. Date, Mater. Lett. 57 (2003) 1066.

[79]   J. C. Yu, L. Zhang, J. Lin, J. Colloid Interface Sci. 260 (2003) 240.

[80]   W. J. Stark, L. Madler, M. Maciejewski, S. E. Pratsinis, A. Baiker, Chem. Commun. (2003) 588.

[81]   S. C. Sharma, N. M. Gokhale, R. Dayal, R. Lal, Bull. Mater. Sci. 25 (2002) 15.

[82]   A. Quinelato, E. Longo, E. R. Leite, M. I. B. Bernardi, J. A. Varela, J. Mater. Sci. 36 (2001) 3825.

[83]   T. Mimani, K. C. Patil, Mater. Phys. Chem. 4 (2001) 134.

[84]   K. Tsukama, M. Shimada, J. Mater. Sci. 20 (1985) 1178.

[85]   W. Liu, M. Flytzani-Stephanopoulos, J. Catal. 153 (1995) 304.

[86]   C. Leitenburg, A. Trovarelli, J. Kaspar, J. Catal. 166 (1997) 98.

[87]   M. Pijolat, M. Prin, M. Soustelle, O. Tourer, P. Nortier, J. Chem. Soc., Faraday Trans. 91 (1995) 3941.

[88]   J. Rynkowski, J. Farbotko, R. Touroude, L. Hilaire, Appl. Catal. A 203 (2000) 335.

[89]   M. P. McDaniel, Adv. Catal. 33 (1985) 47.

[90]   C. P. Poole, D. S. MacIver, Adv. Catal. 17 (1967) 223.

[91]   B. Y. Jibril, S. M. Al-Zahrani, A. E. Abasaeed, R. Hughes, Catal. Commun. 4 (2003) 579.

[92]   P. Moriceau, B. Grzybowska, Y. Barbaux, G. Wrobel, G. Hecquet, Appl. Catal. A 168 (1998) 269.

[93]   P. Moriceau, B. Grzybowska, L. Gengembre, Y. Barbaux, Appl. Catal. A 199 (2000) 73.

[94]   P. G. Harrison, W. Daniell, Chem. Mater. 13(2001) 1708.

[95]   R.P. Viswanath, P. Wilson, Appl. Catal. A 201 (2000) 23.

[96]   S. De Rossi, M. P. Casaletto, G. Ferraris, A. Cimino, G. Minelli, Appl. Catal. A 167 (1998) 257.

[97]   P. G. Harrison, F. J. Allison, W. Daniell, Chem. Mater. 14 (2002) 499.

[98]   Z.Y. Ding, L.X.D. Wade, E.F. Gloyna, Ind. Eng. Chem. Res. 37 (1998) 1707.

[99]   S. Aki, M.A. Abraham, Ind. Eng. Chem. Res. 38 (1999) 358.

[100]   H. Chen, A. Sayari, A. Adnot, F. Larachi, Appl. Catal. B 32 (2001) 195.

[101]   A. M. T. Silva, R. R. N. Marques, R. M. Quinta-Ferreira, Appl. Catal. B 47 (2004) 269.

[102]   G. Qi, R. T. Yang, J. Phys. Chem. B 108 (2004) 15738.

[103]   S. Hamoudi, F. Larachi, A. Sayari, J. Catal. 177 (1998) 247.

[104]   S. Hamoudi, F. Larachi, A. Adnot, A. Sayari, J. Catal. 185 (1999) 333.

[105]   S. Imamura, A. Dol, Ind. Eng. Chem. Prod. Res. Dev. 24 (1985) 75.

[106]   S. Imamura, M. Nakamura, N. Kawabafa, J.-I. Yoshida, Ind. Eng. Chem. Prod. Res. Dev. 25 (1986) 34.

[107]   Y. Kamimura, S. Sato, R. Takahashi, T. Sodesawa, T. Akashi, Appl. Catal. A 252 (2003) 399.

[108]   O. Nagashima, S. Sato, R. Takahashi, T. Sodesawa, J. Mol. Catal. A: Chem. 227 (2005) 231.

[109]   P. A. P. Nascente, D. P. F. de Souza, Appl. Surf. Sci. 144-145 (1999) 228.

[110]   M. B. Mitchell, V. N. Sheinker, A. B. Tesfamichael, E. N. Gatimu, M.

Nunley, J. Phys. Chem. B 107 (2003) 580.

[111]   B. Ernst, L. Hilaire, A. Kiennemann, Catal. Today 50 (1999) 413.

[112]   M. Kang, M. W. Song, C. H. Lee, Appl. Catal. A 251 (2003) 143.

[113]   J. Barrault, A. Derouault, O. Martin, S. Pronier, Surface Chemistry and Catalysis. 2 (1999) 507.

[114]   J. B. Wang, L. E. Kuo, T. J. Huang, Appl. Catal. A 249 (2003) 93.

[115]   J. R. Rostrup-Nielsen, J. H. Bak Hansen, J. Catal. 144 (1993) 38.

[116]   M. C. J. Bradford, M. A. Vannice, Appl. Catal. A 142 (1996) 73.

[117]   Z. Zhang, X. E. Verykios, Appl. Catal. A 138 (1996) 109.

[118]   T. T. Upadhya, S. P. Katdare, D. P. Sabde, Veda Ramaswamy, A. Sudalai, Chem. Commun. (1997) 1119.

[119]   L. Jalowiecki-Duhamel, A. Ponchei, C. Lamonier, A. D'Huysser, Y. Barbaux, Langmuir 17 (2001) 1511.

[120]   T. Inoue, T. Setoguchi, K. Eguchi, H. Arai, Solid State Ionics, 34 (1989).

[121]   U. Lampe, J. Gerblinger, H. Meixner, Sens. Actuators B7 (1992) 787.

[122]   L. S. Kau, D. J. Solomon,   J. E. Penner-Haln, K. O. Hodgson, E. I. Solomon, J. Am. Chem. Soc. 109 (1987) 6433.

[123]   A. Martinez-Arias, A. B. Hungria, M. Fernandez-Garcia, J. Soria, J. C. Conessa, G. Munuera, J. Phys. Chem. B 108 (2004) 17983.

[124]   T. Zhu, L. Kundakovic, A. Dreher, M. Flytzani-Stephanopoulos, Catal. Today 50 (1999) 381.

[125]   E. A. Shaw, T. Rayment, A.P. Walker, R. M. Lambert, T. Gauntlett, R. J. Oldman, A. Dient, Catal. Today 9 (1991) 197.

[126]   S. Hoeevar, J. Batista, J. Levec, J. Catal. 184 (1999) 39.

[127]   V. V. Krishnan, S. McIntosh, R. J. Gorte, J. M. Vohs, Solid State Ionics 166 (2004) 191.

[128]   G. R. Rao, H. R. Sahu, B. G. Mishra, Colloids Surf. A 220 (2003) 261.

[129] A. Martinez-Arias, M. Fernandez-Garcia, A. B. Hungria,, A. Iglesias-Juez, O. Gálvez, J. A. Anderson, J. C. Conesa, J. Soria, G. Munuera , J. Catal. 214 (2003) 261.

[130] X. Zhang, P. Shi, J. Mol. Catal. A: Chem. 194 (2003) 99.

[131] B. Skarman, D. Grandjean, R. E. Benfield, A. Hinz, A. Andersson, L. R. Wallenberg, J. Catal. 211 (2002) 119.

[132] G. Avgouropoulos, T. Ioannides, Ch. Papadopoulou, J. Batista, S. Hocevar, H.K. Matralis, Catal. Today 75 (2002) 157.

[133] J. B. Wang, S. -C. Lin, T.-J. Huang, Appl. Catal. A 232 (2002) 107.

[134] K. Tomishige, H. Yasuda, Y. Yoshida, M. Nurunnabi, B. L. K. Kunimori, Green Chem. 6 (2004) 206.

[135] S. Sato, R. Takahashi, T. Sodesawa, N. Honda, J. Mol. Catal. A: Chem. 221 (2004) 177.

[136] T. Radhika, S. Sugunan, J. Mol. Catal. A: Chem. 250 (2006) 169.

[137] G. R. Bamwenda, H. Arakawa, J. Mol. Catal. A: Chem. 161 (2000) 105.

[138] G. R. Banwenda, K. Sayama, H. Arakawa, Chem. Lett. 30 (1996) 157.

[139] J. M. Coronado, A. J. Maira, A. Martinez-Arians, J. C. Conesa, J. Soria, J. Photochem. Photobiol. A: Chem. 150 (2002) 213.

[140] G. R. Rao, H. R. Sahu, Proc. Indian Acad. Sci. (Chem. Sci.) 113 (2001) 651.

[141] S. Sato, K. Koizumi, F. Nozaki, J. Catal. 178 (1998) 264.

[142] S. Sato, R. Takahashi, T. Sodesawa, K. Matsumoto, Y. Kamimura, J. Catal. 184 (1999) 180.

[143] M. Niwa, N. Katada, M. Sawa, Y. Murakami, J. Phys. Chem. 99 (1995) 8812.

[144] N. Katada, H. Igi, J.H. Kim, M. Niwa, J. Phys. Chem. B 101 (1997) 5969.

[145] N. Katada, T. Miyamoto, H.A. Begum, N. Naito, M. Niwa, A. Matsumoto,

K. Tsutsumi, J. Phys. Chem. B 104 (2000) 5511.

[146]   T. Masuda, Y. Fujikata, S.R. Mukai, K. Hashimoto, Appl. Catal. A 165 (1997) 57.

[147]   N. N. Binitha, S. Sugunan, Microporous Mesoporous Mater. 93 (2006) 82.

[148]   D. E. Jiang, B. Y. Zhao, Y. C. Xie, G. C. Pan, G. P. Ran, E. Z. Min, Appl. Catal. A 219 (2001) 69.

[149]   S. K. Bej, C. A. Bennett, L. T. Thompson, Appl. Catal. A 250 (2003) 197.

[150]   T. Tago, Y. Okubo, S. R. Mukai, T. Tanaka, T. Masuda, Appl. Catal. A 290 (2005) 64.

[151]   C. Morterra, G. Cerrato, F. Pinna, G. Meligrana, Topics in Catalysis 15 (2001).

[152]   E.P. Parry, J. Catal. 2 (1963) 371.

[153]   M. I. Zaki, M. A. Hasan, F. A. Al-Sagheer, L. Pasupulety, Colloids Surf. A: Physicochem. Eng. Aspects 190 (2001) 261.

[154]   M. Lopez Granados, F. Cabello Galisteo, P. S. Lambrou, R. Mariscal, J. Sanz, I. Sobrados, J. L. G. Fierro, A. M. Efstathiou, J. Catal. 239 (2006) 410.

[155]   T. Onfroy, G. Clet, M. Houalla, Microporous and Mesoporous Mater. 82 (2005) 99.

[156]   S. M. Bradley, R. A. Kydd, J. Catal. 141 (1993) 239.

[157]   F. Kooli, J. Bovey, W. Jones, J. Mater. Chem. 7 (1997) 153.

[158]   H. Onoda, H. Nariai, A. Moriwaki, H. Maki, I. Motooka, J. Mater. Chem. 12 (2002) 1754.

[159]   Z. Ma, Y. Yue, X. Deng, Z. Gao, J. Mol. Catal. A: Chem. 178 (2002) 97.

[160]   A. Gedeon, A. Lassoued, J. L. Bonardet, J. Fraissrd, Microporous Mesoporous Mater. 44-45 (2001) 801.

[161]   M. A. Aramendia, V. Borau, C. Jimenez, J. M. Marinas, F. J. Romero, J.

Colloid Interface Sci. 179 (1996) 290.

[162] A. Valente, Z. Lin, P. Brandao, I. Portugal, M. Anderson, J. Rocha, J. Catal. 200 (2001) 99.

[163] R. Jothiramalingam, B. Viswanathan, T. K. Varadarajan, Catal. Commun. 6 (2005) 41.

[164] F. M. Bautista, J. M. Campelo, A. Garcia, D. Luna, J. M. Marinas, R. A. Quiros, A. A. Romero, Appl. Catal. A 243 (2003) 93.

[165] T. Radhika, S. Sugunan, Cat. Commun. 7 (2006) 528.

[166] B. G. Mishra, G. R. Rao, J. Mol. Catal., A: Chem. 243 (2005) 204.

[167] Catalytic Oxidation: Principles and Applications, R. A. Sheldon, R. A. van Santen (Eds.), World Scientific, Singapore (1995).

[168] J. M. Thomas, Angew. Chem. Int. Ed. Engl. 33 (1994) 913.

[169] J. M. Thomas, R. Raja, Chem. Commun. (2001) 675.

[170] S. E. Dapurkar, A. Sakthivel, P. Selvam, New. J. Chem. 27 (2003) 1184.

[171] M. Rogovin, R. Neumann, J. Mol. Catal. A: Chem. 138 (1999) 315.

[172] T. H. Bennur, D. Srinivas, S. Sivasanker, J. Mol. Catal A: Chem. 207 (2004) 163.

[173] E. P. Reddy, R. S. Varma, J. Catal. 221 (2004) 93.

[174] N. K. Mal, A. V. Ramaswamy, Appl. Catal. A 143 (1996) 75.

[175] S. Vetrivel, A. Pandurangan, J. Mol. Catal A: Chem. 217 (2004) 165.

[176] G. A. Olah, in Friedel-Crafts and Related Reactions, Wiley-Interscience, New York (1963).

[177] V. R. Choudhary, S. K. Jana, A. B. Mandale, Catal. Lett. 74 (2001) 95.

[178] H. Suja, C. S. Deepa, K. Sreejarani, S. Sugunan, React. Kinet. Catal. Lett. 79 (2003) 373.

[179] M. Kurian, S. Sankaran, React. Kinet. Catal. Lett. 81 (2004) 57.

[180] S. K. Bhaskaran, V. T. Bhat, React. Kinet. Catal. Lett. 75 (2002) 239.

[181]   S. K. Bhaskaran, T. T. Venugopal, React. Kinet. Catal. Lett. 74 (2001) 99.

[182]   F. J. Palathingal, S. Sugunan, React. Kinet. Catal. Lett. 84 (2005) 207.

[183]   R. Dowbenko, in: J. I. Kroschwit, Mary Houl-Grant (Eds), Kirk-Othmer Encylopedia of Chemical Technology, vol. 2, fourth ed., Wiley, New York, 106.

[184]   K. M. Malshe, P. T. Patil, Shubhangi, B. Umbarkar, M. K. Dongare, J. Mol. Catal. A: Chem. 212 (2004) 337.

[185]   S. Sato, K. Koizumi, F. Nozaki, Appl. Catal. A 133 (1995) L7.

[186]   R. Klimkiewicz, H. Grabowska, H. Teterycz, Appl. Catal. A 246 (2003) 125.

MATERIALS AND EXPERIMENTAL METHODS

Abstract

For many years, the development and preparation of heterogeneous catalysts were considered more as alchemy than science, with the predominance of trial and error experiments. The optimum catalyst is the one that provides the necessary combination of properties (activity, selectivity, lifetime, ease of regeneration and toxicity) at an acceptable cost. The present chapter is focused on the experimental procedures for catalyst preparation, characterization and catalytic activity measurements. The textural characteristics of the catalysts were characterized using XRD, EDX, SEM, BET surface area-pore volume measurements, TGA/DTA, EPR, FT-IR, FT-Raman and DR UV-vis. Ammonia-TPD and thermogravimetric desorption of 2,6-dimethyl pyridine were done to measure the acidity. Cyclohexanol decomposition and cumene cracking were used as test reactions to understand surface acid-base property. Industrially important phenol methylation, o-cresol methylation, oxidation of ethylbenzene, benzylation of toluene and o-xylene were carried out.

2.1 Introduction

The development of novel catalytic materials is a fundamental focal point of catalysis research. After catalyst preparation, the next goal is to perform a detailed and full characterization of the solid yielded by the specific preparation method used. To do this in a systematic way one needs a diverse array of experimental techniques. This chapter gives a detailed description about the preparation of catalytic systems and the characterization techniques.

2.2 Materials

The chemicals used for the preparation of catalyst are given in Table 2.1.

Table 2.1 Chemical used for catalyst preparation

Sl. No.	Chemicals	Company
1.	Cerium nitrate	Indian Rare Earths Ltd., Udyogamandal, Kerala (99.9%)
2.	Zirconium (IV) propoxide	Sigma Aldrich Chemicals Pvt. Ltd
3.	Chromium nitrate	s.d Fine Chem. Ltd
4.	Manganese nitrate	Central Drug House P. Ltd.
5.	Ferric Nitrate	Qualigens Fine Chemicals (25 %)
6.	Cobalt Nitrate	s.d Fine Chem. Ltd.
7.	Nickel Nitrate	s.d Fine Chem. Ltd.
8.	Copper Nitrate	s.d Fine Chem. Ltd.
9.	Ammonia	s.d Fine Chem. Ltd.
10.	Conc. HNO_3	s.d Fine Chem. Ltd.

2.3 Catalyst Preparation

2.3.1 Ceria:– Sol-gel Route

Ceria was prepared via colloidal sol-gel route from aqueous inorganic precursor $Ce(NO_3)_3.6H_2O$[1]. Cerium nitrate was added to 1:1 NH_3 to obtain cerium hydroxide, maintaining the final pH~10. The precipitate was washed to remove nitrate ions and redispersed in water following peptisation using HNO_3 at 80°C. The sol obtained was heated at 90°C to obtain the gel. Gel was dried at 110°C for 12h and calcined at 500°C for 5h to get pure ceria.

2.3.2 Transition Metal modified Ceria

Transition metal (Cr, Mn, Fe, Co, Ni, Cu 2, 5 and 8 wt.%) modified ceria were prepared by the addition of corresponding metal nitrate solution to the previously prepared ceria sol. The resulting sol was stirred for 4h. Gelation and calcination was done as in the case of pure ceria catalyst.

2.3.3. Zirconia (ZrO_2):- Sol-gel Route

Zirconia sol was prepared by adding zirconium propoxide, $Zr(OPr_n)_4$, to an aqueous solution of nitric acid at a volumetric mixing ratio of 1HNO_3: 50H_2O: 3.7 $Zr(OPr_n)_4$[2]. The resulting mixture was stirred mechanically for 72h to obtain zirocnia sol. For preparing pure zirconia, the sol was dried at 110°C for 24h. Then calcined at 500°C for 5h to obtain zirconia powder.

2.3.4 Ceria-Zirconia

To prepare ceria-zirconia mixed oxide appropriate quantity of previously estimated ceria sol and zirconia sol were mixed and stirred for 4h. Kept overnight for ageing, dried at 110°C for 12h to get gel. The gel was calcined at 500°C for 5h to get ceria-zirconia mixed oxide catalyst.

2.3.5 Transition Metal Modified Ceria-Zirconia

Transition metal (Cr, Mn, Fe, Co, Ni, Cu) modified ceria zirconia mixed oxides were prepared by adding appropriate quantity of corresponding metal nitrate solution to the mixed ceria-zirconia sol. Again stirred for 4h and dried at 90°C to get the gel. The gel was submitted to overnight night drying at 110°C and the subsequent calcination at 500°C gave transition metal modified ceria-zirconia catalyst.

2.4 Catalyst Notations

The catalyst notations assigned to the prepared catalysts are listed in Table 2.2.

Table 2.2 Notations of the catalysts prepared

Sl. No.	Catalyst	Notation
1.	CeO_2	Ce
2.	ZrO_2	Zr
3.	CeO_2-ZrO_2	CeZr
4.	$x\%M/CeO_2$	M(x)Ce
5.	$x\%M/CeO_2$-ZrO_2	M(x)CeZr
	M=Cr, Mn, Fe, Co, Ni and Cu	
	X= 2,5 and 8 (M in weight%)	

2.5 Characterization Techniques

In heterogeneous catalysis, the reaction occurs at the surface. Catalysis and catalytic surfaces, hence, need to be characterized by reference to their physical properties and by their actual performance as a catalyst. The variety of techniques used in this work is given below.

2.5.1 Materials

Chemicals used during physico-chemical characterization of catalysts are listed in Table 2.3.

Table 2.3 Chemicals used for physico-chemical characterization

Sl. No.	Chemicals	Company
1.	Conc. H_2SO_4	s.d Fine Chem. Ltd.
2.	Sodium Hydroxide	Merck
3.	Oxalic acid	Merck
4.	Cyclohexanol	Central Drug House P. Ltd.
5.	Cumene	Sigma Aldrich Chemicals Pvt. Ltd
6.	2,6-dimethylpyridine	Sigma Aldrich Chemicals Pvt. Ltd.
7.	Liquid Nitrogen	Sterling Gases Pvt. Ltd.
8.	Magnesium oxide	Merck

2.5.2 Powder X-ray Diffraction

X-ray diffraction (XRD) is an extremely important technique in the field of material characterization to obtain information on an atomic scale from both crystalline and noncrystalline materials. Application of X-ray diffraction to structure determination in 1913 (by W. L. Bragg and W. H. Bragg) paved the way of successful utilization of this technique to determine the crystal structure of metals and alloys, minerals, inorganic compounds, polymers and organic materials infact all crystalline materials[3]. Subsequently the technique of X-ray diffraction was also applied to derive information on the fine structure of materials- crystallite size, lattice strain, chemical composition, state of ordering etc.

The diffraction principle developed by W. L. Bragg is based on diffraction from two scattering planes that are separated by the distance d (in Å) and the intercept

X-radiation of wavelength λ (in Å) at the incident angle θ. Constructive interference occurs when the Bragg's law, $n\lambda = 2\ d\ \sin\theta$ (where n is the order of diffraction) is obeyed.

The crystallite size was calculated using Scherrer equation,

$$L= 0.9\lambda/\beta\cos\theta$$

β= Full width at half maximum (FWHM) of the peak which have maximum intensity.

Powder X-ray diffraction data were recorded using Rigaku D-Max Ni filtered Cu Kα radiation ($\lambda = 1.5418$ Å) diffractometer equipped with a diffracted beam monochromator at a scan rate of 4°/min.

2.5.3. Energy Dispersive X-ray Analysis

Energy Dispersive X-ray analysis is referred to as EDS or EDAX analysis. It is a technique used for identifying the elemental composition of the specimen, or an area of interest thereof. The EDX analysis system works as an integrated feature of a scanning electron microscope (SEM), and cannot operate on its own without the latter. During EDX Analysis, the specimen is bombarded with an electron beam inside the scanning electron microscope. The bombarding electrons collide with the specimen atom's own electrons, knocking some of them off in the process. A position vacated by an ejected inner shell electron is eventually occupied by a higher-energy electron from an outer shell. To be able to do so, however, the transferring outer electron must give up some of its energy by emitting an X-ray.

The amount of energy released by the transferring electron depends on which shell it is transferring from, as well as which shell it is transferring to. Furthermore, the atom of every element releases X-rays with unique amounts of energy during the transferring process. Thus, by measuring the amounts of energy present in the X-rays being released by a specimen during electron beam bombardment, the identity of the

atom from which the X-ray was emitted can be established. The output of an EDX analysis is an EDX spectrum. The EDX spectrum is just a plot of how frequently an X-ray is received for each energy level. An EDX spectrum normally displays peaks corresponding to the energy levels for which the most X-rays had been received. Each of these peaks is unique to an atom, and therefore corresponds to a single element. The higher a peak in a spectrum, the more concentrated the element is in the specimen. An EDX spectrum plot not only identifies the element corresponding to each of its peaks, but the type of X-ray to which it corresponds as well. For example, a peak corresponding to the amount of energy possessed by X-rays emitted by an electron in the L-shell going down to the K-shell is identified as a K-Alpha peak. The peak corresponding to X-rays emitted by M-shell electrons going to the K-shell is identified as a K-Beta peak.

The chemical compositions of catalysts were obtained from Stereoscan 440 Cambridge, UK energy dispersive X-ray analyzer used in conjunction with SEM.

2.5.4 Surface area and Pore volume measurements

The most common method of measuring surface area and one used routinely in most catalyst studies is that developed by Brunauer, Emmett and Teller[4]. In essence, the Langmuir adsorption isotherm is extended to multilayer adsorption. As in the Langmuir approach, for the first layer the rate of evaporation is considered to be equal to the rate of condensation, and the heat of adsorption is taken to be independent of coverage. For layers beyond the first, the rate of adsorption is taken to be proportional to the fraction of the lowest layer still vacant. The rate of desorption is taken to be proportional to the amount present in that layer. The heat of adsorption for all layers except the first layer is assumed to be equal to the heat of liquefaction of the adsorbed gas. Summation over an infinite number of adsorbed layers gives the final expression as follows:

$$P/V (P_o - P) = 1/V_m C + (C-1)P/(CV_m P_o)$$

where V= Volume of gas adsorbed at pressure P

V_m= Volume of gas adsorbed in monolayer, same units as V

P_o= Saturation pressure of adsorbate gas at the experimental temperature.

C= a constant related exponentially to the heats of adsorption and liquefaction of the gas.

A graph of $P/V(P_o-P)$ versus P/Po should give a straight line, the slope and intercept of which can be used to evaluate V_m and C. The surface area of the catalyst can be calculated from V_m if the average area occupied by an adsorbed molecule is known.

Liquid nitrogen is a readily available coolant, and nitrogen is usually used as the adsorbate since it is relatively cheap and readily available in high purity. The surface area is then calculated using:

$$S_{BET} = V_m A_m N_a / V_{mol}$$

where;

N_a: Avogadro's number (6.0238×10^{23}), V_{mol}: molar volume of absorbate gas at STP ($22.41 mol^{-1}$) and A_m: Cross sectional area of adsorbed gas (A_m (N_2) = 0.162 nm^2).

When nitrogen is the adsorbing gas, this reduces to:

$$S_{BET} = 4.353 \ V_m$$

BET surface areas and pore volume values of the catalysts were acquired by nitrogen adsorption and subsequent desorption at liquid nitrogen temperature (77K) with a Micromeritics Flow Prep-060 Gemini 2360 instrument.

2.5.5 Scanning Electron Microscopy

The fundamental principles of Scanning Electron Microscopy (SEM) were discovered in the 1930s. Generally speaking, the signals from the interaction between

electrons and sample are used to obtain the information of the sample, either topographical, or compositional, or elemental, or structural images, depending on which signal is used. The scanning electron microscope generates a beam of electrons in a vacuum. That beam is collimated by electromagnetic condenser lenses, focused by an objective lens, and scanned across the surface of the sample by electromagnetic deflection coils. The primary imaging method is by collecting secondary electrons that are released by the sample. The secondary electrons are detected by a scintillation material that produces flashes of light from the electrons. The light flashes are then detected and amplified by a photomultiplier tube. By correlating the sample scan position with the resulting signal, an image can be formed that is strikingly similar to what would be seen through an optical microscope. The illumination and shadowing shows a quite natural looking surface topography.

SEM pictures were obtained on Cambridge Oxford 7060 scanning electron microscope connected to a 4-quadrant backscattered electron detector under a resolution of 1.38 eV coated with a layer of gold to minimum charge effects.

2.5.6 Thermogravimetric Analysis

A generally accepted definition of thermal analysis is: "A group of techniques in which a physical property of a substance and/or its reaction products is measured as a function of temperature whilst the substance is subjected to controlled temperature programme". Thermogravimetric analysis (TGA) provides a quantitative measurement of any weight changes associated with thermally induced transitions[5]. For example, TG can record directly the loss in weight as a function of temperature or time for transitions involve dehydration or decomposition. Thermogravimetric curves are characteristic of a given compound or material due to the unique sequence of physical transitions and chemical reactions that occur over definite temperature range. Changes in weight results from physical and chemical bonds forming and breaking at

elevated temperatures. These processes may evolve volatile products or form reaction products that result in a change in weight of the sample[2].

Differential thermal analysis (DTA) is a technique in which the difference in temperature between a substance and a reference material is measured as a function of temperature while the substance and reference material are subjected to a controlled temperature program. Thermogravimetry, a valuable tool in its own right, is perhaps most useful when it complements differential thermal analysis studies, virtually all weight change processes absorb or release energy and are thus measurable by DTA, but all energy change processes are accompanied by changes in weight. This difference in two techniques enables a clear distinction to be made between physical and chemical changes when samples are subjected to both DTA and TGA.

TGA/DTA analysis were done on a Perkin Elmer Pyris Diamond thermogravimetric/differential thermal analyzer instrument under nitrogen atmosphere at heating rate of 20°C/ min from room temperature to 800°C with samples mounted on an alumina sample holder.

2.5.7 FT-Infrared Spectroscopy

Infrared (IR) spectroscopy undoubtedly represents one of the most important tools in catalysis research[7,8]. It is the most widely used, and usually most effective, spectroscopic method for characterization of the surface chemistry of heterogeneous catalysts. Vibrational spectroscopy has become a very powerful tool for characterizing the molecular structures of these supported metal oxides. Infrared spectroscopy has been used to study the interactions of the surface metal oxide species with the surface hydroxyls of the support. It can also be used to measure the distribution of surface Bronsted and Lewis acid sites by adsorption of pyridine. The number of surface sites on these catalysts can also be estimated by measuring the

amount of chemisorbed CO_2. IR can also be used to detect the terminal metal-oxygen stretches (M=O) on supported metal oxides.

Infrared spectra were recorded with KBr pellets on an ABB BOMEM (MB Series) FT-IR spectrometer model in the range 400-4000 cm^{-1}.

2.5.8 UV-vis Diffuse Reflectance Spectroscopy

In surface chemistry, the UV–Vis spectroscopic method is usually used in its diffuse reflection modification. The radiation reflected from a powdered crystalline surface consists of two components, i.e. (i) that reflected from the surface without any transmission (mirror or specular reflection), and (ii) that absorbed into the material and which then reappears at the surface after multiple scattering. Modern spectrometers minimize the first component, and the term 'reflectance' is thus used for diffusely reflected radiation[9]. Since only a part of the diffuse radiation is returned to the detector, measurement of the diffused intensity is difficult. For this purpose, a special integrative sphere, coated inside with a highly reflecting layer, such as MgO or $BaSO_4$, is used. Such a sphere increases the part of the diffused intensity that reaches the detector (30-50%). Spectra are recorded 'in ratio' with a sample which has similar diffusion characteristics to the sample under investigation, but without any absorption losses. The evaluation of the intensities of diffuse reflectance spectra is based on the theory of Kubelka and Munk.

DR UV-vis spectroscopy may be used to determine the local symmetry and oxidation state of a transition metal, and thus it is a sensitive probe for the type of site in which such an ion exists. The applicability of this method is not limited to transition-metal-containing systems. It can be also used to measure the electronic spectra of adsorbed molecules and to obtain direct information about the excited and ground states of such species.

DR UV-vis spectra were taken in the range 200-800 nm on an Ocean Optics, Inc. SD 2000, Fiber Optic Spectrometer with a charged coupled device detector. The spectra were recorded at room temperature using MgO as a reference. Prior to measurement, the samples were pretreated for 1h at the calcination temperature.

2.5.9 FT-Raman Spectroscopy

Raman spectroscopy (FT-Raman) can provide molecular-level structural information about the nature of the active surface sites, especially in highly dispersed catalyst systems, and the surface reaction intermediates. Surface metal oxide species typically vibrate in the 100-1100 cm^{-1} region. Common oxide supports, such as alumina and amorphous silica, absorb strongly below approximately 1000 cm^{-1}. Consequently, the IR bands of the surface metal oxide species are usually masked by the strong IR bands of the oxide support. In contrast, the Raman bands of these oxides support are weak or Raman inactive in the same region. Because of this, Raman spectroscopy is preferred over IR spectroscopy for measuring the vibrational spectra of supported metal oxides. Since the Raman spectrum of each molecular structure is unique, Raman spectroscopy can discriminate between different molecular structures of the supported metal oxides[10].

For the Raman spectra measurements the catalysts calcined at 773K were introduced into a metallic sample holder. FT-Raman spectra were collected on Bruker FRA 106 FT-Raman Accessory and the RES 100 FT-Raman spectrometer.

2.5.10 Electron Paramagnetic Resonance Spectroscopy

Electron paramagnetic resonance (EPR) spectroscopy has long been recognized as a powerful tool for the catalytic chemist, as the high sensitivity of the techniques permits the detection of low concentrations of active sites, even under in situ conditions. EPR techniques are widely used to study paramagnetic centers on

various solid surfaces. These centres may be surface defects, inorganic or organic radicals, metal cations or supported metal complexes and clusters. Each of these paramagnetic species will produce a characteristic EPR profile with well defined spin-Hamiltonian parameters. However the magnetic properties, stability and reactivity of these centres can vary dramatically depending on the nature of the support. In some case, radicals, which are stable on one surface will be transient on another, while variations in the EPR spectra of these radicals may be observed simply by altering the pretreatment conditions of the support. EPR techniques provide a deeper understanding of catalyst preparation, the nature of surface-active sites and the types of reaction intermediates as well as details of the catalytic reaction mechanisms[14]. When the molecules of solid exhibits paramagnetism, transitions can be induced between spin states by applying magnetic filed and then supplying electromagnetic energy, usually in the microwave frequencies. The resulting EPR spectra provide information about the material.

The EPR measurements were determined on a VARIAN E-line Century Series instrument at X-band at liquid nitrogen temperature.

2.6 Surface Acidity measurements

2.6.1 Temperature Programmed Desorption of Ammonia

Temperature programmed desorption of basic molecules such as ammonia (TPD-NH_3), pyridine, n-butylamine, etc. is frequently used to characterize the acid strength as well as acid amount on a solid surface. However, ammonia and n-butylamine in which hydrogen atoms are attached to the nitrogen atom have a tendency to dissociate (e. g., $NH_3 \rightarrow NH_2^- + H^+$) and adsorb on both acidic and basic sites depending on the kinds of solids and the adsorption condition. Methods utilizing adsorption and desorption of gaseous bases have the advantage that the acid amount

for a solid at high temperatures, or under its actual working conditions as a catalyst, can be determined[11].

Prior to the experiment, the catalysts were activated inside the reactor at 300°C for 30 min with continuous flow of nitrogen. After cooling to the room temperature, a specific volume of ammonia was injected in the absence of the carrier gas and allowed to attain equilibrium. Excess physisorbed ammonia was removed by the flow of nitrogen. Then the temperature program is done from room temperature to 600°C in a stepwise manner. The ammonia desorbed at each interval of 100°C was collected in a known volume of dilute sulfuric acid and estimated volumetrically by titration with standardized NaOH.

2.6.2 Thermodesorption of 2,6-dimethyl pyridine

The thermodesorption of study of 2,6-dimethyl pyridine (2,6-DMP) adsorbed catalyst samples to get an idea about Bronsted acid sites present on the catalyst surface. 2,6-dimethyl pyridine adsorbs strongly on Brönsted acid sites and forms weak bonds with Lewis acid sites. The 2,6-dimethyl pyridine weakly bound to the Lewis acid sites get desorbed below 300°C. Hence thermodesorption study of 2,6-dimethyl pyridine adsorbed sample beyond 300°C can give the measure of Bronsted acid sites. The samples were activated at 500°C for 1h and kept in a dessicator saturated with 2,6-dimethyl pyridine for 48 h. Further subjected to TG analysis at a heating rate of 20°C/min. in nitrogen atmosphere. The percentage of weight loss in the temperature region 300-600°Cis divided in to weak (300-400°C), medium (400-500°C) and strong (500-600°C) acid sites.

2.6.3 Cumene Cracking

Cumene cracking has been used extensively as a test reaction to investigate the characteristics of any newly developed catalyst. Bronsted acid sites catalyse

cracking of cumene to Benzene and propylene and Lewis acid sites catalyze dehydrogenation to α-methylstyrene. The relative amounts of benzene and α-methylstyrene in the product mixture can therefore be a good indication of the types of acidities possessed by catalyst[12]. All the prepared catalysts were subjected to cumene cracking in vapor phase at optimized reaction conditions.

2.6.4 Cyclohexanol Decomposition

Cyclohexanol decomposition was carried out to study the acid-base properties of the catalyst systems. Being amphoteric in nature, cyclohexanol can interact with both the acidic and basic sites on the catalyst surface resulting in dehydration and dehydrogenation reactions. Dehydration activity is linked to the acidic property and dehydrogenation activity to the combined effect of both acidic and basic properties of the catalyst[13]. Vapour phase cyclohexanol decomposition was done using the prepared catalysts under optimized conditions.

2.7 Catalytic Activity

The chemicals used for catalytic activity studies are presented in the following Table 2.4.

Table 2.4 Chemicals used for catalytic activity studies

Sl. No.	Chemicals	Company
1.	Toluene	s.d Fine Chem. Ltd.
2.	*o*-xylene	s.d Fine Chem. Ltd.
3.	Benzyl chloride	s.d Fine Chem. Ltd.
4.	Phenol	Merck
5.	*o*-cresol	Merck
6.	methanol	s.d Fine Chem. Ltd.
7.	Ethylbenzene	s.d Fine Chem. Ltd.

8.	Tert-butyl hydroperoxide	Sigma Aldrich Chemicals Pvt. Ltd
9.	Acetonitrile	Qualigens Fine Chemicals (99%)
10.	Acetone	Qualigens Fine Chemicals (99%)
11.	Acetic acid	Qualigens Fine Chemicals (99%)
12.	Dichloromethane	Qualigens Fine Chemicals (99%)

2.7.1 Ethylbenzene Oxidation

Ethyl benzene oxidation was conducted in a 50mL Glass round bottom flask placed in a thermostated oil bath fitted with a magnetic stirrer and water cooled condenser. In a typical oxidation, required quantity of ethyl benzene, solvent and catalyst were taken in the R.B and after attaining the reaction temperature tertiary butyl hydroperoxide was added in drops. The products were identified by GC-MS and conversion and product selectivity were monitored using a Chemito 8610 GC using a FID detector and an SE-30 column.

2.7.2 Benzylation of Toluene and *o*-xylene

Liquid phase benzylation of toluene and *o*-xylene was carried using benzyl chloride as the benzylating agent. The reactants in the required mole ratio and definite amount of the catalyst were taken in a 50mL double necked round bottom flask and refluxed in an oil bath using water condenser. The temperature of the oil bath was adjusted according to the requirement of the reaction studied and kept constant by means of a dimmerstat. The reaction mixture was stirred magnetically and the products were analyzed using a Chemito 8610 GC using a FID detector and an SE-30 column.

2.7.3 Methylation of Phenol and *o*-cresol

Methylation was carried out in a vertical down flow glass reactor. All the reactions were carried out using 0.5 g charge of the catalyst. Prior to the reaction the

catalysts were activated in the muffle furnace for 1h at 500°C. The catalyst was packed between the layers of quartz wool, and the upper portion of the reactor was filled with glass beads, which served as pre-heaters for the reactants. The reactor was placed inside a temperature-controlled furnace with a thermocouple placed at the centre of the catalyst bed for measuring the reaction temperature. In a typical reaction, a mixture of phenol or cresol and methanol in required molar ratio was fed into the reactor at pre-determined flow rate through a syringe pump at a particular reaction temperature. The products were condensed and collected in an ice trap. The products were identified by GC-MS and were analyzed by a Chemito 8610 GC using a FID detector and an OV-17 column. The conversion was expressed in terms of o-cresol reacted and the product selectivity was obtained as the amount of the particular product divided by the total amount of products multiplied by 100.

Gas chromatographic analysis conditions are given in Table 2.6.

Table 2.6 GC analysis conditions of various reactions

| Reaction | Column | Temperature (°C) | | |
		Injector	Detector	Programme of Analysis
Cumene cracking	BP-1	230	230	110°C-Isothermal
Cyclohexanol decomposition	Carbowax	200	200	90°C-Isothermal
Ethylbenzene oxidation	SE-30	250	250	120°C-3 min-20°/min-280°C
Toluene/o-xylene benzylation	SE-30	230	230	80°C-2 min-3°/min-230°C
Phenol/o-cresol methylation	OV-17	250	250	80°C-2 min-10°/min-280°C

References

[1]   A. Atkinson, R. M. Guppy, J. Mater. Sci. 26 (1999) 3869.

[2]   Michael E. Zorn, Dean T. Tompkins, Walter A. Zeltner, Marc A. Anderson, Appl. Catal. B 23 (1999) 1.

[3]   C. Suryanarayana, M. G. Norton, X-Ray Diffraction A Practical Approach, Plenum Press, New York (1998).

[4]   C. N. Satterfield, Heterogeneous Catalysis in Industrial Practice, McGraw – Hill Inc., New York (1991).

[5]   D. A. Skoog, F. J. Holler, T. A. Nieman, Principles of Instrumental analysis, fifth edition, Thomson Learning Inc. (1998).

[6]   H. H. Willard, L. L. Merritt, Jr, J. A. Dean, F. A. Settle, Jr Instrumental Methods of Analysis, CBS Publishers and Distributors, New Delhi (1986).

[7]   J. W. Niemantsverdriet, Spectroscopy in Catalysis An Introduction, VCH Publishers, New York (1995).

[8]   J. Ryczkowski, Catal. Today 68 (2001) 263.

[9]   H. G. Hecht, Modern aspects of Reflectance Spectroscopy, W. W. Wendlandt (Ed.), Plenum Press, New York (1968)

[10]   V. S. Escribano, E. F. Lopez, M. Panizza, C. Resini, J. M. l. Amores, G. Busca, Solid State Sciences 5 (2003) 1369.

[11]   K. Tanabe, M. Misono, Y. Ono, H. Hattora, Solid Acids and Bases, Elsevier Science Publishers B. V, The Netherlands (1989).

[12]   S. M. Bradley and R. A. Kydd, J. Catal. 141 (1993) 239.

[13]   R. Jothiramalingam, B. Viswanathan, T. K. Varadarajan, Catal. Commun. 6 (2005) 41.

[14]   D. M. Murphy, E. Giamello, Electron Paramagnetic Resonance, The Royal Society of Chemistry, 18 (2002).

PHYSICO-CHEMICAL CHARACTERIZATION

Abstract

Catalyst characterization is a lively and highly relevant discipline in catalysis. There are many ways to obtain information on the physico chemical properties of materials. Characterization of the prepared catalysts were done by different techniques such as X-ray diffraction analysis, surface area and pore volume measurements, energy dispersive X-ray analysis, scanning electron microscopy, infrared spectroscopy, UV-visible diffuse reflectance spectroscopy, FT-Raman spectroscopy, electron paramagnetic resonance spectroscopy. The acidity of the catalyst were measured by TPD of ammonia and thermogravimetric desorption of 2,6-dimethyl pyridine. Surface acidic properties were studied by two test reactions, cyclohexanol decomposition and cumene cracking.

3.1 Introduction

In heterogeneous catalysis, the reaction occurs at the surface. Catalytic surfaces need to be characterized with reference to their physical properties and their actual performance as catalyst. The most important physical properties are those relating to the surface because catalyst performance is determined by surface parameters. A detailed investigation on the structural and surface characterization of the catalyst was carried out and the results are discussed in the present chapter.

3.2 Physical Characterization

3.2.1 X-ray Diffraction Analysis

X-ray diffraction (XRD) analysis was used to determine the phase composition and to estimate the crystallite size of the powders.

Figure 3.1 shows the XRD patterns of ceria, zirconia and ceria-zirconia. The diffraction pattern of ceria shows reflections characteristic of cubic phase with fluorite structure. The four typical peaks were observed at $2\theta \approx 28.5$, 33.0, 47.5, 56.5 (°), corresponding to the planes of (111), (200), (220) and (311) respectively (space group Fm3m)[1]. For pure zirconia, tetragonal phase is dominant with a small amount of monoclinic phase as evident from the diffraction pattern[2,3]. The phase diagram for CeO_2-ZrO_2 system reported in the literature depicts three major phases, i.e., cubic, tetragonal, and monoclinic. The tetragonal phase is further divided into stable t and metastable t' and t'' structures[4,5]. Sanchez Escribano et al.[6] reported that the symmetry of solid solution phases or the presence of minor amounts of tetragonal phases in the Ce-rich materials cannot be determined with certainty using XRD.
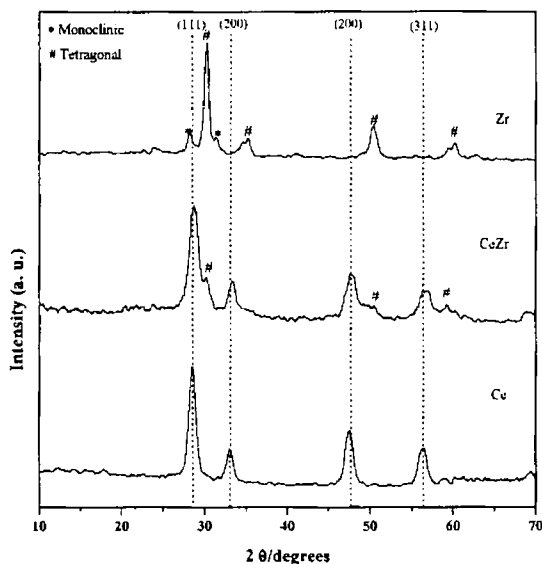
Figure 3.1 XRD patterns of Ce, Zr and CeZr

The XRD pattern of ceria-zirconia mixed oxide contains peaks similar to pure ceria confirming the formation of cubic solid solution and stabilization of fluorite structure by zirconia substitution[7]. The high 2θ shoulders in the pattern reveal the presence of a minor zirconia rich phase. The shift of the peaks towards higher 2θ values is due to the small ionic radius of Zr^{4+} (0.84 Å) in comparison with that of Ce^{4+} (0.97 Å)[8].

Diffractograms of chromium, manganese, iron and cobalt modified catalysts are illustrated in figure 3.2. All the catalysts gave almost identical diffractograms. According to Viswanath et al., the absence of chromia phase in the diffraction pattern for the supported catalysts may be attributed to the fact that chromium species are randomly dispersed, disordered, and the crystallite size may be smaller than the detection limit[9]. Harisson et al. observed that phase separation of Cr_2O_3 is detectable

only after calcination at 876K for chromia promoted ceria catalysts[10]. The peaks corresponding to the MnO_x phase are absent in the diffraction patterns. It is reported that the replacement of Ce^{4+} by Mn^{3+} in the fluorite structures is possible by their structural similarity[11]. The crystallization of Mn_2O_3 takes place only when the Mn content $> 50\%$[12,13]. Thus for the prepared Mn series the MnO_x crystallites are efficiently dispersed on the surface of the catalyst. Iron modified series shows peaks corresponds to typical fluorite structure. No peaks of iron oxide are detected. Decrease in cell parameter is observed after iron modification due to the incorporation of Fe^{3+} (0.67 Å) in the structure of CeO_2[14]. No formation of crystalline CoO was observed in the case of cobalt modified catalysts. Kraum et al.[15] reported that among Co supported on ceria, zirconia and titania, only on ceria no cobalt oxide crystallites are formed. An increase in cobalt dispersion is attributed to the efficient metal-support interaction.
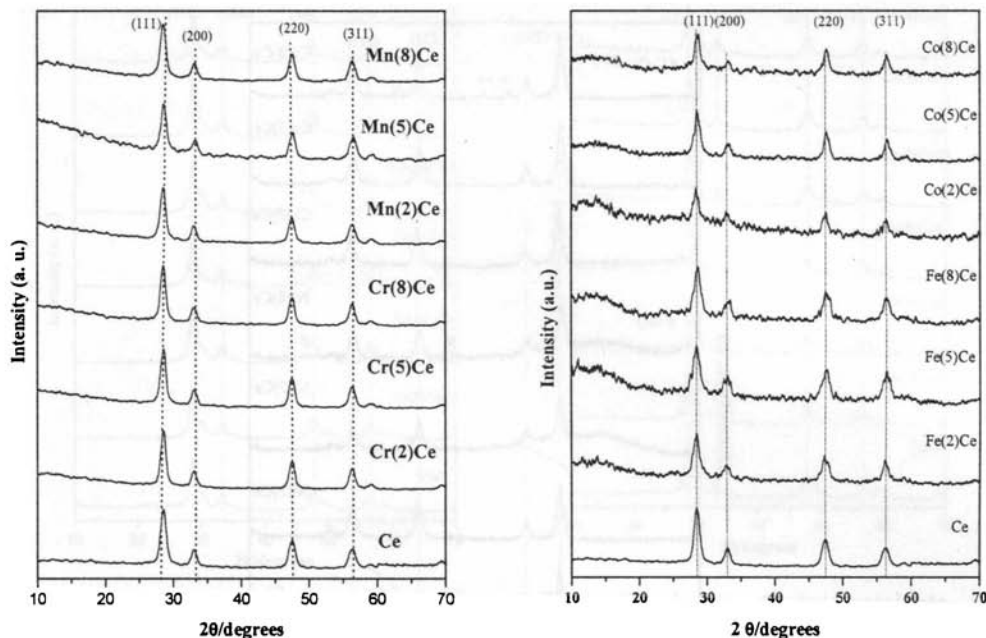
Figure 3.2 XRD patterns of Cr, Mn, Fe and Co modified ceria catalysts

For nickel modified catalysts, no nickel compounds are seen at low Ni loading (Figure 3.3). 8 wt.% Ni containing catalyst shows NiO reflections at $2\theta \approx 43.7$ and $62.9°$ similar to that reported by Li et al.[16]. In the diffraction patterns of the catalysts containing 2 and 5 wt.% copper, no peaks corresponding to crystalline CuO appear. In 8 wt.% Cu containing catalysts two peaks corresponding to the crystalline CuO were observed ($2\theta \approx 35.4, 38.8°$)[17].
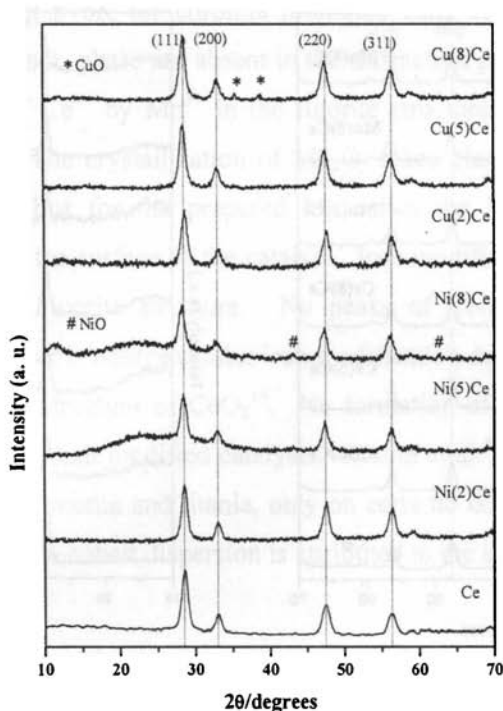
Figure 3.3 XRD patterns of Co and Ni modified ceria catalysts

XRD patterns of chromium, manganese, iron and cobalt modified ceria-zirconia catalysts (Figure 3.4) resembles that of fluorite structure. No peaks corresponding to incorporated metal oxide are found. This suggests efficient dispersion of metal oxides on the ceria-zirconia support. Reflections due to crystalline CuO and NiO phase is found in the case of 8 wt.% copper and nickel loaded ceria-zirconia catalysts (Figure 3.5). But the intensity of metal oxide reflections is low compared to the corresponding metal modified ceria catalysts suggesting that ceria-zirconia support is more efficient in dispersing incorporated metal rather than pure ceria.
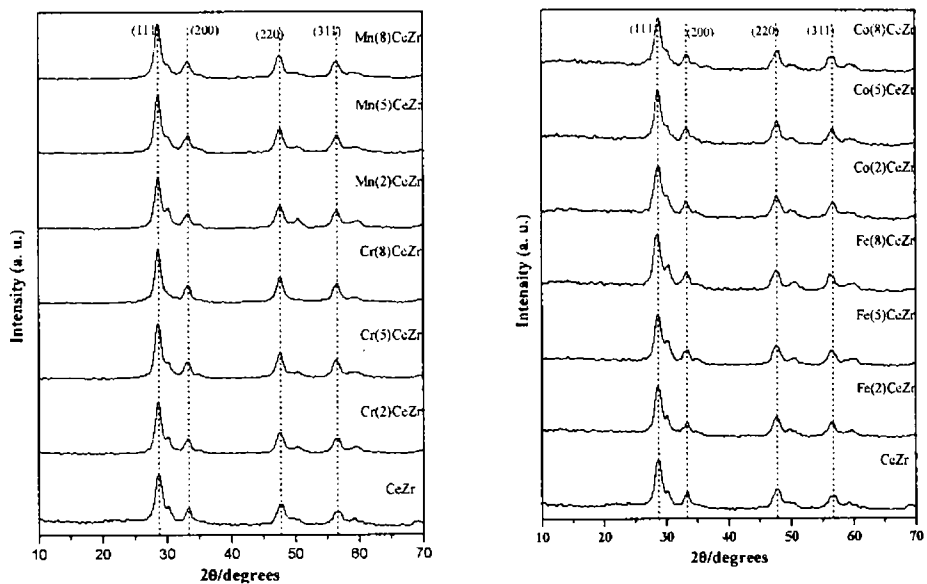
Figure 3.4 XRD patterns of Cr, Mn, Fe and Co modified ceria-zirconia catalysts
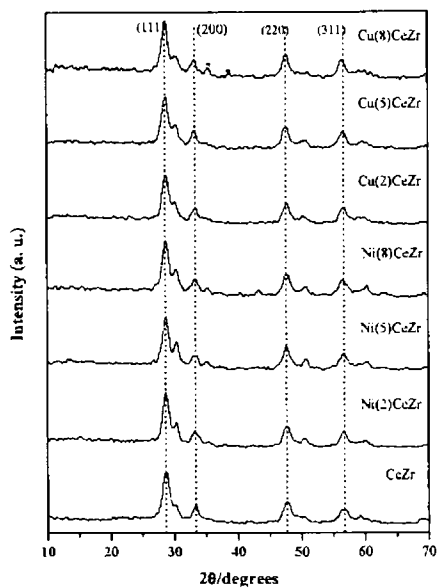
Figure 3.5 XRD patterns of Ni and Cu modified ceria-zirconia catalysts

The average crystallite size was estimated from the peak broadening using Scherrer equation and is tabulated as in Table 3.1. Cr and Mn modified ceria catalysts have crystallite size comparable to pure ceria. Fe, Co and Ni modification of ceria and ceria-zirconia results a decrease in crystallite size.

Table 3.1 Crystallite size of catalysts

Catalyst	Crystallite size (nm)	Catalyst	Crystallite size (nm)
Ce	10.3	Zr	10.2
Cr(2)Ce	11.5	CeZr	8.0
Cr(5)Ce	10.9	Cr(2)CeZr	8.5
Cr(8)Ce	11.2	Cr(5)CeZr	8.3
Mn(2)Ce	10.8	Cr(8)CeZr	9.5
Mn(5)Ce	10.5	Mn(2)CeZr	8.3
Mn(8)Ce	10.3	Mn(5)CeZr	9.1
Fe(2)Ce	6.9	Mn(8)CeZr	9.2
Fe(5)Ce	4.5	Fe(2)CeZr	5.2
Fe(8)Ce	7.1	Fe(5)CeZr	7.6
Co(2)Ce	5.0	Fe(8)CeZr	7.3
Co(5)Ce	3.2	Co(2)CeZr	6.9
Co(8)Ce	9.8	Co(5)CeZr	7.5
Ni(2)Ce	7.1	Co(8)CeZr	7.5
Ni(5)Ce	6.9	Ni(2)CeZr	8.3
Ni(8)Ce	6.7	Ni(5)CeZr	8.2
Cu(2)Ce	6.2	Ni(8)CeZr	8.5
Cu(5)Ce	5.9	Cu(2)CeZr	7.8
Cu(8)Ce	5.9	Cu(5)CeZr	8.3
		Cu(8)CeZr	9.9

3.2.2 Energy Dispersive X-ray Analysis

The catalyst composition obtained from energy dispersive X-ray analysis (EDX) of metal modified ceria catalysts are presented in Table 3.2. It is observed that the experimental atom percentage is close to the expected (theoretical) values. It can be concluded that the sol-gel method is effective for the preparation of metal modified ceria catalysts with required composition.

Table 3.3 give the composition of metal modified ceria-zirconia mixed oxide catalysts. The expected Ce/Zr ratio is 50:50 and the experimentally obtained ratio is 51.9: 48.1. In the case of Cr, Mn and Fe doped catalysts the Ce/Zr atom ratio is ≈1 as theoretically expected. But for Co, Ni and Cu the ratio shows deviation from unity. Martinez-Arias et al. investigated the preparation of ceria-zirconia mixed oxides with Ce/Zr ratio1. They found the presence of Ce-rich layer at the external surface and predicted some degree of heterogeneity in the sample[5].

Table 3.2 Elemental composition of metal modified ceria catalysts

Catalyst	Composition (atom %)			
	Ce		Metal	
	Theo.	Exp.	Theo.	Exp.
Ce	100	100	-	-
Cr(2)Ce	93.8	92.9	6.2	7.1
Cr(5)Ce	85.8	85.6	14.2	14.4
Cr(8)Ce	79.1	77.0	20.9	23.0
Mn(2)Ce	94.1	91.6	5.9	8.4
Mn(5)Ce	86.5	81.3	13.5	18.7
Mn(8)Ce	80.0	76.1	20.0	23.9
Fe(2)Ce	94.2	95.7	5.8	4.3
Fe(5)Ce	86.7	86.9	13.3	13.0
Fe(8)Ce	80.2	77.7	19.8	22.3
Co(2)Ce	94.5	95.3	5.5	4.7
Co(5)Ce	87.3	85.2	12.7	14.8
Co(8)Ce	81.1	76.3	18.9	23.7
Ni(2)Ce	94.5	94.5	5.5	5.5
Ni(5)Ce	87.2	86.2	12.8	13.8
Ni(8)Ce	81.0	80.2	19.0	19.8
Cu(2)Ce	94.9	91.3	5.1	8.7
Cu(5)Ce	88.1	89.8	11.9	10.2
Cu(8)Ce	82.2	80.9	17.8	19.1

Table 3.3 Elemental composition of metal modified ceria-zirconia catalysts

| Catalyst | Composition (atom %) | | | | | |
| | Ce | | Zr | | Metal | |
	Theo.	Exp.	Theo.	Exp.	Theo.	Exp.
Zr	-	-	100	100	-	-
CeZr	50.0	51.9	50.0	48.1	-	-
Cr(2)CeZr	47.3	48.9	47.3	43.3	5.4	7.8
Cr(5)CeZr	43.8	42.8	43.8	41.0	12.4	16.2
Cr(8)CeZr	40.7	39.7	40.7	39.6	18.4	20.7
Mn(2)CeZr	47.5	47.2	47.5	46.2	5.0	6.6
Mn(5)CeZr	44.1	42.8	44.1	41.2	11.8	16.0
Mn(8)CeZr	41.2	39.8	41.2	40.1	17.6	20.1
Fe(2)CeZr	47.5	47.7	47.5	46.3	5.0	6.0
Fe(5)CeZr	44.2	42.8	44.2	44.9	11.6	12.3
Fe(8)CeZr	41.3	42.0	41.3	40.5	17.4	17.5
Co(2)CeZr	47.6	50.0	47.6	45.2	4.8	4.8
Co(5)CeZr	44.4	47.4	44.4	40.5	11.1	12.0
Co(8)CeZr	41.7	44.6	41.7	38.4	16.6	17.0
Ni(2)CeZr	47.6	50.3	47.6	44.7	4.8	5.0
Ni(5)CeZr	44.4	46.3	44.4	41.2	11.2	12.5
Ni(8)CeZr	41.6	39.5	41.6	37.7	16.8	22.8
Cu(2)CeZr	47.8	44.9	47.8	47.3	4.4	7.7
Cu(5)CeZr	44.8	44.6	44.8	39.6	10.4	15.8
Cu(8)CeZr	42.2	42.3	42.2	39.5	15.6	18.2

3.2.3 Surface area and pore volume measurements

The BET surface area and pore volume measurement (S_{BET}) results of different transition metal modified ceria catalysts are presented in Table 3.4. On

incorporating Cr, Mn and Fe, the surface area is found to be enhanced with enhancement in pore volume. In the case of chromium modified systems, the surface area increases up to 5 wt.% metal content and then decreases. For Mn and Fe modified systems, the highest surface area is obtained for 2 wt.% metal containing systems. Further increase in metal content results a decrease in surface area. Considering the surface area values of Co, Ni and Cu systems, an opposite trend is observed. Even though there is reduction in surface area on incorporating these metals compared to pure ceria, among the metal modified systems surface area increases with increase in metal content. Neri et al.[14] reported that on addition of iron to ceria an increase in surface area is observed. Addition of iron favors the creation of structural defects. The formation of structural defects in turn favors the increase of surface area. Akashi et al.[13] reported that Cr, Mn, Fe, Co and Ni modified ceria prepared through amorphous citrate process have high surface area compared to pure ceria. Mn content of about 20-90 mol% does not affect the specific surface area of CeO_2-MnO_x catalyst. But with the same preparation method Sato et al. found that addition of Fe, Co and Ni to ceria cause a decrease in surface area[18]. It is found that different methods of preparation lead to ceria catalysts with different surface characteristics[19]. Viswanath et al.[9] reported that for ceria supported chromium catalyst by impregnation, the deposition of chromium species on the CeO_2 support caused a decrease in specific surface area and is attributed to the plugging of pores on the support by chromia phase. The BET surface area of CuO_x/CeO_2 catalysts prepared by inert gas condensation technique is found to be independent of the copper content and is primarily influenced by the particle morphology[20].

The specific surface area of metal modified ceria-zirconia catalysts are given in Table 3.5. Here also the surface area values are comparatively higher for the Cr, Mn and Fe modified catalysts. Ni and Cu modified catalysts have surface area comparable to ceria-zirconia catalysts. On Co modification there is slight decrease in

surface area. Srinivas et al.[21] found that for hydrothermally synthesized $NiO-CeO_2$-ZrO_2 catalyst the surface area increased with increase in Ni content up to 20 wt% and then decreased. Wang et al.[22] reported that for $CuO-ZrO_2$ nano powders the surface area is seen initially to increase with the increase in Cu content with a maximum for 30% copper, and decrease for copper content of 50%. The increase of surface area with the increase of Cu content is expected to be due to the contribution of Cu species.

Table 3.4 Surface area and pore volume of metal modified ceria catalysts

Catalyst	Surface area $(m^2 g^{-1})$		Pore volume $(*10^{-6} m^3)$
	BET	Langmuir	
Ce	61	93	0.050
Cr(2)Ce	59	90	0.066
Cr(5)Ce	63	97	0.066
Cr(8)Ce	58	89	0.067
Mn(2)Ce	69	105	0.068
Mn(5)Ce	67	104	0.065
Mn(8)Ce	58	89	0.064
Fe(2)Ce	69	105	0.064
Fe(5)Ce	59	89	0.062
Fe(8)Ce	55	83	0.063
Co(2)Ce	35	54	0.028
Co(5)Ce	37	55	0.033
Co(8)Ce	42	64	0.034
Ni(2)Ce	43	65	0.035
Ni(5)Ce	44	67	0.033
Ni(8)Ce	55	82	0.044
Cu(2)Ce	53	86	0.040
Cu(5)Ce	59	89	0.041
Cu(8)Ce	59	89	0.040

Table 3.5 Surface area and pore volume of metal modified ceria-zirconia catalysts

Catalyst	Surface area (m^2g^{-1})		Pore volume $(*10^{-6})$
	BET	Langmuir	
Zr	22	32	0.040
CeZr	42	63	0.072
Cr(2)CeZr	61	145	0.090
Cr(5)CeZr	68	161	0.083
Cr(8)CeZr	76	180	0.076
Mn(2)CeZr	43	103	0.088
Mn(5)CeZr	59	144	0.089
Mn(8)CeZr	65	155	0.097
Fe(2)CeZr	44	66	0.072
Fe(5)CeZr	48	72	0.072
Fe(8)CeZr	54	81	0.093
Co(2)CeZr	38	57	0.067
Co(5)CeZr	37	56	0.062
Co(8)CeZr	39	58	0.059
Ni(2)CeZr	41	63	0.066
Ni(5)CeZr	40	61	0.056
Ni(8)CeZr	44	66	0.073
Cu(2)CeZr	41	61	0.654
Cu(5)CeZr	42	63	0.060
Cu(8)CeZr	44	67	0.056

From the BET surface area results it can be proposed that the surface area of doped ceria catalysts strongly depend on the nature and loading of the promoter.

Unlike that of impregnation method, the plugging of pores is not evident for Cr, Mn and Fe modified systems. The sol-gel method is effective for the preparation of supported metal catalysts since it produces homogenous materials with highly dispersed metals on the support.

3.2.4 Scanning Electron Microscopy

Figures 3.6 and 3.7 contain scanning electron microscopic (SEM) pictures of some representative catalysts. Similar surface morphology is observed in all cases.
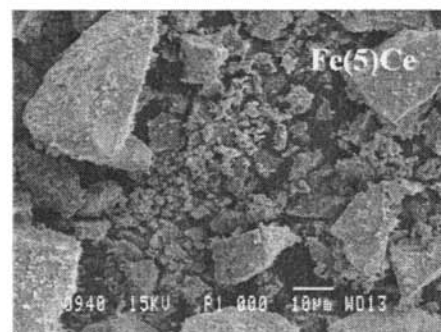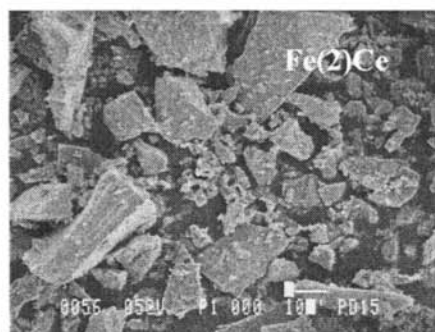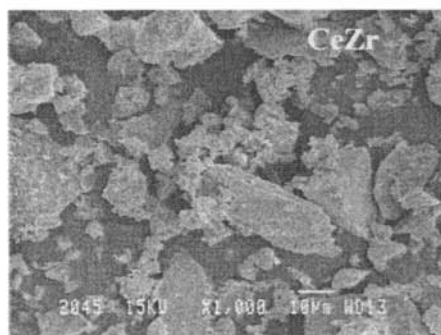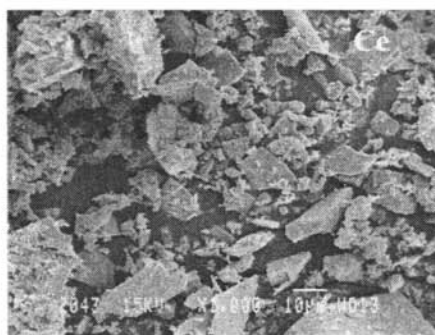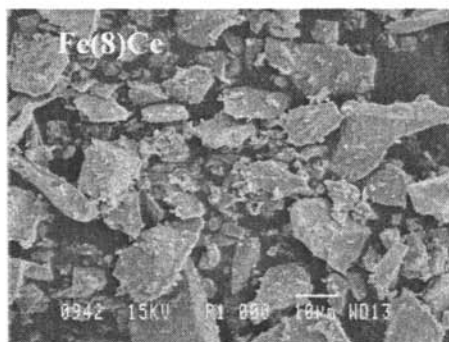
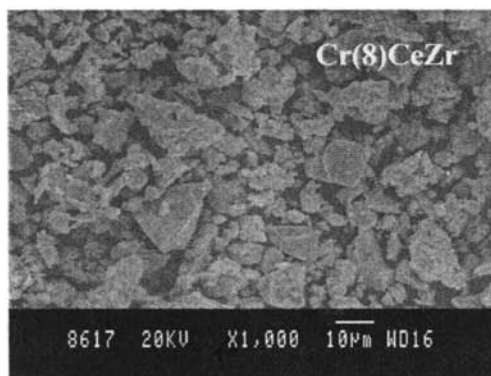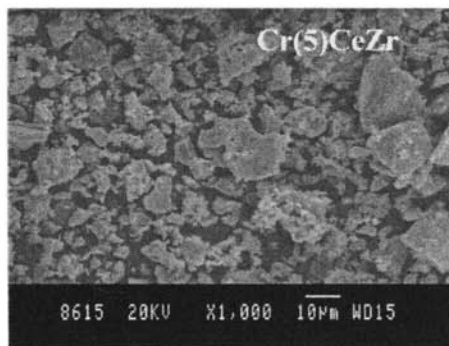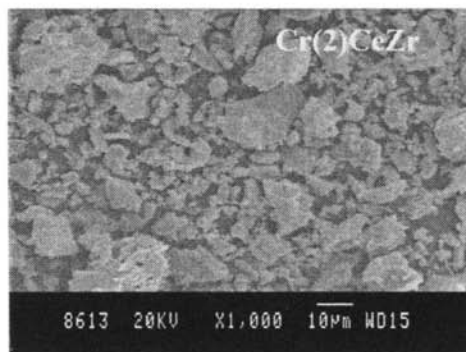**Figure 3.6** SEM pictures of Ce, CeZr and Fe modified ceria catalysts

Figure 3.7 SEM pictures of Cr modified ceria-zirconia catalysts

3.2.5 Thermogravimetric Analysis

The dried gels were analyzed by thermogravimetry (TGA/DTA) in nitrogen with a heating rate of 20°C/min. Figure 3.8 shows the TGA/DTA curves of Ce, Zr and CeZr. According to Zou et al.[23] the dried ceria sample may consist of three portions of materials: (1) crystalline ceria, CeO_2, (2) crystalline ceria with structural water, $CeO_2.2H_2O$, and (3) amorphous cerium hydroxide, $Ce(OH)_4$. The endothermic peak (figure 3.8) in 50-105°C could be due to crystallization of the amorphous portion in the sample, $Ce(OH)_4$ to crystalline CeO_2. The small endothermic peak at about 442°C can be attributed to the loss of structural water molecules. These results suggest that dried ceria sample is a mixture of three materials, $Ce(OH)_4$, CeO_2 and $CeO_2.2H_2O$. The prominent exothermic peak at 350°C can be attributed to change in oxidation state of cerium from Ce^{3+} to Ce^{4+} [24].

The sample Zr shows an endothermic peak around 100°C that corresponding to desorption of physically adsorbed water[25]. The thermogram corresponding to ceria-zirconia mixed oxide shows an endothermic peak at about 237°C attributed to the formation of ceria-zirconia solid solution with cubic structure[26]. An exotherm exhibited by ZrO_2 at 479°C can be proposed as being due to a phase transition from an amorphous into a crystalline form.
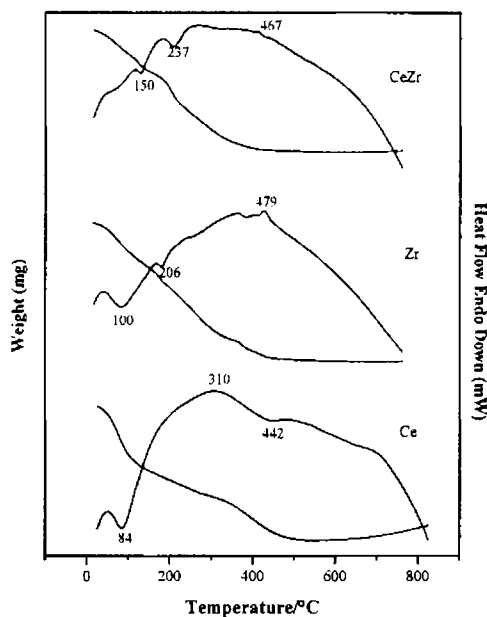
Figure 3.8 TGA/DTA profiles of Ce, Zr and CeZr

To study the effect of metal content, thermogravimetric analysis of iron modified ceria and ceria-zirconia catalysts was carried out and the thermograms are given in Figure 3.9. There is no significant difference between the thermograms of catalysts containing various metal contents.
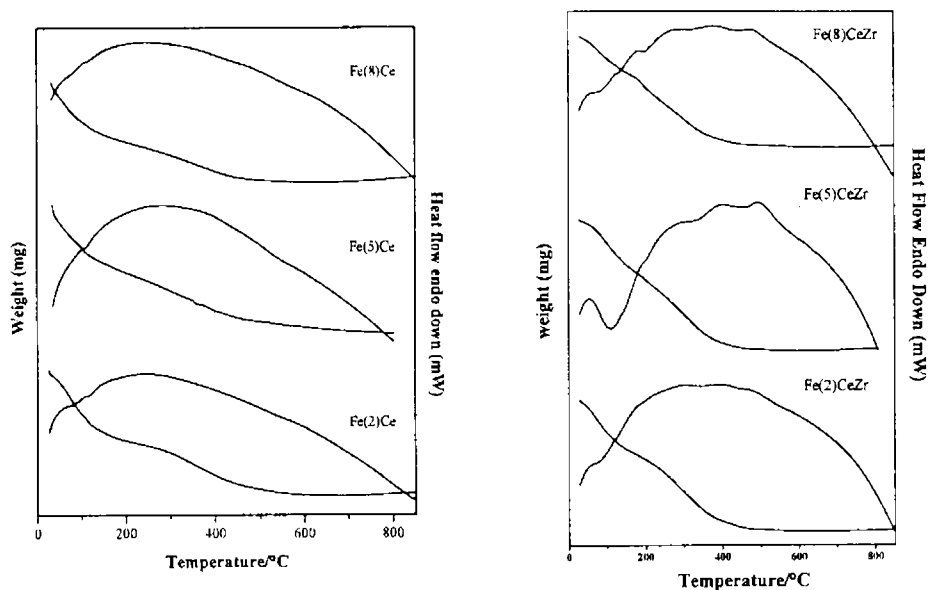
Figure 3.9 TGA/DTA profiles of Fe modified ceria and ceria-zirconia catalysts

    TGA/DTA profiles of Co, Ni and Cu modified systems are presented in Figure 3.10. The DTA profile as a whole resembles a broad exotherm, results from the removal of hydrated water, organic and nitrate residual and solid solution formation.
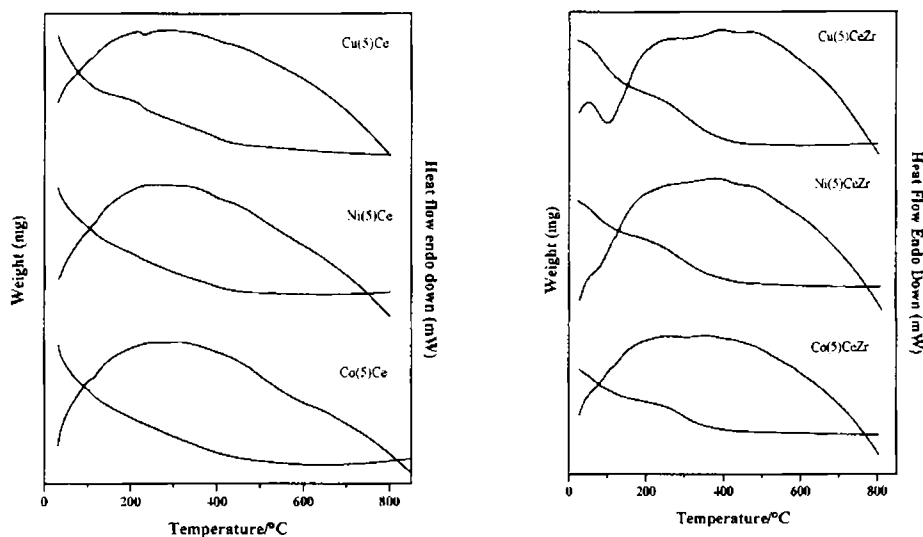
Figure 3.10 TGA/DTA profiles of representative catalysts

From the TGA/DTA profiles of the representative catalysts it is clear that the weight loss due to dehydration and decomposition of the residual organics and nitrates finished below 450°C. Hence the catalysts which are calcined at 500°C contain only metal oxides without any impurity. Up to 800°C no further weight loss is observed which confirms the thermal stability of prepared catalysts.

3.2.6 UV-vis-NIR Diffuse Reflectance Spectra

The surface structure of the prepared catalysts was investigated by UV-vis-NIR diffuse reflectance spectroscopy (DR UV-vis). This technique is based on the reflection of light in the ultraviolet (10-420 nm), visible (420-700 nm) and near infrared (700-2500 nm) regions by a powder sample. From the spectra information on surface coordination and different oxidation states of metal ions can be obtained[27].

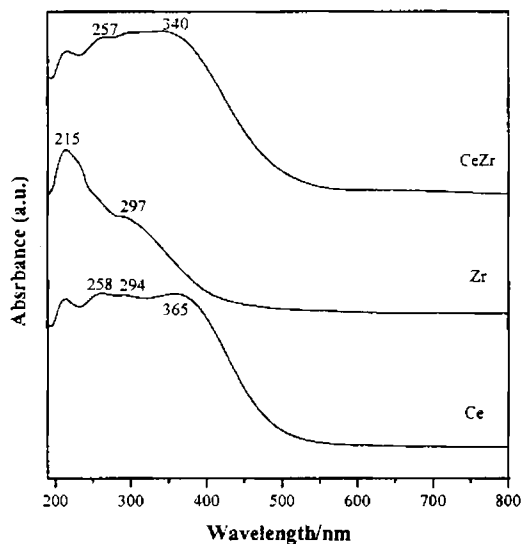**Figure 3.11** DR UV-vis spectra of Ce, Zr and CeZr

The DR UV-vis spectra of ceria, zirconia and ceria-zirconia mixed oxide catalysts are given in Figure 3.11. Crystalline CeO_2 has a band gap of 3.1 eV and absorbs strongly in the UV region with the absorption threshold near 400 nm. The absorption bands at 256 and 294 nm are attributed to $O^{2-} \rightarrow Ce^{3-}$ and $O^{2-} \rightarrow Ce^{4+}$ charge transfer transitions[27]. The spectra of ZrO_2 contain absorption at 215 nm which is attributed to monoclinic zirconia[7]. In the case of ceria-zirconia mixed oxide two bands are observed at 257 and 340 nm. The band at 257 nm is similar to that of ceria corresponding to $O^{2-} \rightarrow Ce^{3+}$ transition in the solid solution. The band around 340 nm may consist of interband and $O^{2-} \rightarrow Zr^{4+}$ transitions of substituted fluorite lattice[28].

The DR UV-vis spectra of chromium modified catalysts (Figure 3.12) show a band around 360 nm corresponding to the tetrahedral chromate transitions (O-Cr^{6-} charge transfer transitions), corresponding to chromium (VI) [9,29]. The band around 470 nm, assigned to Cr^{6-} present in supported chromate is also observed[30]. The band around 590 nm corresponds to octahedrally coordinated Cr^{3-} state due to $A_{2g} \rightarrow T_{2g}$

transitions[31]. It is also suggested that the band at 600 nm could be due to the presence of Cr^{6+} and Cr^{3+} ions, which could interact through d↔d electron exchange. According to Khaddar-Zine et al[32]. the identification of chromate and dichromate species are difficult, since Cr^{4+} $(3d^2)$ and $Cr^{5+}(3d^1)$ in octahedral symmetry, produce transitions at almost identical values to propose unequivocal identification of the existing chromium species.
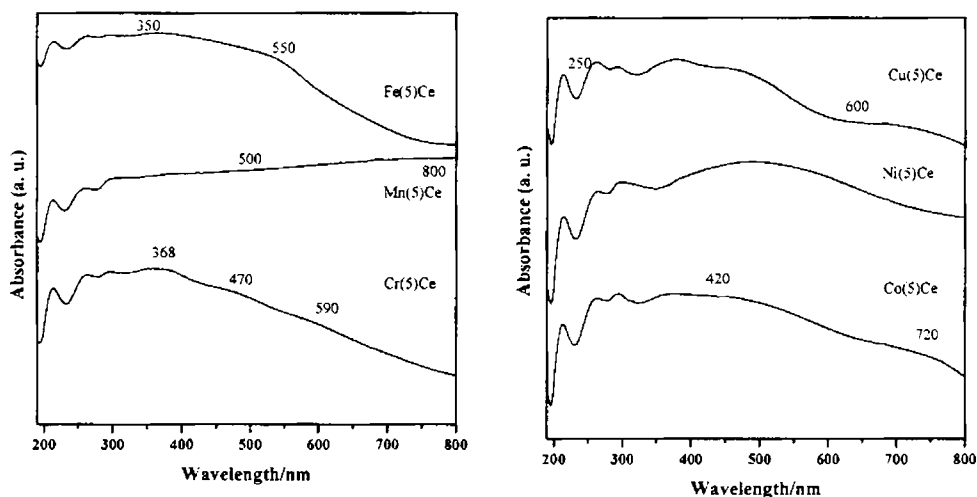
Figure 3.12 DR UV-vis spectra of representative ceria catalysts

Mn modified ceria catalyst shows an intense band centered around 800 nm, which indicates the presence of Mn(II) in tetrahedral coordination and this band is due to ligand to metal charge transfer involving transition metal sites[33]. A band observed around 500 nm is assigned to $^6A_{1g}{\rightarrow}^4T_{2g}$ crystal field transition. The broad band around 380 nm is attributed to $O^{2-}{\rightarrow}Mn^{3+}$ charge transfer transitions superimposed on $^5B_{1g}{\rightarrow}^5E_g$ crystal field d-d transition[34]. Introduction of iron into ceria and ceria-zirconia results in the appearance of very broad band in the range of 350-550 nm. This band is assigned to symmetrical spin-forbidden d-d transitions of Fe^{3+} [31]. Bachari et al.[35] observed for iron containing mesoporous silicas, a very broad band appeared with

a maximum around 350 nm which is the characteristic of iron oxide. Cobalt modified ceria-zirconia catalyst shows a band around 580 nm corresponding to cobalt in the octahedral environment and is assigned to the $^5T_{2g} \rightarrow ^5E_g$ transition[51]. For copper modified catalysts the band observed in the region between 600-800 nm can be attributed to d-d transitions of Cu with octahedral environment in CuO^{31}.
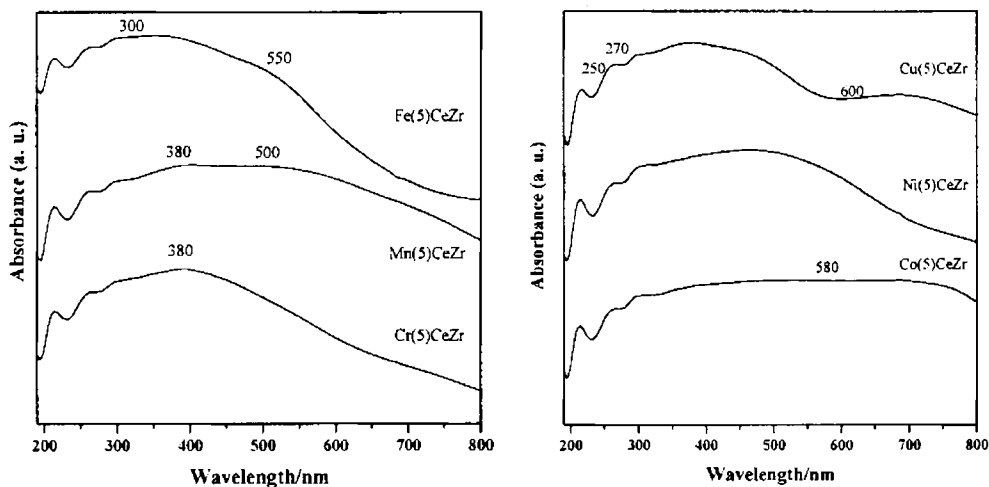
Figure 3.13 DR UV-vis spectra of representative ceria-zirconia catalysts

The near infrared portion of diffuse reflectance spectrum covers the overtones and combination bands of fundamental stretching frequencies of surface molecular groups such as H_2O and -OH. The bands observed at 1443 and 1941 nm in the NIR region of all the catalysts are due to the first overtone of hydroxyl groups ($2v_{O-H}$) and combination band corresponding to hydroxyl stretching and bending vibrations respectively (Figures 3.14 and 3.15). On modification with transition metal, the intensity of band at 1443 nm decreases owing to consumption of -OH groups as a result of dehydroxylation occurring between the active metal oxide and the support phase[9]. Only cobalt modified catalysts show an increase in the intensity in the hydroxyl region.
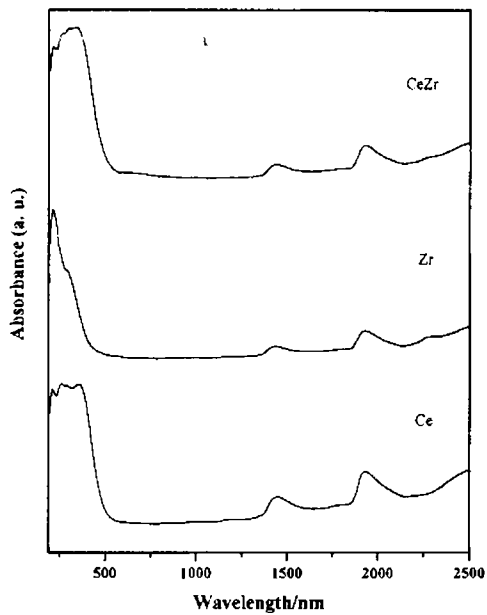
Figure 3.14 DR UV-vis NIR spectra of Ce, Zr and CeZr
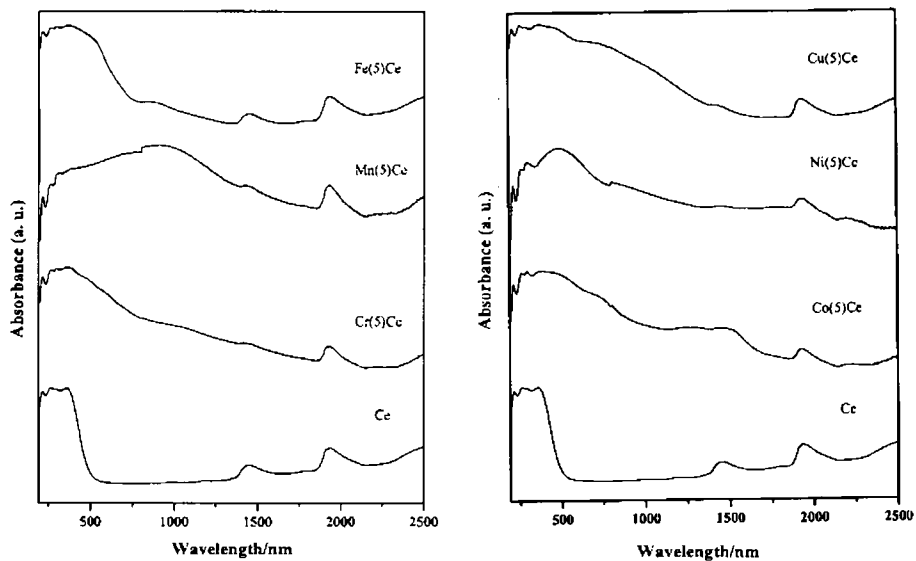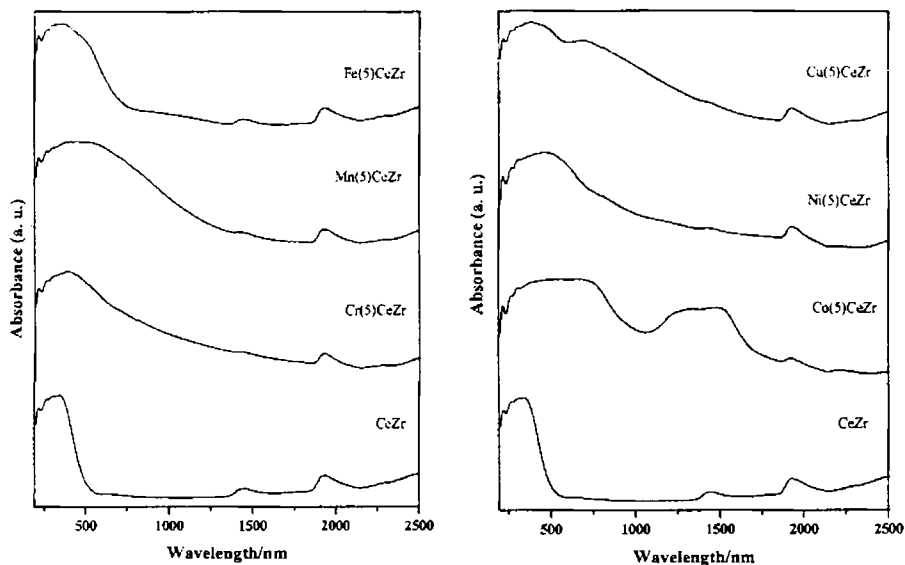
Figure 3.15 DR UV-vis NIR spectra of representative ceria and ceria-zirconia catalysts

3.2.7 FT-Infrared Spectra

The FT-Infrared (FT-IR) spectra of representative catalysts are shown in Figure 3.16. The broad absorption band located in the area from 3200 to 3600 cm^{-1} approximately corresponds to the O-H stretching vibration, and the one located in the area from 450 to 700 cm^{-1} to the CeO_2 stretching vibration. The absorption peaks at 1600 and 1340 cm^{-1} correspond to H_2O bending vibration and Ce-OH stretching vibration respectively[36]. The spectra of iron modified catalysts resemble that of pure ceria.
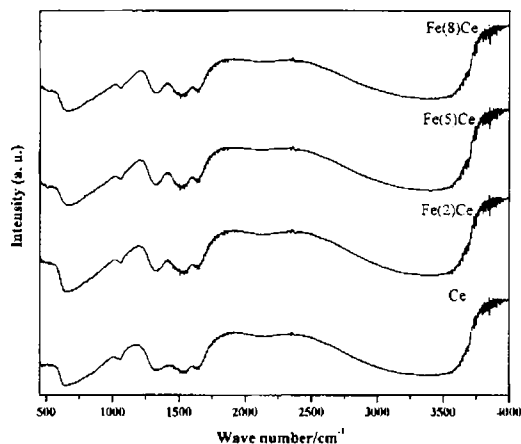
Figure 3.16 FT-IR spectra of ceria and Fe modified ceria

3.2.8 FT-Raman Spectra

The FT-Raman spectrum of pure ceria in Figure 3.17 show only one peak at 478 cm^{-1} which corresponds to the fundamental F_{2g} symmetry, which can be regarded as a symmetric O-Ce-O stretching as reported by Sanchez et al[6]. For Zirconia sample, peaks are observed at 164, 285, 334, 484, 627, 662 cm^{-1} correspond to the theoretical bands predicted for tetragonal zirconia. The presence of small peak at 198 cm^{-1} reveals the presence of monoclinic zirconia. The Ceria-zirconia mixed oxide shows only one peak at 483 cm^{-1} characteristic of cubic fluorite-like structure.
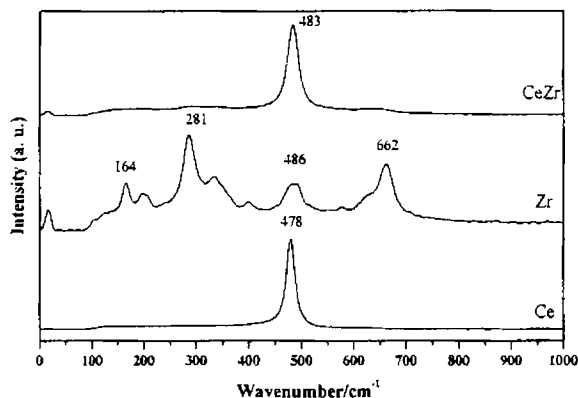
Figure 3.17 FT-Raman spectra of Ce, Zr and CeZr.

3.2.9 Electron Paramagnetic Resonance Spectra

The electron paramagnetic resonance (EPR) spectra obtained for ceria and ceria-zirconia catalysts at 77 K are presented in Figure 3.18. The ceria as well as ceria-zirconia spectra show a line at g=1.96 which has been assigned to impurity related defects (Table 3.6). g factor around 1.94 can be attributed to Ce^{3+} with removable ligands[37]. In addition to the line at g=1.96, the ceria-zirconia sample exhibits a strong resonance line, the fine structure of which is poorly resolved. Since Zr^{4+} cations do not contribute to EPR, this strong line is probably due to the presence of Ce^{3+} ions and corresponding oxygen vacancies. Such vacancies may trap electrons that give rise to the paramagnetic signal. Besides, Ce^{3+} ions themselves may contribute to the resonance line at g=2.05. The strong extra line in the ceria-zirconia EPR spectrum shows that its electronic structure is substantially different from that of undoped ceria. The difference is due to the presence of extra oxygen vacancies in oxygen deficient ceria-zirconia[50].
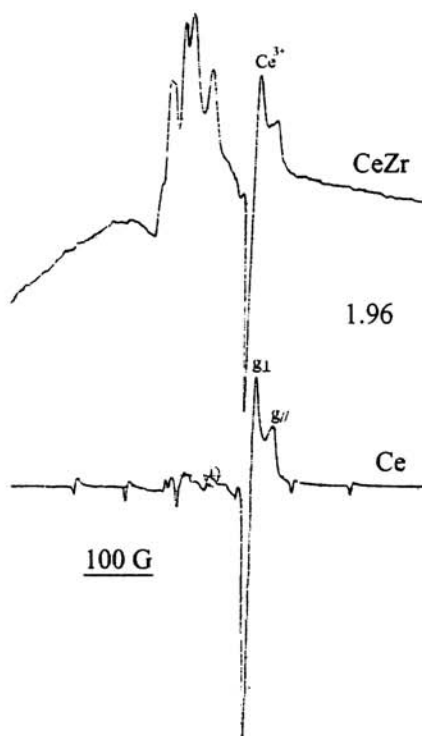
Figure 3.18 EPR spectra of Ce and CeZr

Table 3.6 EPR parameters of Ce and CeZr

Catalyst	g factor
Ce	1.966, 1.942
CeZr	1.966, 1.943, 2.05

The EPR spectra taken for Cr modified ceria and ceria-zirconia catalysts are shown in Figure 3.19 and the g values are given in the Table 3.7. The spectra of chromium modified ceria catalysts contain a broad peak with g values at 1.972 and 1.94. Studies by Weckhuysen et al.[38,39] on Cr(VI)/SiO$_2$ and Cr(VI)/Al$_2$O$_3$ catalysts have shown that three different chromium signals are observable in the EPR

depending on the treatment history of the catalysts. These are referred to as the δ-, γ-, β-signals. The δ- and β-signals are broad and occur in the g_{eff} ranges 5 and 1.96-2.45 respectively. The δ- signal results from dispersed Cr^{3+} ions where as β- signal is assigned to the clusters as indicated by broad range of g values. The γ- signal is much sharper and occurs at g=1.97. The signals obtained in the present study can be assigned as γ-signal in agreement with the report by Harrison et al.[10]. The origin of the signal can be attributed to the formation of mixed valence species. Spitz[40] has attributed the signal to mixed-valence trimers, Cr(VI)-O-Cr(III)-O-Cr(VI), with an average Cr oxidation state of Cr(V). For chromium modified ceria-zirconia catalysts, the β signals at 2.07 and 2.20 are attributed to clusters of Cr^{3+} on the catalyst surface.
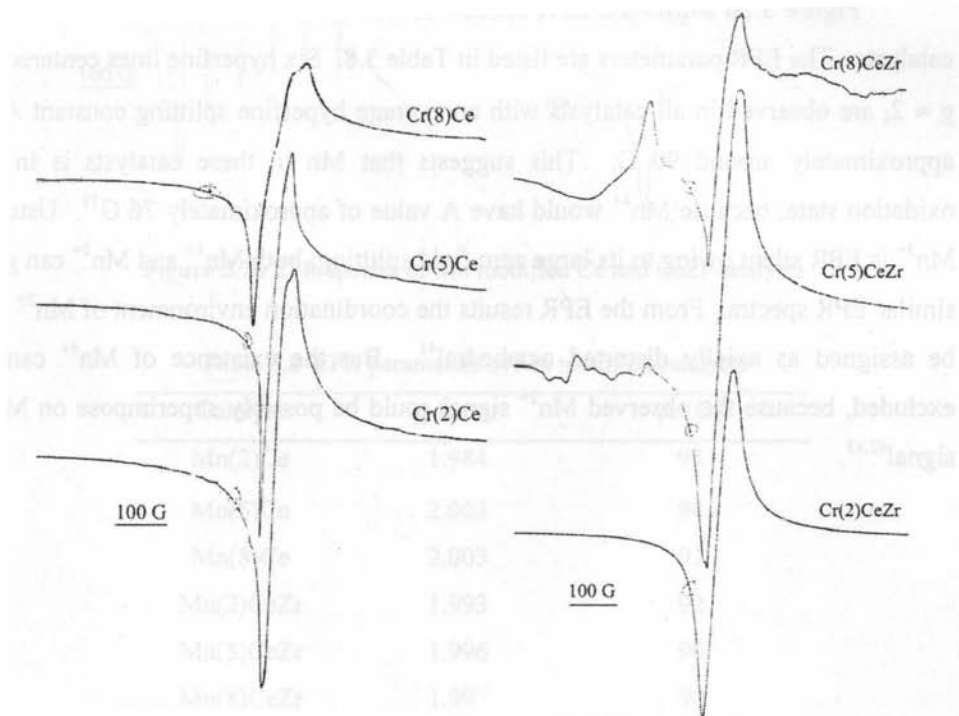
Figure 3.19 EPR spectra of Cr modified Ce and CeZr catalysts

Table 3.7 EPR parameters of Cr
modified Ce and CeZr catalysts

Catalyst	g values
Cr(2)Ce	1.972, 1.94
Cr(5)Ce	1.972, 1.94
Cr(8)Ce	1.972, 1.94
Cr(2)CeZr	1.966
Cr(5)CeZr	1.969, 2.20, 2.07
Cr(8)CeZr	1.972, 1.94, 2.07

Figure 3.20 shows the EPR spectra of Mn modified ceria and ceria-zirconia catalysts. The EPR parameters are listed in Table 3.8. Six hyperfine lines centered on $g \approx 2$, are observed in all catalysts with an average hyperfine splitting constant A of approximately around 90 G. This suggests that Mn in these catalysts is in +2 oxidation state, because Mn^{4+} would have A value of approximately 76 G^{11}. Usually Mn^{3+} is EPR silent owing to its large zero field splitting; both Mn^{4+} and Mn^{2+} can give similar EPR spectra. From the EPR results the coordination environment of Mn^{2+} can be assigned as axially distorted octahedral[41]. But the existence of Mn^{4+} cannot excluded, because the observed Mn^{2+} signal could be possibly superimpose on Mn^{4+} signal[42,43].
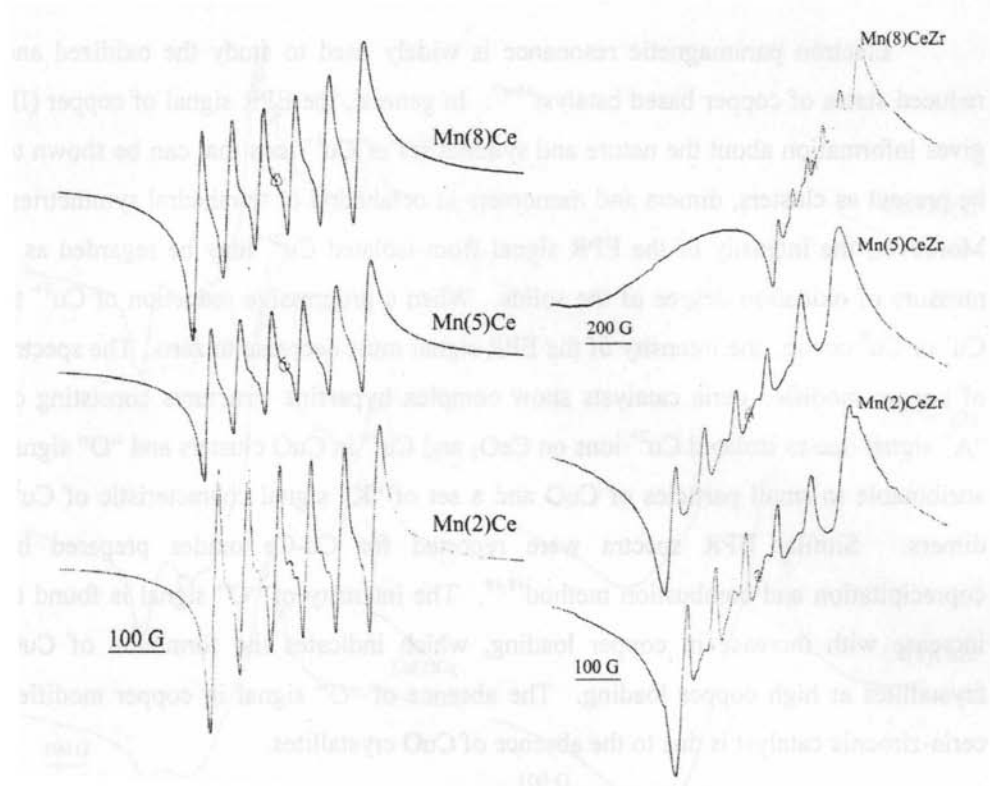
Figure 3.20 EPR spectra of Mn modified Ce and CeZr catalysts

Table 3.8 EPR parameters of Mn modified catalysts

Catalyst	g factor	A (G)
Mn(2)Ce	1.984	95
Mn(5)Ce	2.003	94
Mn(8)Ce	2.003	91
Mn(2)CeZr	1.993	92
Mn(5)CeZr	1.996	90
Mn(8)CeZr	1.997	90

Electron paramagnetic resonance is widely used to study the oxidized and reduced states of copper based catalyst[44-47]. In general, the EPR signal of copper (II) gives information about the nature and symmetries of Cu^{2+} ions that can be shown to be present as clusters, dimers and monomers in octahedral or tetrahedral symmetries. Moreover, the intensity of the EPR signal from isolated Cu^{2+} may be regarded as a measure of oxidation degree of the solids. When a progressive reduction of Cu^{2+} to Cu^{+} or Cu^{0} occurs, the intensity of the EPR signal must decrease to zero. The spectra of copper modified ceria catalysts show complex hyperfine structures consisting of "A" signal due to isolated Cu^{2+} ions on CeO_2 and Cu^{2+} in CuO clusters and "O" signal attributable to small particles of CuO and a set of "K" signal characteristic of Cu^{2+} dimers. Similar EPR spectra were reported for Cu-Ce oxides prepared by coprecipitation and combustion method[48,49]. The intensity of "O" signal is found to increase with increase in copper loading, which indicates the formation of CuO crystallites at high copper loading. The absence of "O" signal in copper modified ceria-zirocnia catalyst is due to the absence of CuO crystallites.
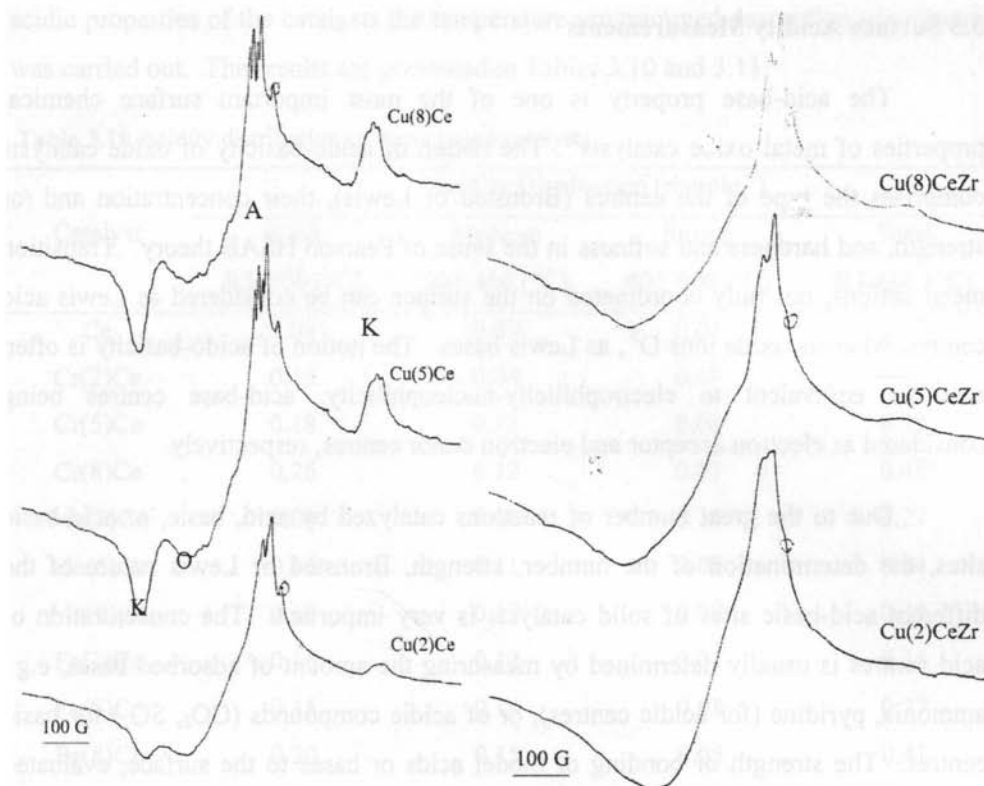
Figure 3.21 EPR spectra of Cu modified Ce and CeZr catalysts

Table 3.9 EPR parameters of Cu modified catalysts

Catalyst	g factor		
	A	O	K
Cu(2)Ce	2.027	2.192	2.283, 1.833
Cu(5)Ce	2.033	2.181	2.299, 1.833
Cu(8)Ce	2.037	2.192	2.299, 1.833
Cu(2)CeZr	2.033	-	2.229
Cu(5)CeZr	2.033	-	2.213, 1.833
Cu(8)CeZr	2.033	-	2.213, 1.833

3.3 Surface Acidity Measurements

The acid-base property is one of the most important surface chemical properties of metal oxide catalysts[51]. The notion of acido-basicity of oxide catalysts comprises the type of the centres (Bronsted or Lewis), their concentration and /or strength, and hardness and softness in the sense of Pearson HSAB theory. Transition metal cations, not fully coordinated on the surface can be considered as Lewis acid centres, whereas oxide ions O^{2-}, as Lewis bases. The notion of acido-basicity is often used as equivalent to electrophilicity-nucleophilicity, acid-base centres being considered as electron acceptor and electron donor centres, respectively.

Due to the great number of reactions catalyzed by acid, basic, or acid-basic sites, the determination of the number, strength, Bronsted or Lewis nature of the different acid-basic sites of solid catalysts is very important. The concentration of acid centres is usually determined by measuring the amount of adsorbed bases, e.g., ammonia, pyridine (for acidic centres), or of acidic compounds (CO_2, SO_2) for basic centres. The strength of bonding of model acids or bases to the surface, evaluated from the heat of their adsorption, the desorption temperature in TPD measurements, or a shift of the IR bands of adsorbed model compounds, is usually taken as a measure of the acid or basic strength. One can also estimate the strength of acid centres from the type of model reactions, assuming the analogy with typical acidic oxides that dehydration of alcohols and double-bond isomerization indicate the presence of weak acid centres, whereas cracking of hydrocarbons and skeletal isomerization require high acid strength.

3.3.1 Temperature Programmed Desorption-Ammonia

Temperature programmed desorption of ammonia (TPD-NH_3) is a powerful tool to examine the acidic nature of metal oxides. In order to investigate the surface

acidic properties of the catalysts the temperature programmed desorption of ammonia was carried out. The results are presented in Tables 3.10 and 3.11.

Table 3.10 Acidity distribution of Ceria based catalysts

Catalyst	Acidity Distribution (mmolg^{-1})			
	Weak RT-200 (°C)	Medium 201-400 (°C)	Strong 401-600 (°C)	Total RT-600 (°C)
Ce	0.09	0.03	0.03	0.15
Cr(2)Ce	0.15	0.04	0.13	0.32
Cr(5)Ce	0.18	0.12	0.09	0.39
Cr(8)Ce	0.26	0.12	0.07	0.45
Mn(2)Ce	0.09	0.08	0.10	0.27
Mn(5)Ce	0.16	0.11	0.07	0.34
Mn(8)Ce	0.18	0.12	0.08	0.38
Fe(2)Ce	0.16	0.12	0.07	0.35
Fe(5)Ce	0.15	0.14	0.08	0.37
Fe(8)Ce	0.20	0.15	0.05	0.41
Co(2)Ce	0.16	0.12	0.08	0.36
Co(5)Ce	0.20	0.14	0.07	0.41
Co(8)Ce	0.22	0.14	0.07	0.43
Ni(2)Ce	0.16	0.12	0.07	0.35
Ni(5)Ce	0.15	0.13	0.08	0.36
Ni(8)Ce	0.17	0.13	0.10	0.38
Cu(2)Ce	0.10	0.08	0.07	0.25
Cu(5)Ce	0.14	0.07	0.07	0.28
Cu(8)Ce	0.14	0.08	0.06	0.28

Table 3.11 Acidity distribution of Ceria-zirconia based catalysts

Catalyst	Acidity Distribution (mmolg^{-1})			
	Weak	Medium	Strong	Total
	RT-200 (°C)	201-400 (°C)	401-600 (°C)	RT-600 (°C)
Zr	0.10	0.04	0.03	0.17
CeZr	0.15	0.05	0.04	0.24
Cr(2)Ce Zr	0.22	0.15	0.10	0.47
Cr(5)CeZr	0.24	0.16	0.12	0.52
Cr(8)CeZr	0.24	0.15	0.12	0.51
Mn(2)CeZr	0.21	0.17	0.08	0.46
Mn(5)CeZr	0.19	0.16	0.08	0.43
Mn(8)CeZr	0.24	0.10	0.10	0.44
Fe(2)CeZr	0.25	0.10	0.09	0.44
Fe(5)CeZr	0.24	0.09	0.09	0.42
Fe(8)CeZr	0.23	0.11	0.12	0.46
Co(2)CeZr	0.20	0.12	0.07	0.39
Co(5)CeZr	0.25	0.12	0.10	0.47
Co(8)CeZr	0.25	0.11	0.05	0.41
Ni(2)CeZr	0.21	0.11	0.09	0.39
Ni(5)CeZr	0.24	0.12	0.13	0.49
Ni(8)CeZr	0.18	0.11	0.07	0.36
Cu(2)CeZr	0.20	0.12	0.04	0.36
Cu(5)CeZr	0.19	0.12	0.06	0.37
Cu(8)CeZr	0.18	0.14	0.05	0.35

Ceria, being a basic oxide shows lowest acidity. On incorporation of metal there is enhancement in acidity. Transition metal incorporated ceria-zirconia systems show more acidity than ceria systems. It is generally agreed that the surface acidity of ceria catalyst is due to surface Ce^{4+} species and $OH^{\delta+}$ species[27]. The transition metal

modification results in more coordination unsaturated cations and these sites gave higher acidity. Ceria-zirconia mixed oxide had acidity greater than that of pure ceria and zirconia[52]. The incorporation of zirconia into ceria lattice modifies surface acidic properties due to exposed Ce^{4+} and Zr^{4+} ions. The zirconium ion radius is 0.84 Å smaller than that of the Ce^{4+} ion and it is likely to exhibit acidic nature in solid solutions[7]. On transition metal modification there is enhancement in acidity.

3.3.2 Thermodesorption studies of 2,6-dimethyl pyridine

It is reported that 2,6-dimethyl pyridine (2,6-DMP) adsorbs strongly on Bronsted acid sites and forms weak bonds with Lewis acid sites[53]. According to Satsuma et al.[54] the 2,6-DMP weakly bound to Lewis acid sites, get desorbed below 300°C. Hence the thermodesorption study of 2,6-DMP adsorbed beyond 300°C can give a measure of Bronsted acid sites. The results obtained for the thermodesorption of 2,6-DMP are given in Tables 3.12 and 3.13.

From the results it is clear that ceria possesses appreciably good Bronsted acidity. Metal modification results in enhancement in Bronsted acidity. Ceria-zirconia has got acidity less than pure ceria. Cobalt and iron modified ceria systems show comparatively high Bronsted acidity. Among ceria-zirconia systems, Cr, Fe and Co modified systems gave higher acidity values.

Table 3.12 Acidity measurement of ceria based catalysts by thermodesorption of 2,6-DMP

Catalyst	Amount of 2,6-DMP desorbed (mg)			
	Weak	Medium	Strong	Total
	300-400 (°C)	400-500 (°C)	500-600 (°C)	300-600 (°C)
Ce	0.27	0.08	0.01	0.36
Cr(2)Ce	0.38	0.06	0.06	0.5
Cr(5)Ce	0.40	0.12	0.01	0.53
Cr(8)Ce	0.42	0.15	0.02	0.59
Mn(2)Ce	0.29	0.11	0.04	0.43
Mn(2)Ce	0.38	0.12	0.02	0.52
Mn(2)Ce	0.41	0.09	0.04	0.54
Fe(2)Ce	0.37	0.09	0.04	0.51
Fe(5)Ce	0.40	0.17	0.01	0.58
Fe(8)Ce	0.36	0.41	0.05	0.83
Co(2)Ce	0.43	0.09	0.01	0.53
Co(5)Ce	0.35	0.22	0.01	0.58
Co(8)Ce	0.63	0.22	0.07	0.92
Ni(2)Ce	0.32	0.12	0.00	0.44
Ni(5)Ce	0.30	0.10	0.01	0.40
Ni(8)Ce	0.40	0.41	0.10	0.91
Cu(2)Ce	0.25	0.05	0.02	0.32
Cu(5)Ce	0.29	0.04	0.02	0.35
Cu(8)Ce	0.30	0.04	0.03	0..37

Table 3.13 Acidity measurement of ceria-zirconia based catalysts by thermodesorption of 2,6-DMP

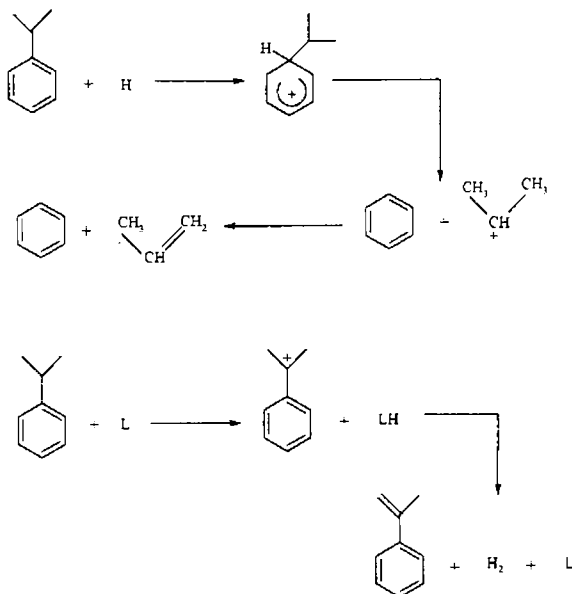| Catalyst	Amount of 2,6-DMP desorbed			
	Weak	Medium	Strong	Total
	300-400 (°C)	400-500 (°C)	500-600 (°C)	300-600 (°C)
Zr	0.11	0.1	0.07	0.28
CeZr	0.19	0.08	0.05	0.32
Cr(2)Ce Zr	0.34	0.36	0.08	0.78
Cr(5)CeZr	0.37	0.40	0.07	0.84
Cr(8)CeZr	0.50	0.35	0.09	0.94
Mn(2)CeZr	0.30	0.15	0.07	0.52
Mn(5)CeZr	0.33	0.16	0.09	0.58
Mn(8)CeZr	0.33	0.17	0.08	0.59
Fe(2)CeZr	0.28	0.13	0.03	0.44
Fe(5)CeZr	0.26	0.11	0.01	0.38
Fe(8)CeZr	0.24	0.46	0.08	0.78
Co(2)CeZr	0.38	0.38	0.07	0.82
Co(5)CeZr	0.36	0.37	0.07	0.8
Co(8)CeZr	0.38	0.20	11.0	0.69
Ni(2)CeZr	0.30	0.12	0.05	0.47
Ni(5)CeZr	0.29	0.11	0.05	0.45
Ni(8)CeZr	0.39	0.20	0.11	0.70
Cu(2)CeZr	0.30	0.16	0.04	0.50
Cu(5)CeZr	0.25	0.11	0.06	0.42
Cu(8)CeZr	0.27	0.12	0.06	0.45

3.3.3 Cumene Cracking

The conversion of cumene is a model reaction for identifying the Lewis/Bronsted acid site ratio of a catalyst: cumene is cracked to benzene and propene over Bronsted acid sites, whereas dehydrogenation to α-methylstyrene occurs over Lewis acid sites (Scheme 3.1). The relative amounts of benzene and α-methylstyrene in the product mixture can therefore be a good indication of the types of acidities possessed by catalyst [55]. Mechanism for cumene conversion may be represented as in Scheme 3.2.

α-methylstyrene

Major Products

Cumene

Benzene

Toluene   Ethylbenzene   Styrene

Minor Products
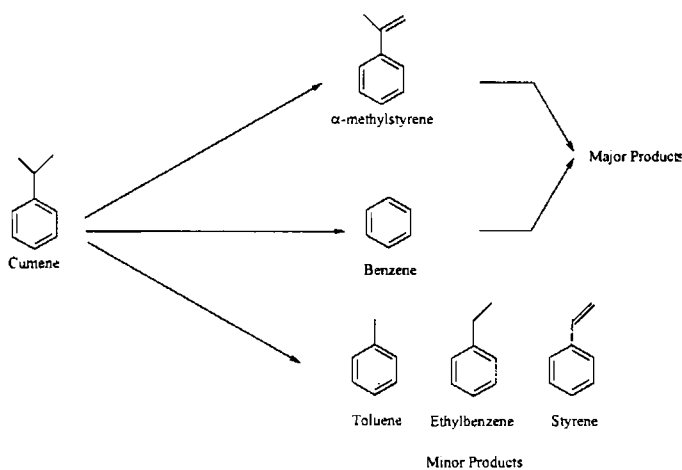
Scheme 3.1 Cumene cracking

Scheme 3.2 Mechanism of cumene cracking

3.3.3.1 Influence of Reaction conditions

3.3.3.1.1 Effect of Temperature

On increasing reaction temperature from 350 to 500°C there is considerable increase in cumene conversion. α-methyl styrene selectivity decreases at high temperature due to the formation of styrene at high temperatures. Benzene selectivity remains more or less same through out the temperature studied.
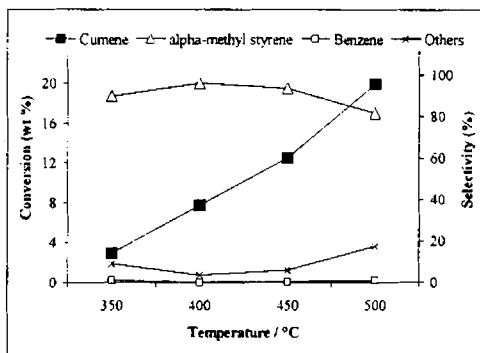
Reaction conditions:- Co(5)CeZr-0.5g, Flow rate-4mLh^{-1},

Time-2h.

Figure 3.22 Effect of temperature on cumene cracking

3.3.3.1.2 Effect of Flow rate

As the flow rate increases from 2 to 6mL there is decrease in cumene conversion due to the decrease in contact time between cumene and catalyst surface. α-methyl styrene selectivity increased first and then remains constant.
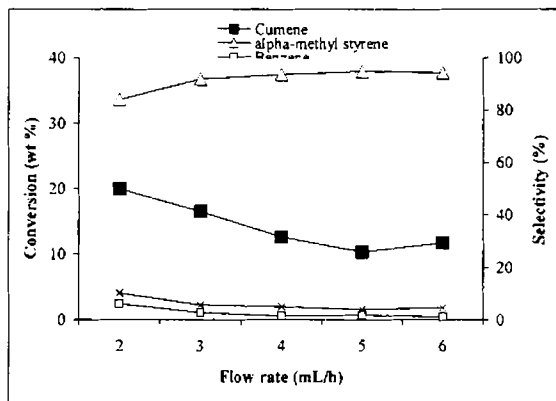
Reaction conditions:- Co(5)CeZr-0.5g, Temperature-450°C, Time-2h.

Figure 3.23 Effect of flow rate on cumene cracking

3.3.3.1.3 Effect of Time-Deactivation

The catalysts were tested towards deactivation by conducting the experiment for 8h. It is found that compared to pure ceria and zirconia, the rate of deactivation is less for ceria-zirconia mixed oxide catalyst (Figure 3.24). Time on stream profiles of representative transition metal modified ceria and ceria-zirconia catalysts are given in Figure 3.25. Chromium modified systems show comparatively less deactivation. Ni and Cu systems show very fast deactivation.
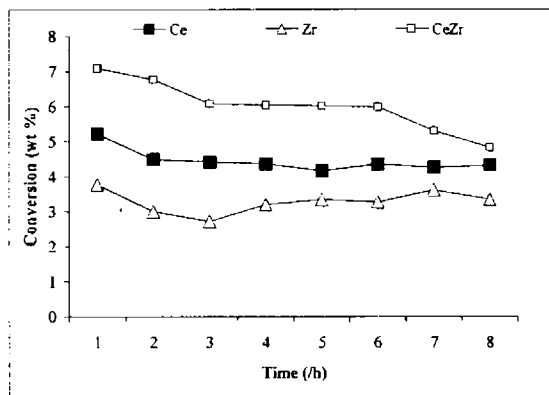
Reaction conditions:- Temperature-450°C, Flow rate-3mLh^{-1}.

Figure 3.24 Effect of time on cumene cracking
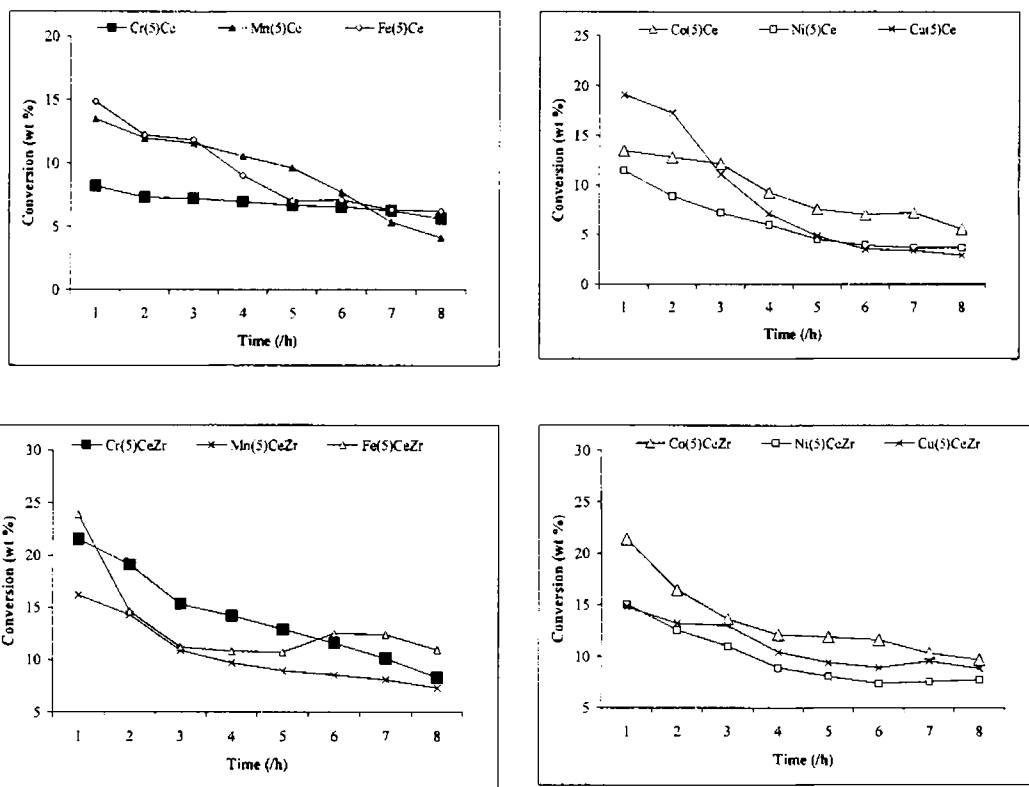
Reaction conditions:- Temperature-450°C, Flow rate-3mLh^{-1}

Figure 3.25 Effect of time on cumene cracking for representative catalysts

3.3.3.2 Comparison of Catalysts

Cumene cracking reaction was carried out using all the prepared catalysts at a temperature of 450°C, flow rate of 3mLh^{-1} and time on stream of 2h. The results of cumene cracking over transition metal modified ceria and ceria-zirconia catalysts are given in Tables 3.14 and 3.15. On metal modification both the ceria and ceria-zirconia catalysts show increase in conversion. α-methyl styrene selectivity is about 90% which indicate the presence of Lewis acid sites on the catalyst surface.

Table 3.14 Cumene cracking over metal modified ceria catalysts

Catalyst	Conversion (wt.%)	Selectivity (%)		
		α-methyl styrene	Benzene	Others
Ce	4.5	87.3	7.2	5.6
Cr(2)Ce	9.2	93.4	2.7	3.9
Cr(5)Ce	11.2	94.3	1.9	3.8
Cr(8)Ce	14.5	96	1.2	2.8
Mn(2)Ce	11.3	91.2	1.4	7.4
Mn(5)Ce	12	92.7	1.5	5.8
Mn(8)Ce	14.2	94.2	2.5	3.3
Fe(2)Ce	10.8	93.6	2.9	3.5
Fe(5)Ce	12.2	93.9	1.9	4.3
Fe(8)Ce	14.9	88.9	2.8	8.4
Co(2)Ce	10.3	88.7	4.3	6.9
Co(5)Ce	12.8	92.7	2.8	4.5
Co(8)Ce	15.8	90.8	3.0	6.2
Ni(2)Ce	10.5	92.8	2.1	5.1
Ni(5)Ce	8.9	91.9	4.6	3.5
Ni(8)Ce	12.9	94.2	2.7	3.1
Cu(2)Ce	8.6	89.3	2.8	7.9
Cu(5)Ce	10.2	91.5	2.9	5.6
Cu(8)Ce	12.1	90.9	2.1	6.9

Table 3.15 Cumene cracking over metal modified ceria-zirconia catalysts

Catalyst	Conversion (wt.%)	Selectivity (%)		
		α-methyl styrene	Benzene	Others
Zr	3.0	86.5	7.3	6.2
CeZr	6.0	80.3	15.3	4.3
Cr(2)CeZr	16.2	94.3	2.3	3.6
Cr(5)CeZr	19.1	92.6	3.4	4.0
Cr(8)CeZr	17.5	92.5	2.6	4.9
Mn(2)CeZr	16.2	88.3	7.6	4.1
Mn(5)CeZr	14.3	89.9	4.4	5.8
Mn(8)CeZr	15.3	87.5	8.9	3.6
Fe(2)CeZr	15.1	92.6	1.7	5.7
Fe(5)CeZr	14.6	92.1	1.6	6.3
Fe(8)CeZr	15.5	89.8	3.6	6.7
Co(2)CeZr	12.8	94.4	1.6	4.0
Co(5)CeZr	16.5	91.9	2.6	5.6
Co(8)CeZr	16.1	91.1	4.3	4.7
Ni(2)CeZr	14.1	93.3	2.5	4.2
Ni(5)CeZr	18.8	92.5	3.0	4.5
Ni(8)CeZr	12.6	88.0	6.4	5.7
Cu(2)CeZr	11.6	93.3	2.1	4.6
Cu(5)CeZr	13.2	93.2	2.4	4.4
Cu(8)CeZr	11.6	91.7	3.5	4.9

Cumene conversion and total acidity from ammonia TPD measurements show good correlation, which confirms the acidity results obtained from desorption measurements (Figure 3.26).
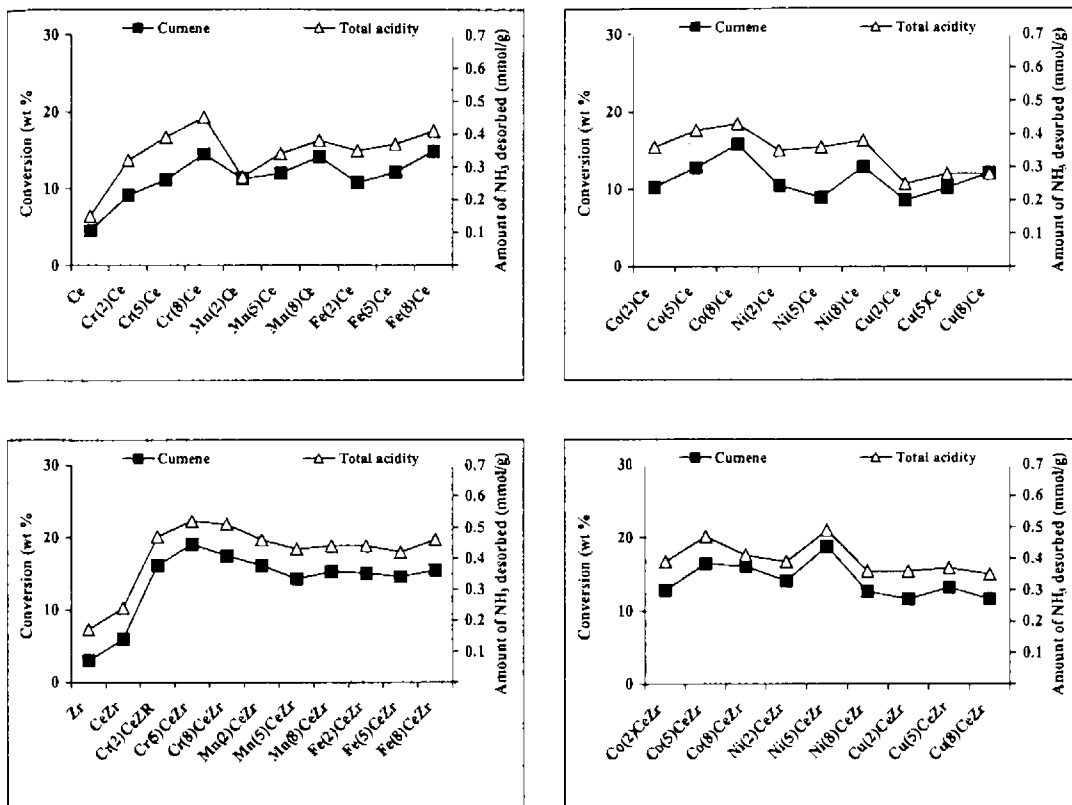
Figure 3.26 Cumene cracking vs total acidity

3.3.4 Cyclohexanol Decomposition

Alcohol decomposition reaction has been widely studied because it is a simple model reaction to determine the functionality of an oxide catalyst. Dehydration activity is linked to the acidic property and dehydrogenation activity to the combined effect of both acidic and basic properties of the catalyst. The general scheme for cyclohexanol decomposition is given in Scheme 3.3. A proposed mechanism for the decomposition of cyclohexanol is depicted in Scheme 3.4.
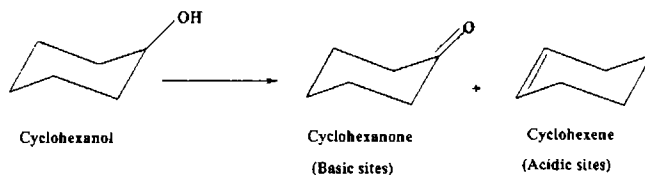
Scheme 3.3 Cyclohexanol decomposition
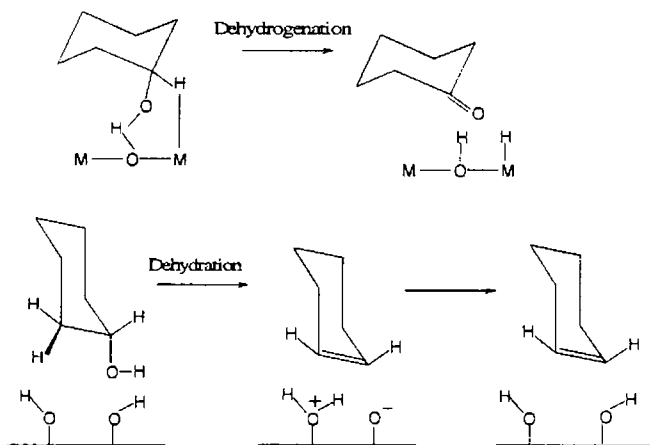
Scheme 3.4 Mechanism of cyclohexanol decomposition

3.3.4.1 Influence of Reaction conditions

3.3.4.1.1 Effect of Temperature

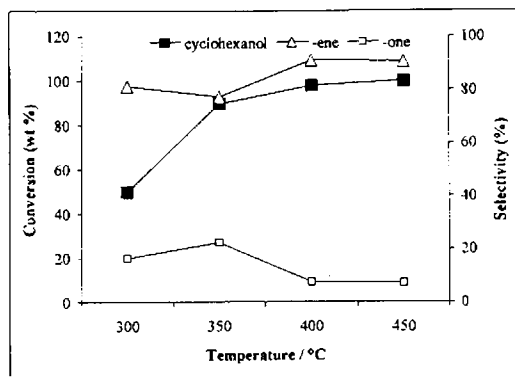The results obtained in the decomposition of cyclohexanol at various temperatures are represented in Figure 3.27. Cyclohexanol conversion increased with increase in temperature. The conversion reached a maximum of 99% at 450°C. Cyclohexene selectivity shows an increase with increase in temperature.

Reaction conditions:- Ni(8)Ce-0.5g, Flow rate-4mLh⁻¹, Time-2h.

Figure 3.27 Effect of temperature on cyclohexanol decomposition

3.3.4.1.2 Effect of Flow rate

Figure 3.28 illustrates the effect of flow rate on cyclohexanol conversion and selectivity. Initially, there is an increase in conversion as the flow rate increased from 3 to 4mL. Thereafter the conversion decreased with increase in flow rate. Cyclohexene selectivity increases with increase in the flow rate.
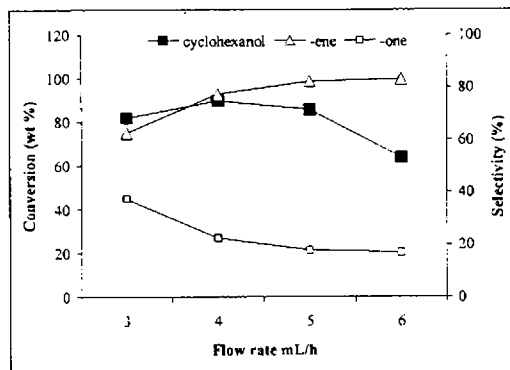
Reaction conditions:- Ni(8)Ce-0.5g, Temperature- 350°C, Time-2h.

Figure 3.28 Effect of flow rate on cyclohexanol decomposition

3.3.4.2 Comparison of Catalysts

The cyclohexanol decomposition activity of the prepared catalysts was carried out at a temperature of 350°C and flow rate of 4mLh^{-1}. Cyclohexanol conversion and selectivity are given in Tables 3.16 and 3.17.

Table 3.16 Cyclohexanol decomposition over ceria based catalysts

Catalyst	Conversion (wt.%)	Selectivity (%)	
		-ene	-one
Ce	74.7	92.9	6.1
Cr(2)Ce	90.2	87.2	12.1
Cr(5)Ce	93.1	89.8	10.2
Cr(8)Ce	97.9	93.2	6.6
Mn(2)Ce	82.3	91.3	9.2
Mn(5)Ce	89.2	94.1	5.8
Mn(8)Ce	84.3	93.2	6.1
Fe(2)Ce	76.3	87.5	12.2
Fe(5)Ce	79.5	87.6	11.6
Fe(8)Ce	84.4	85.7	14.3
Co(2)Ce	81.9	85.4	14.6
Co(5)Ce	84.3	79.9	20.0
Co(8)Ce	92.6	76.6	23.3
Ni(2)Ce	97.2	89.8	8.8
Ni(5)Ce	95.3	93.9	6.0
Ni(8)Ce	94.3	77.2	18.5
Cu(2)Ce	84.3	96.3	2.5
Cu(5)Ce	90.1	96.3	3.7
Cu(8)Ce	90.2	86.7	5.9

Table 3.17 Cyclohexanol decomposition over
ceria-zirconia based catalysts

Catalyst	Conversion (wt.%)	Selectivity (%)	
		-ene	-one
Zr	75.5	98.1	1.9
CeZr	86.6	96.7	3.3
Cr(2)CeZr	96.2	94.2	5.6
Cr(5)CeZr	98.9	93.1	6.7
Cr(8)CeZr	92.3	89.2	9.7
Mn(2)CeZr	89.3	94.2	5.5
Mn(5)CeZr	90.4	96.2	3.7
Mn(8)CeZr	88.3	98.3	1.3
Fe(2)CeZr	85.8	93.4	6.5
Fe(5)CeZr	91.2	96.8	3.2
Fe(8)CeZr	93.2	80.4	19.3
Co(2)CeZr	90.2	93.0	9.0
Co(5)CeZv	94.3	95.3	4.7
Co(8)CeZr	89.3	82.6	19.8
Ni(2)CeZr	82.3	98.2	1.6
Ni(5)CeZr	85.4	90.6	5.9
Ni(8)CeZr	92.6	81.3	17.7
Cu(2)CeZr	83.4	99.1	0.9
Cu(5)CeZr	76.3	94.6	5.3
Cu(8)CeZr	80.3	96.7	3.2

On transition metal modification, there is enhancement in cyclohexanol conversion for both ceria and ceria-zirconia catalysts. The metal content plays an important role in cyclohexanol decomposition reaction.

Cyclohexanol decomposition activity of the prepared catalysts was correlated with the weak and medium acid centres on the catalyst surface (Figure 3.29).

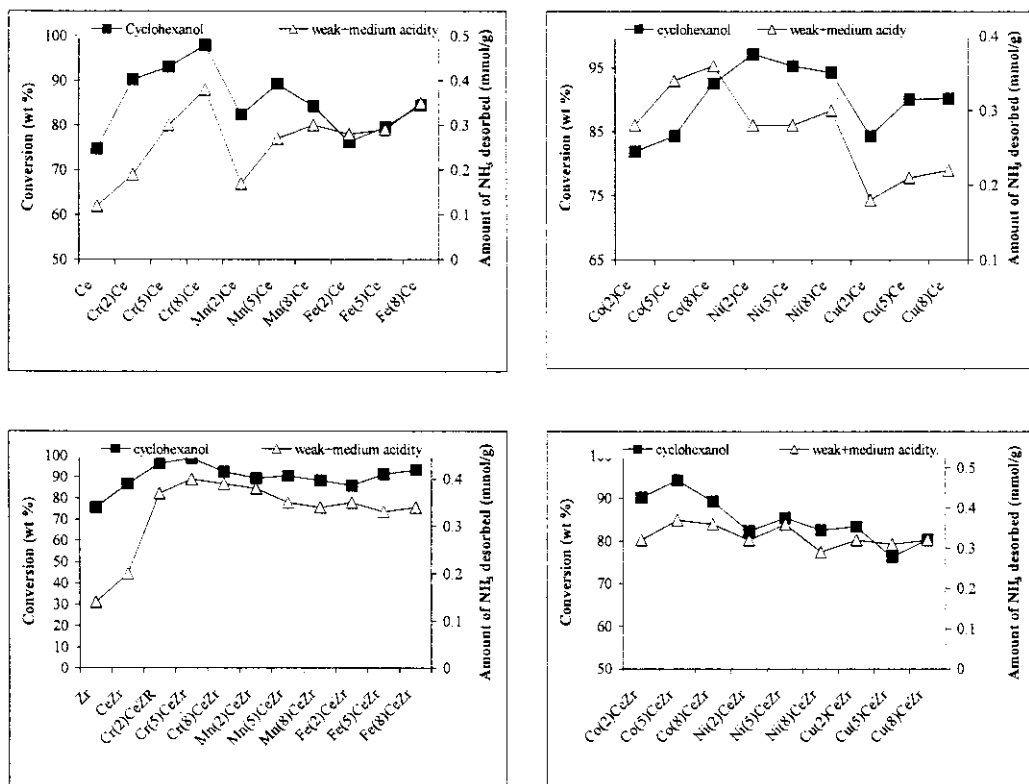**Figure 3.29** Cyclohexanol conversion vs weak+medium acidity

3.4 Conclusions

The powder X-ray diffraction analyses confirm the fluorite structure of transition metal modified ceria and ceria-zirconia mixed oxides. The composition of the catalyst obtained from the EDX analysis is close to the theoretical value. From the BET surface area results it can be proposed that the surface area of doped ceria

catalysts strongly depend on the nature and loading of the promoter. Unlike that of impregnation method, the plugging of pores is not evident for Cr, Mn and Fe modified systems. The sol-gel method is effective for the preparation of supported metal catalysts since it produces homogenous materials with highly dispersed metals on the support. From the TGA/DTA profiles of the representative catalysts, it is clear that the weight loss due to dehydration and decomposition of the residual organics and nitrates is complete below 450°C. Hence the catalysts which are calcined at 500°C contain only metal oxides without any impurity. Up to 800°C no further weight loss is observed which confirms the thermal stability of prepared catalysts. From the DR UV-vis spectra information on surface coordination and different oxidation state of transition metal ions incorporated can be obtained. In Raman spectra, the Ceria-zirconia mixed oxides shows only one peak at 483cm^{-1} characteristic of cubic fluorite-like structure. EPR spectra revealed the presence of extra oxygen vacancies in ceria-zirconia catalyst. The various oxidation states of the incorporated metal ions could be obtained from the EPR analysis. TPD of NH$_3$ and thermogravimetric desorption of 2,6-DMP measurements confirms the enhancement of surface acidity upon modification with transition metals. Activity towards cumene cracking could be correlated to total acidity obtained from ammonia TPD. A relation between cyclohexanol decomposition and weak+medium acidity from ammonia TPD is established.

References

[1]   S. Sato, K. Koizumi, F. Nozaki, J. Catal. 178 (1998) 264.

[2]   I. Ferino, M. F. Casula, A. Corrias, M. G. Cutrufello, R. Monaci, G. Paschina, Phys. Chem. Chem. Phys. 2 (2000) 1847.

[3]   Y. Wang, R. A. Caruso, J. Mater. Chem. 12 (2002) 1442.

[4]   A. S. Deshpande, N. Pinna, P. Beato, M. Antonietti, M. Niederberger, Chem.

Mater. 16 (2004) 2599.

[5]   A. Martinez-Arias, M. Fernandez-Garcia, V. Ballesteros, L. N. Salamanca, J. C. Conesa, C. Otero, J. Soria, Langmuir 15 (1999) 4796.

[6]   Vincente Sanchez Escribano, Enrique Fernandez Lopez, Marta Panizza, Carlo Resini, Jose Manuel Gallardo Amores, Guido Busca, Solid State Sciences, 5 (2003) 1369.

[7]   G. Ranga Rao, H. Ranjan Sahu, Proc. Indian. Acad. Sci. (Chem. Sci.), 113 (2001) 651.

[8]   V. Solinas, E. Rombi, I. Ferino, M. G. Cutrufello, G. Colon, J. A. Navio, J. Mol. Catal., A: Chem. 204-205 (2003) 629.

[9]   R. P. Viswanath, P. Wilson, Appl. Catal. A: Gen. 201 (2000) 23.

[10]   P. G. Harrison, W. Daniell, Chem. Mater. 13 (2001) 1708.

[11]   G. Qi, R. T. Yang, J. Phys. Chem. B 108 (2004) 15738.

[12]   M. Machida, M. Uto, D. Kurogi, T. Kijima, Chem. Mater. 12 (2000) 3158.

[13]   T. Akashi, S. Sato, R. Takahashi, T. Sodesawa, K. Inui, Catal. Commun. 4 (2003) 411.

[14]   G. Neri, A. Pistone, C. Milone, S. Galvagno, Appl. Catal. B: Env. 38 (2002) 321.

[15]   M Kraum, M. Baerns, Appl. Catal. A 186 (1999) 189.

[16]   Y. Li, Q. Fu, M. Flytzani-Stephanopoulos, Appl. Catal. B 27 (2000) 179.

[17]   Y. Hu, L. Dong, J. Wang, W. Ding, Y. Chen, J. Mol. Catal. A: Chem. 162 (2000) 307.

[18]   S. Sato, R. Takahashi, T. Sodesawa, N. Honda, H. Shimizu, Catal. Commun. 4 (2003) 77-81.

[19]   Ching-Huei Wang, Shiow-Shyung Lin, Appl. Catal. A 268 (2004) 227.

[20]   B. Skarman, T. Nakayama, D. Grandjean, R. E. Benfield, E. Olsson, K. Nihara, L. R. Wallenberg, Chem. Mater. 14 (2002) 3686.

[21] D. Srinivas, C. V. V. Satyanarayana, H. S. Potdar, P. Ratnasamy, Appl. Catal. A: Chem. 246 (2003) 323.

[22] Y. Wang, R. A. Caruso, J. Mater. Chem. 12 (2002) 1442.

[23] H. Zou, Y. S. Lin, N. Rane, T. He, Ind. Eng. Chem. Res. 43 (2004) 3019.

[24] N. Rane, H. Zou, G. Buelna, Jerry Y. S. Lin, J. Membr. Sci. 256 (2005) 89.

[25] J. Zhao, W. Fan, D. Wu, Y. Sun, J. Non-Cryst. Solids, 261 (2000) 15.

[26] S. Rossignol, F. Gerard, D. Duprez, J. Mater. Chem. 9 (1999) 1615.

[27] B. J. Mishra, G. Ranga Rao, J. Mol. Catal. A: Chem. 243 (2005) 204.

[28] R. Brayner, D. Ciuparu, G. M. da Cruz, F. F. Vincent, F. Bozon-Verduraz, Catal. Today 57 (2000) 261.

[29] L. Huiyun, Y. Yinghong, M. Changxi, X. Zaiku, H. Weiming, G. Zi, Chin. J. Catal. 27 (2006) 4.

[30] B. M. Weckhuysen, A. A. Verberckmoes, A. R. De Baets, R. A. Schoonheydt, J. Catal. 166 (1997) 160.

[31] P. Kustrowski, L. Chmielarz, R. Dziembaj, P. Cool, E. F. Vasant, J. Phys. Chem. A 109 (2005) 330.

[32] S. Khaddar-Zine, A. Ghorbel, C. Naccache, J. Mol. Catal. A: Chem. 150 (1999) 223.

[33] S. Vetrivel, A. Pandurangan, J. Mol. Catal. A: Chem. 217 (2004) 165.

[34] S. Velu, N. Shah, T. M. Jyothi, S. Sivasanker, Microporous Mesoporous Mater. 33 (1999) 61.

[35] K. Bachari, J. M. M. Millet, B. Benaichouba, O. Cherifi, F. Figueras, J. Catal. 221 (2004) 55.

[36] Nan-Chun Wu, Er-Wei Shi, Yan-Qing Zheng, Wen-Jun Li, J. Am. Ceram. Soc., 85, 2462-68 (2002).

[37] T. Radhika, S. Sugunan, J. Mol. Catal. A: Chem. 250 (2006) 169.

[38] B. M. Weckhuysen, R. A. Schoonheydt, F. E. Mabbs, D. J. Collison, J. Chem. Soc., Faraday Trans. 92 (1996) 2431.

[39] B. M. Weckhuysen, L. M. De Ridder, P. J. Grobert, R. A. Schoonheydt, J. Phys. Chem. 99 (1995) 320.

[40] R. J. Spitz, J. Catal. 35 (1974) 345.

[41] S. Vetrivel, A. Pandurangan, Ind. Eng. Chem. Res. 44 (2005) 692.

[42] S. Imamura, M. Nakamura, N. Kawabata, J. Yoshida, Ind. Eng. Chem. Prod. Res. Dev. 25 (1986) 34.

[43] W. S. Kijlstra, E. K. Poels, A. Bliek, B. M. Weckhuysen, R. A. Schoonheydt, J. Phys. Chem. B 101 (1997) 309.

[44] C. Decarne, E. Abi-Aad, B. G. Kostyuk, V. V. Lunin, A. Aboukais, J. Mater. Sci. 39 (2004) 3249.

[45] M. Fernandez-Garcia, E. G. Rebollo, A. G. Ruiz, J. C. Conesa, J. Soria, J.Catal. 172 (1997) 146.

[46] P. G. Harrison, I. K. Ball, W. Azelee, W. Daniell, D. Goldfarb, Chem. Mater. 12 (2000) 3715.

[47] Ta-Jen Huang, Yung-Chien Kung, Catalysis Lett. 85 (2003) 51.

[48] G. R. Rao, H. R. Sahu, B. J. Mishra, Colloids and Surfaces A: Physicochem. Eng. Aspects 220 (2003) 261.

[49] A. Aboukais, A. Bennani, C. Lamonier-Dulongpont, E. Abi-Aad, G. Wrobel, Colloids Surf. A, 155 (1996) 171.

[50] E. Mamontov, T. Egami, R. Brezny, M. Koranne, S. Tyagi J. Phys. Chem. B 104 (2000) 11110.

[51] K. Tanabe, T. Yamaguchi, Catal. Today 20 (1994) 185.

[52] K. Tomishige, H. Yasuda, Y. Yoshida, M. Nurunnabi, B. Li, K. Kunimori, Green Chem. 6 (2004) 206.

[53] P. A. Jacobs, C. F. Heylen, J. Catal. 34 (1974) 2.

[54] A. Satsuma, Y. Kamiya, Y. Westi, T. Hattori, Appl. Catal. 194-195 (2000) 253.

[55] S. M. Bradley, R. A. Kydd, J. Catal. 141 (1993) 239.

CHAPTER 4

OXIDATION OF ETHYLBENZENE

Abstract

Side-chain oxidation of alkyl aromatics using cleaner peroxide oxidants catalyzed by heterogeneous catalysts still attracts interests. Classical synthetic laboratory procedures preferably use stoichiometric oxidants such as permanganate and dichromate which are hazardous. Hence, there has been an interest to develop ecofriendly catalysts for the oxidation of alkyl aromatics. Heterogeneous catalysts have the advantage, compared to their homogeneous counterparts, of facile recovering and recycling. The present chapter deals with liquid phase oxidation of ethylbenzene with tert-butyl hydroperoxide over the prepared catalysts. Influence of various reaction parameters was studied. Cr and Mn modified catalysts gave good ethylbenzene conversion and acetophenone selectivity.

4.1 Introduction

Effective utilization of ethylbenzene, available in the xylene stream of the petrochemical industry for more value added products, is an interesting proposition. Oxidation of ethylbenzene to the different products can take place in two ways. One is the aromatic ring hydroxylation under which the hydroxylation at the *para*-positon is preferred to some extent to the *ortho*-position. The other is the side chain oxidation at primary and secondary carbon atoms. The primary and secondary carbinols formed from the side chain oxidation undergo further oxidation to the respective aldehydes and ketones. The pathways of ethylbenzene oxidation are represented in Scheme 4.1. The side chain oxidation at the secondary carbon predominates over the primary carbon. Acetophenone is one of the key products in the industries. It is used as a component of perfumes and as an intermediate for the manufacture of pharmaceuticals, resins, alcohols, and tear gas (chloroacetophenone).

Wang et al.[1] reported that the polymer supported 4-(2-pyridylazo) resorcinol copper complex is an effective catalyst for the oxidation of ethylbenzene by molecular oxygen. The main products were 1-phenyl ethanol and acetophenone. Mn-MCM41 molecular sieves were found to be active for the oxidation of ethylbenzene with tert-butyl hydroperoxide in liquid phase and with air in vapor phase[2-4]. Choudhary et al.[5] were showed that a stoichiometric $KMnO_4$ reagent, commonly employed for oxidations, can be transformed into a highly active, stable, easily separable, and reusable environmental friendly catalysts for the oxidation of ethylbenzene to acetophenone or similar reactions by immobilizing MnO_4^{1-} anions in highly basic Mg-Al-hydrotalcite at its anion-exchange sites and the activity could be improved by optimizing the catalyst composition parameters.
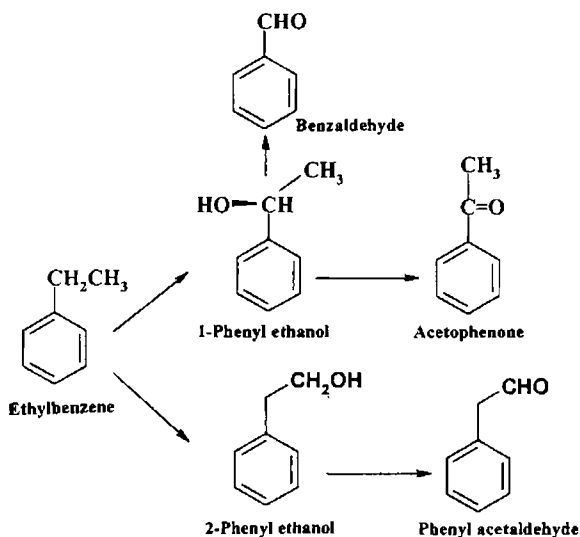
Scheme 4.1 Oxidation of Ethylbenzene

Ti-, V- and Sn- containing silicates are found to give acetophenone and 1-phenyl ethanol as major products and ring hydroxylated aromatics as minor products[6]. The "neat" and zeolite Y-encapsulated copper tri- and tetraza macrocyclic complexes exhibit efficient catalytic activity in the regioselective oxidation of ethylbenzene using TBHP[7]. Framework substituted MeAPO-11s are found to be active for ethylbenzene oxidation[8]. Alumina-supported vanadia catalysts favor the formation of acetophenone and benzaldehyde[9]. Baek et al.[10] investigated the promotional effect of CO_2 in the liquid phase oxidation of ethylbenzene to acetophenone with Co/Mn/Br catalyst system. CO_2 assisted oxidation resulted in an enhancement in ethylbenzene conversion and high acetophenone selectivity. Oxidation of ethylbenzene with air catalyzed by μ-oxo dimeric metalloporphyrins yields acetophenone and 1-phenylethanol[11]. Cobalt containing silicate was found to be especially active and selective for the oxidation of alkyl aromatics with TBHP[12]. Muzart et al.[13] studied the chromium (VI) oxide catalyzed oxidations of alcohols and activated methylenes by

aqueous tert-butyl hydroxide using benzotrifluoride as solvent. The oxidation of alkylaromatics with hydrogen peroxide in the presence of several manganese (III) porphyrins was studied, under mild conditions using ammonium acetate as co-catalyst[14]. Torbio et al.[15] used barium compounds as catalyst for liquid-phase oxidation of ethylbenzene with molecular oxygen yielding ethylbenzene hydroperoxide as the major product with small amounts of acetophenone and 1-phenylethanol.

Ethylbenzene oxidation was conducted in a 50mL glass round bottom flask placed in a thermostated oil bath fitted with a magnetic stirrer and water cooled condenser. In a typical oxidation, required quantity of ethyl benzene, solvent and catalyst were taken in the R. B flask and after attaining the reaction temperature tertiary butyl hydroperoxide was added in drops. The products were identified by GC-MS and conversion and product selectivity were monitored using a Chemito 8610 GC with FID detector and SE-30 column.
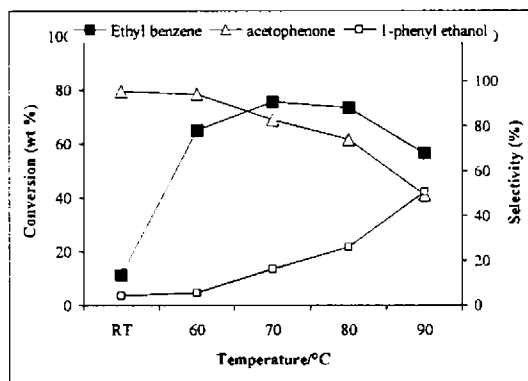
4.2 Influence of Reaction conditions

4.2.1 Effect of Oxidant

Oxidation of ethylbenzene was conducted using *tert*-butyl hydroperoxide (TBHP) and hydrogen peroxide (H_2O_2) as oxidants. No conversion was observed in presence of H_2O_2. According to Sheldon et al.[16] metal ions which catalyze oxygen transfer reactions with H_2O_2 or RO_2H are divided into two types based on the active intermediate: a peroxometal or an oxometal complex. Transition elements with d^0 configuration, like Mo(VI), W(VI), V(V), Ti(IV) follow peroxometal pathways and late or first row transition metals like Cr(VI), V(V), Mn(V), Ru(VI), Ru(VIII), Os(VIII) employ oxometal pathways. The prepared catalysts contain elements from first row transition metals and they are likely to follow oxometal pathway with TBHP as oxidant.

4.2.2 Effect of Temperature

Ethylbenzene conversion is investigated as a function of temperature at room temperature, 60, 70, 80 and 90°C and the results are s given in Figure 4.1. With the increasing of the temperature form RT to 70°C, the conversion was increasing, but when the temperature increased from 70 to 90°C, the conversion was decreasing continuously. Conversion and acetophenone selectivity at 70°C is found to be more as compared to that at 60°C. This increase is attributed to the higher activation of TBHP at 70°C. Further increase in temperature causes decrease in ethylbenzene conversion and 1-phenyl ethanol selectivity which can be explained as due to the decomposition of t-butylhydroperoxide[2].
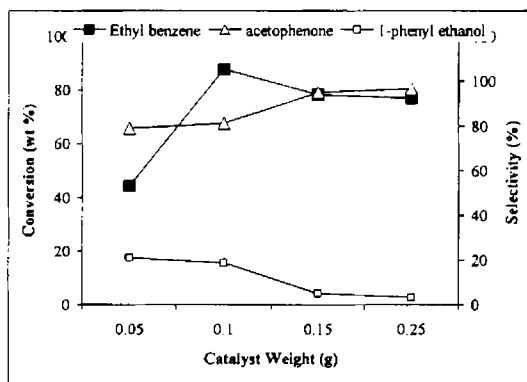

Reaction conditions:- Cr(5)CeZr- 0.1g, Acetonitrile- 10mL,

EB:TBHP- 1:3, Time- 12h.

Figure 4.1 Effect of temperature on ethylbenzene oxidation

4.2.3 Effect of Catalyst weight

The results of oxidation of ethyl benzene in the presence of various amount of catalyst are represented in Figure 4.2. When the amount of catalyst increased from 0.05 to 0.1g, the conversion increased from 44 to 84%. Further increase in catalyst

amount decreases conversion and then remains constant. This result is in agreement with that reported by Wang et al.[1]. They concluded that the amount of catalyst has the best quantity when the amount of substrate is fixed. Otherwise, on increasing or decreasing the amount of catalyst, the conversion of the substrate decreases. A similar observation is found in the case of ethylbenzene autoxidation in the presence of variable amounts of barium oxide[15].
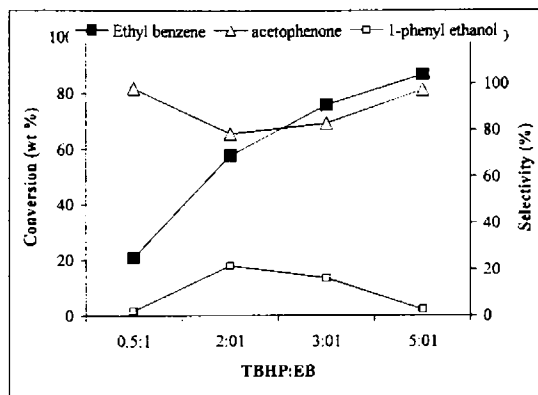

Reaction conditions:- Cr(5)CeZr, Acetonitrile- 10mL,
EB:TBHP- 1:3, Temperature- 70°C, Time- 12h

Figure 4.2 Effect of catalyst weight on ethylbenzene oxidation

4.2.4 Effect of Ethylbenzene to TBHP mole ratio

Effect of reactant to oxidant mole ratio on conversion and product selectivity is studied and the results are given in Figure 4.3. The ratios were changed by keeping the amount of ethylbenzene constant. The conversion raised from 20 to 86 wt% as the TBHP/EB ratio increased from 0.5 to 5. The selectivity to acetophenone is increased with the increase in molar ratio.
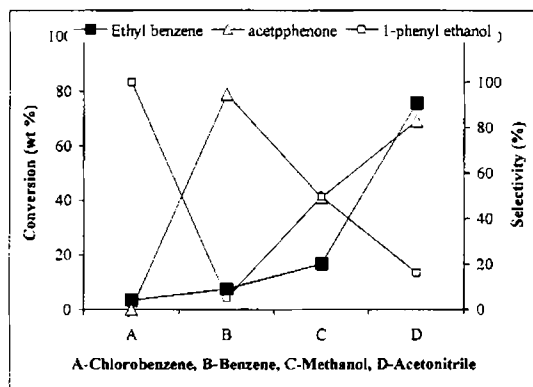
Reaction conditions:- Cr(5)CeZr- 0.1g, Acetonitrile-10mL,

Temperature- 70°C, Time-12h.

Figure 4.3 Effect of EB:TBHP ratio on ethylbenzene oxidation

4.2.5 Effect of Solvent

The effect of various solvents such as chlorobenzene, benzene, acetonitrile and methanol used in the oxidation of ethylbenzene is illustrated in Figure 4.4. The role of solvent on the reaction is very complex, especially on product distribution. Chlorobenzene has a negative influence on the reaction. Acetonitrile is found to be the best solvent. Kishore Mal et al.[6] studied the influence of various solvents for ethylbenzene oxidation. They also found acetonitrile and water as the best solvents compared to acetone and tert-butanol, the reasons for the observation being unclear. Bhoware et al.[17] investigated the role of solvent in the oxidation of ethylbenzene over Co-HMS catalysts. Among a series of solvents like acetonitrile, dichloromethane, acetone and ethyl alcohol, acetonitrile is found to give high conversion. Belifa et al.[18] observed that the presence of polar solvent makes the vanadia-titania catalyst more active for cyclohexane oxidation, due to the efficient removal of oxidation products from the active sites of the catalysts by the polar solvent. It is reported that an

increase in solvent polarity brought about an enhanced rate of toluene oxidation and a better selectivity for benzoic acid[19].

Reaction conditions:- Cr(5)CeZr-0.1g, Solvent-10mL,
Temperature- 70°C, EB:TBHP- 1:3.

Figure 4.4 Effect of solvent on ethylbenzene oxidation

4.2.6 Effect of Solvent volume

The influence of solvent volume in ethylbenzene oxidation is investigated and the findings are presented in Figure 4.5. Appreciably high ethylbenzene conversion and acetophenone selectivity is obtained in the absence of solvent. When the reaction is conducted in presence of solvent (with low solvent volume), ethylbenzene conversion is increased to 87%. But on increasing solvent volume, conversion decreases suggesting that there is an optimum solvent concentration for maximum conversion. For Co-HMS catalyst, it is reported that when solvents are used for the oxidation of ethylbenzene, the conversions are less and interestingly, the maximum conversion was obtained in the absence of solvent. It is suggested that solvent had negative influence over the performance of cobalt containing catalyst, which may possibly arise from the blocking of the active catalytic sites by the solvent molecules[17].
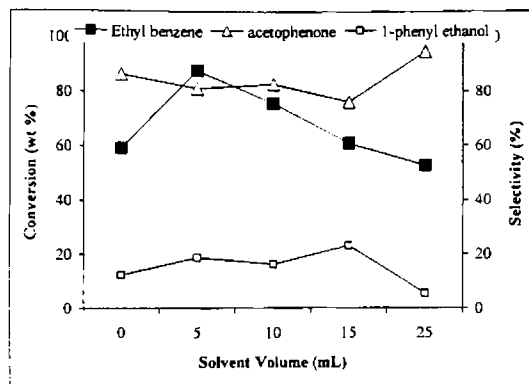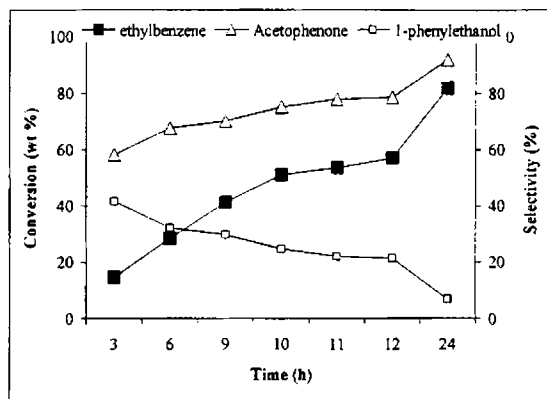
Reaction conditions:- Cr(5)CeZr- 0.1g, Solvent-Acetonitrile,

Temperature- 70°C, EB:TBHP- 1:3, Time- 12h.

Figure 4.5 Effect of solvent volume on ethylbenzene oxidation

4.2.7 Effect of Time

Figure 4.6 shows the results of oxidation of ethylbenzene with TBHP with respect to reaction time at 70°C. Selective formation of acetophenone increases, whereas formation of 1-phenylethanol decreases with reaction time. The selectivity to acetophenone increases with increase in time since acetophenone is not a precursor of any daughter product. Selectivity to α-phenyl ethanol decreases with time as its further converts to acetophenone. The reaction is almost complete after about 24h.

Reaction conditions:- Cr(5)CeZr- 0.1g, Solvent-Acetonitrile,

Temperature- 70°C, EB:TBHP- 1:2.

Figure 4.6 Effect of time on ethylbenzene oxidation

The influence of reaction time on ethylbenzene conversion at temperatures 60, 70 and 80°C are represented in Figure 4.7. Ethylbenzene conversion increased with time whatever may be the temperature.
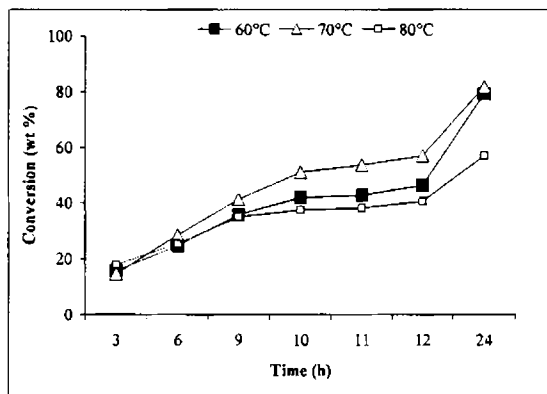
Reaction conditions:- Cr(5)CeZr- 0.1g, Acetonitrile-

10mL, EB:TBHP- 1:2.

Figure 4.7 Effect of time on ethylbenzene oxidation

4.2.8 Leaching

In order to address the issue of leaching, hot filtration studies were performed with the two promising metal containing catalysts, Cr and Mn. After 1h of reaction, the reaction mixture was filtered hot, and the reaction was continued with the filtrate in the absence of any solid catalyst[20]. The results obtained for leaching studies are given in Table 4.1. More ethylbenzene oxidation activity is observed in the filtrate for all catalysts. Thus it is clear that the catalyst loses traces of Cr, and Mn which catalyzed at least part of the reaction in homogeneous phase. Sheldon et al.[16] stated that no heterogeneous chromium catalysts have been reported, which have been unequivocally stable under liquid-phase oxidation conditions by performing appropriate rigorous tests for leaching.

Table 4.1 Leaching studies over Cr and Mn modified catalysts

Catalyst	Time/h	Ethylbenzene conversion (wt.%)	Acetophenone selectivity (%)
Cr(5)Ce	1	9.7	49.3
Filtrate	6	11.6	65.5
Mn(5)Ce	1	13.2	88.3
Filtrate	6	15.3	93.5
Cr(5)CeZr	1	16.3	75.3
Filtrate	6	21.3	88.5
Mn(5)CeZr	1	14.2	74.4
Filtrate	6	18.3	83.9

4.2.9 Reusability

Catalysts recycling experiments were carried out with repeated uses of representative catalysts. For the recycling studies, the catalyst was removed from the

reaction mixture after 12h by filtration, washed with acetone, heated at 500°C for 12h, and subjected to the next catalytic run, with same molar ratio of the substrate under the same reaction conditions. From the Table 4.2, it is clear that, the reuse of the catalysts did not appreciably decrease the conversion of ethylbenzene. The acetophenone selectivity remained nearly similar in all recycle experiments. Thus the catalysts can be recycled four times without significant loss of activity.

Table 4.2 Recycling studies of representative catalysts

Catalyst	Cycle	Ethylbenzene conversion (wt.%)	Acetophenone selectivity (%)
Cr(5)Ce	1	72.1	91.5
	2	74.5	88.6
	3	73.2	86.5
	4	71.4	85.3
Mn(5)Ce	1	36.7	95.9
	2	40.2	93.3
	3	38.2	86.7
	4	35.7	92.6
Cr(5)CeZr	1	87.8	81.2
	2	84.3	79.2
	3	83.8	76.6
	4	79.4	75.2
Mn(5)CeZr	1	39.8	85.9
	2	42.2	92.3
	3	38.3	86.5
	4	36.4	90.2

4.3 Comparison of Catalysts

The prepared catalysts were tested for liquid phase oxidation of ethylbenzene and the results are presented in Tables 4.3 and 4.4.

Table 4.3 Ethylbenzene oxidation over ceria based catalysts

Catalyst	Conversion	Selectivity (%)	
	(wt.%)	Acetophenone	1-phenyl ethanol
Ce	1.7	3.4	92.3
Cr(2)Ce	31.7	86.0	14.0
Cr(5)Ce	72.1	91.5	8.5
Cr(8)Ce	40.9	88.3	11.7
Mn(2)Ce	32.5	93.9	6.1
Mn(5)Ce	36.7	95.9	4.3
Mn(8)Ce	33.0	93.9	6.1
Fe(2)Ce	9.6	15.5	84.4
Fe(5)Ce	8.1	8.2	83.4
Fe(8)Ce	7.4	12.6	84.2
Co(2)Ce	13.8	86.3	3.5
Co(5)Ce	16.0	81.2	4.6
Co(8)Ce	16.5	68.5	15.5
Ni(2)Ce	6.6	7.7	81.3
Ni(5)Ce	10.2	50.2	40.8
Ni(8)Ce	8.2	90.1	9.1
Cu(2)Ce	27.8	62.1	26.7
Cu(5)Ce	22.6	69.9	17.3
Cu(8)Ce	29.1	55.8	35.0

Reaction conditions:-Catalyst-0.1g, Acetonitrile-5mL, Temperature-70°C, EB:TBHP-1:3, Time-12h.

Table 4. 4 Ethylbenzene oxidation over ceria-zirconia based catalysts

Catalyst	Conversion (wt.%)	Selectivity (%)	
		Acetophenone	1-phenyl ethanol
Zr	2.5	6.9	92.4
CeZr	5.7	30.2	68.2
Cr(2)CeZr	31.9	92.3	7.6
Cr(5)CeZr	87.8	81.2	18.8
Cr(8)CeZr	85.7	94.8	5.3
Mn(2)CeZr	23.2	84.2	3.9
Mn(5)CeZr	39.8	85.9	4.5
Mn(8)CeZr	45.9	88.4	4.0
Fe(2)CeZr	6.8	71.8	2.2
Fe(5)CeZr	6.6	74.9	12.5
Fe(8)CeZr	6.6	74.7	25.3
Co(2)CeZr	17.8	84.5	3.5
Co(5)CeZr	18.3	82.3	4.4
Co(8)CeZr	17.1	85.2	3.5
Ni(2)CeZr	11.1	83.2	3.3
Ni(5)CeZr	5.7	81.2	3.3
Ni(8)CeZr	5.4	90.8	1.6
Cu(2)CeZr	16.7	70.4	16.0
Cu(5)CeZr	43.2	58.9	32.8
Cu(8)CeZr	26.2	61.9	21.2

Reaction conditions:-Catalyst- 0.1g, Solvent- 5mL, Temperature- 70°C,
EB:TBHP- 1:3, Time-12h

Pure ceria catalyst gave negligibly small conversion of 1.7% with α-phenyl ethanol selectivity of 92.3%. Among different metal modified systems, Cr incorporated catalysts show highest conversion with high acetophenone selectivity. Mn modified systems also show good conversion with acetophenone selectivity >90%. Among Fe, Co, Ni and Cu modified systems, comparatively good conversion is shown by Cu modified systems. But acetophenone selectivity for Cu systems is less compared to Cr and Mn modified systems.

The results obtained towards ethylbenzene conversion and product selectivity for transition metal modified ceria and ceria-zirconia mixed oxide catalysts are tabulated in the Table 4.2. Here also the unmodified ZrO_2 gave less conversion, with high 1-phenylethanol selectivity. CeZr catalyst contributes 5.7% conversion. Compared to pure ceria and zirconia, the unmodified ceria-zirocnia catalyst showed better conversion and acetophenone selectivity. Chromium modified catalyst showed increase in ethylbenzene conversion with increase in chromium content. 5 and 8 wt.% chromium containing catalysts showed almost same ethylbenzene conversion. Mn modified catalysts gave better conversion at high Mn content. Comparatively good conversion is obtained for copper containing catalysts. Iron and nickel modification did not result in better catalytic activity compared to ceria-zirconia catalyst. The conversion of ethylbenzene and acetophenone selectivity remained constant over Co modified catalysts with different cobalt content.

4.4 Discussion

From the DR UV-vis analysis of the catalysts, it is clear that Cr exists in different oxidation states, ie Cr^{6-} and Cr^{3+}. The presence of Mn^{2+} and Mn^{3+} ions in the manganese modified catalyst was also confirmed from the DR UV-vis analysis. EPR spectra of chromium modified ceria and ceria-zirconia catalysts reveals the presence of mixed-valence trimers, Cr(VI)-O-Cr(III)-O-Cr(VI), with an average Cr oxidation

state of Cr(V). Cr modified ceria-zirconia catalysts showed an additional β signals which are attributed to the clusters of Cr^{3+} on the ceria-surface. The presence of Mn^{2+} ions is evident from the EPR spectral analysis of Mn modified ceria and ceria-zirconia catalysts. The possibility for the existence of Mn^{4+} is also considered because the observed Mn^{2+} signal could be possibly superimposed on Mn^{4+} signal. It is reported that the oxidation of toluene with TBHP in the presence of chromium silicate-1 catalyst proceeds through the reversible transformation of Cr^{3+} and Cr^{5+} [21]. Parentis et al.[22] suggested that in presence of TBHP, Cr(III) is oxidized to Cr(VI) in Cr/SiO_2 catalysts which in turn oxidizes the substrate via redox mechanism. Velu et al[19]. reported that the catalytic activity for toluene oxidation increases with increasing Mn content in Mg-Al layered double hydroxides and the Mn^{2+}/Mn^{3+} ions present in the LDH structure show better catalytic performance than a mixture of $Mn(OH)_2$ and $MnCO_3$. Imamura et al.[23] studied the catalytic activity of Mn/Ce composite oxide in the wet oxidation of organic compounds. They concluded that the effect of ceria was to produce manganese species with lower valence states (Mn^{3+}, Mn^{2+}), and the combination of Mn^{4+} with Mn^{3+} or Mn^{2+} was assumed to be the cause of the high activity of the catalyst. According to Sheldon et al. first row transition elements generally employ oxometal pathway which involves two-electron redox reactions of the metal ion. The highest catalytic activity is observed for Mn and Cr modified catalyst, which can easily undergo redox reactions through oxometal pathways. The presence of various oxidation states confirmed by EPR and DR UV-vis also support this argument. A general mechanism is shown in Scheme 4.2.
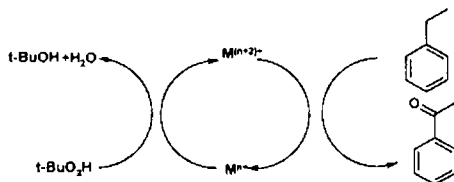
Scheme 4.2 General mechanism of ethylbenzene oxidation

4.5 Conclusions

The conclusions from the present results can be summarized as follows.

✓ Ethylbenzene oxidation with tert butyl hydroperoxide over transition metal modified ceria and ceria-zirconia catalysts gave acetophenone as the major product and 1-phenyl ethanol as the minor product.

✓ Reaction variables such as temperature, ethylbenzene to TBHP mole ratio, catalyst concentration, time and solvent have strong influence on the conversion and product selectivity.

✓ Chromium and Manganese modified systems show very good conversion and acetophenone selectivity. These catalysts can be a convenient ecofriendly substitute for hazardous stoichiometric oxidants.

✓ From the reusability studies, it is confirmed that the catalysts can be efficiently reused.

✓ The oxidation is expected to involve a redox mechanism.

References

[1]   Y. Wang, Y. Chang, R. Wang, F. Zha, J. Mol. Catal. A: Chem. 159 (2000) 31.

[2]   S. Vetrivel, A. Pandurangan, J. Mol. Catal. A: Chem. 217 (2004) 165.

[3]   S. Vetrivel, A. Pandurangan, Ind. Eng. Chem. Res. 44 (2005) 692.

[4]   S. Vetrivel, A. Pandurangan, Appl. Catal. A 264 (2004) 243.

[5]   V. R. Choudhary, J. R. Indurkar, V. S. Narkhede, R. Jha, J. Catal. 227 (2004) 257.

[6]   N. K. Mal, A. V. Ramaswamy, Appl. Catal. A 143 (1996 75.

[7]   T. H. Bennur, D. Srinivas, S. Sivasanker, J. Mol. Catal. A: Chem. 207 (2004) 163.

[8]   P. S. Singh, K. Kosuge, V. Ramaswamy, B. S. Rao, Appl. Catal. A 177 (1999) 149.

[9]   E. P. Reddy, R. S. Varma, J. Catal. 221 (2004) 93.

[10] S. –C. Baek, H. –S Roh, S. A. Chavan, M.-H. Choi, K. –W. Jun, S. –E. Park, J. S. Yoo, K. –J. Kim, Appl. Catal. A 244 (2003) 19.

[11] C. Guo, Q. Peng, Q. Liu, G. Jiang, J. Mol. Catal. A: Chem. 192 (2003) 295.

[12] M. Rogovin, R. Neumann, J. Mol. Catal. A: Chem. 138 (1999) 315.

[13] S. Boitsov, A. Riahi, J. Muzart, Chemistry 3 (2000) 747.

[14] S. L. H. Rebelo, M. M. Q. Simoes, M. Graca, P. M. S. Neves, J. A. S. Cavaleiro, J. Mol. Catal. A: Chem. 201 (2003) 9.

[15] P. P. Toribio, J. M. Campos-Martin, J. L. G. Fierro, J. Mol. Catal. A: Chem. 227 (2005) 101.

[16] I. W. C. E. Arends, R. A. Sheldon, Appl. Catal. A 212 (2001) 175.

[17] S. K. Bhoware, S. Shylesh, K. R. Kamble, A. P. Singh, J. Mol. Catal. A: Chem. 255 (2006) 123.

[18] A. Belifa, D. Lahcene, Y. N. Tchenar, A. Choukchou-Braham, R. Bachir, S. Bedrane, C. Kappenstein, Appl. Catal. A 305 (2006) 1.

[19] S. Velu, N. Shah, T. M. Jyothi, S. Sivasankar, Microporous Mesoporous Mater. 33 (1999) 61.

[20] R. Anand, M. S. Hamdy, P. Gkourgkoulas, Th. Maschmeyer, J. C. Jansen, U. Hanefeld, Catal. Today 117 (2006) 279.

[21] A. P. Singh, T. Selvam, J. Mol. Catal. A: Chem. 113 (1996) 489.

[22] M. L. Parentis, N. A. Bonini, E. E. Gonzo, React. Kinet. Catal. Lett. 76 (2002) 243.

[23] S. Imamura, M. Nakamura, N. Kawabata, J. Yoshida, S. Ishida, Ind. Eng. Chem. Prod. Res. Dev. 25 (1986) 34.

FRIEDEL-CRAFTS BENZYLATION OF TOLUENE AND *o*-XYLENE

Abstract

The present chapter deals with Liquid phase benzylation of toluene and o-xylene using benzyl chloride as alkylating agent. Influence of various reaction parameters on conversion and selectivity were studied. Lewis acid sites present on the surface of the catalysts were correlated with the alkylation activity. Metal incorporation could generate Lewis acid sites on the catalyst surface which in turn catalyze the alkylation reaction.

5.1 Introduction

Friedel-crafts alkylation is an important means for attaching alkyl chains to aromatic rings. The alkylation is traditionally performed with alkyl halides using Lewis acid catalysts such as HF and $AlCl_3$ or with alcohols using Bronsted acids, typically H_2SO_4. However, the homogeneous catalysts are not easily separable after the reaction or cause large amounts of acid waste generation[1]. Development of reusable solid acid catalysts having high activity in the Friedel-Crafts reaction is, therefore, of great practical importance. Benzyl toluene and isomeric mixtures thereof are compounds useful as dielectric liquids for such components as transformers, capacitors and cables[2].

Benzylation of benzene and toluene over zeolite catalysts have been reported[3]. Choudhary et al.[4] reported alkylation of benzene by benzyl chloride over zeolite partially substituted by Fe or Ga. Iron promoted sulfated zirconia catalysts were found to catalyze benzylation of toluene using benzyl chloride[5]. Al-promoted sulfated super acids were employed for benzoylation of toluene with benzoyl chloride[6]. The liquid phase benzylation and benzoylation of o-xylene with benzyl chloride to 3,4-dimethyldiphenylmethane and 3,4-dimethylbenzophenone over rare earth catalysts like CeO_2 and Pr_2O_3 were studied by Bhaskaran et al.[7,8]. Sugunan et al.[9] investigated selective benzylation of toluene over tungsten promoted ceria catalysts prepared through pseudo-template method.

Bachari et al.[10] studied benzylation of benzene and substituted benzene employing benzyl chloride as alkylating agent over a series of Cu containing mesoporous silica. Correlation between surface properties and benzylation of clay catalysts was done by Pushpalatha el al.[11]. Sugunan et al.[12] concluded that Lewis acid sites are responsible for benzylation of arenes with benzyl chloride over nanocrystalline chromia loaded sulfated titania. Liquid-phase benzylation of o-xylene

to 3,4-dimethyl diphenylmethane (3,4-DMDPM) with benzyl chloride has been investigated in the presence of various zeolite catalysts[13]. The formation of DMDPM is explained by an electrophilic attack of the benzyl cation ($C_6H_5CH^+_2$) on the *o*-xylene ring whose formation is facilitated by acid sites of the zeolite catalysts. Coq et al.[14] studied benzylation of toluene by benzyl chloride over protonic zeolites. Monobenzylation to benzyltoluenes was the main reaction, usually higher than 90% selectivity when a toluene/benzyl chloride molar ratio of 5 was used. Secondary reactions to dibenzyl- and tribenzyltoluenes occurred to various extents depending on the reaction conditions and catalysts. Pillared clay catalysts were found to be highly active and selective for the benzylation of benzene at room temperature[15]. Ghorpade et al.[16] investigated liquid phase Friedel Crafts alkylation over $CuCr_{2-x}Fe_xO_4$ spinel catalysts. Choudary et al.[17] reported Friedel-Crafts Benzylation reaction were solid bases are used as starting catalytic materials, namely different crystallites of MgO.

Liquid phase benzylation of toluene and *o*-xylene were carried out over the prepared catalysts. The general scheme for Friedel crafts benzylation of toluene and *o*-xylene are shown in Scheme 5.1.

R1=H, R2=CH3:Toluene   R1=R2=CH3:*o*-Xylene
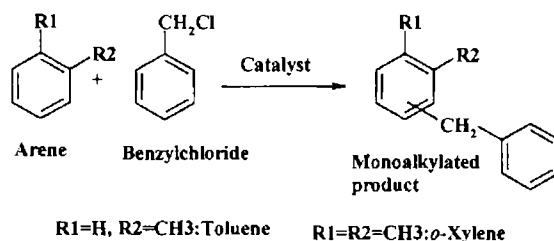
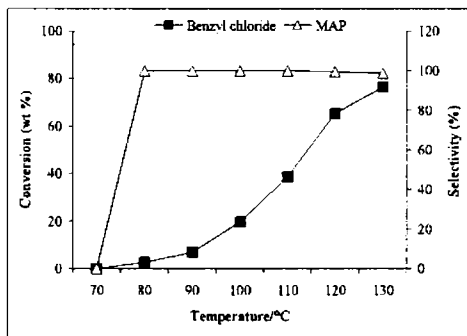**Scheme 5.1** Benzylation of toluene and *o*-xylene

The reactions were carried out in a closed 50mL glass round bottom flask with a reflux condenser. In typical run appropriate amounts of toluene/*o*-xylene, benzyl chloride and catalyst were allowed to react at specified temperatures under magnetic stirring. The reaction mixtures were analyzed periodically using Chemito

8610 GC equipped with SE-30 column and FID detector. As toluene/*o*-xylene was taken in excess, the yield of the reaction was expressed as the total percentage of benzyl chloride transformed. The product formed was identified as mono alkylated and is designated as MAP (Mono Alkylated Product).

5.2 Influence of Reaction conditions
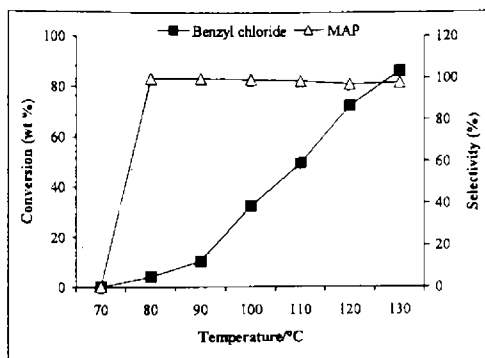
5.2.1 Effect of Temperature

The influence of temperature on benzylation of toluene and *o*-xylene are illustrated in Figures 5.1a and 5.1b. Up to 70°C, there was no reaction observed in the case of toluene benzylation. As the temperature increases the benzyl chloride conversion also increases. Selectivity remains 100% to MAP of toluene up to 120°C then slight decreases is observed, which could be attributed to the consecutive alkylation at high temperatures.

Reaction conditions:- Ni(8)CeZr-0.2g, Toluene:Benzyl chloride- 10:1,Time-3h.

Figure 5.1a Effect of temperature on benzylation of toluene

Benzylation of *o*-xylene also reveals temperature dependence identical to that of toluene. Here also the possibility for consecutive alkylation at high temperature is observed.
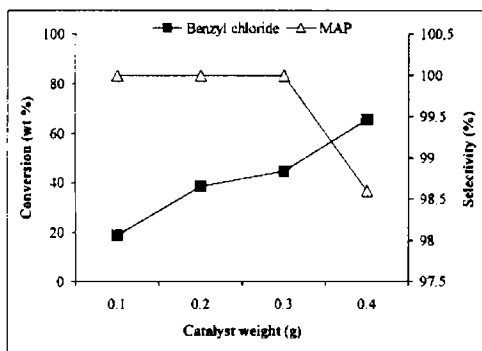
Reaction conditions:- Ni(8)CeZr-0.2g, *o*-xylene:Benzyl
chloride- 10:1,Time-3h.

Figure 5.1b Effect of temperature on benzylation of *o*-xylene
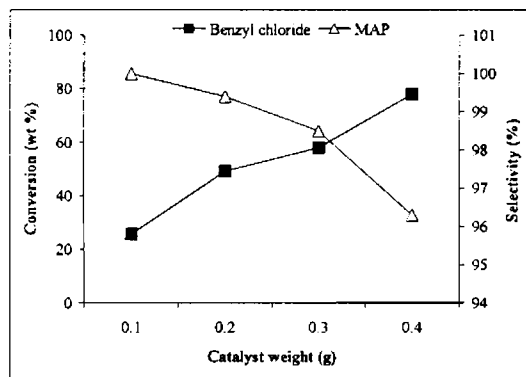
5.2.2 Effect of Catalyst weight

Effect of catalyst concentration on benzylation of toluene and *o*-xylene was studied by varying catalyst weight and keeping the reactant ratio constant and the results are represented in Figures 5.2a and 5.2b. As the catalyst concentration increases, the benzyl chloride conversion increases significantly for both toluene and *o*-xylene. This shows that the catalysis is truly heterogeneous in nature. On increasing the catalyst concentration, the number of active sites available for the reaction increases which favors the easy adsorption and desorption of reactants and products and hence increases the catalytic activity.

Reaction conditions:- Catalyst- Ni(8)CeZr, Toluene: Benzyl
chloride- 10:1,Time-3h, Temperature-110°C.

Figure 5.2 a Effect of catalyst weight on benzylation of toluene
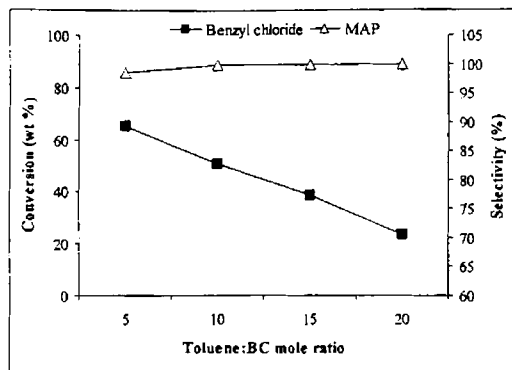

Reaction conditions:- Catalyst- Ni(8)CeZr, *o*-xylene: Benzyl
chloride- 10:1,Time-3h, Temperature-110°C.

Figure 5.2 b Effect of catalyst weight on benzylation of *o*-xylene

## 5.2.3 Effect of substrate to benzyl chloride mole ratio

The influence of substrate to benzyl chloride ratio on the benzylation reaction
was investigated by varying the mole ratio, keeping the amount of substrate constant.
The results are presented in Figures 5.3a and 5.3b. Lower conversion with an increase

in substrate to benzyl chloride molar ratio is due to the dilution effect of excess substrate.

Reaction conditions:- Ni(8)CeZr-0.2g, Time-3h.,

Temperature-110°C.

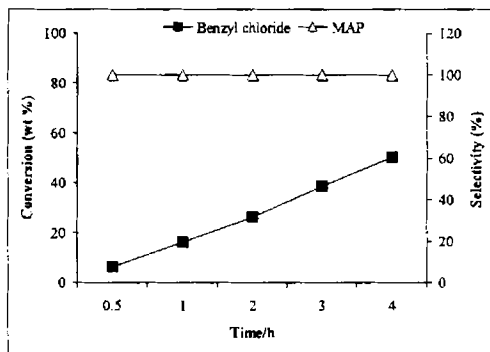**Figure 5.3 a** Effect of toluene:BC ratio on benzylation
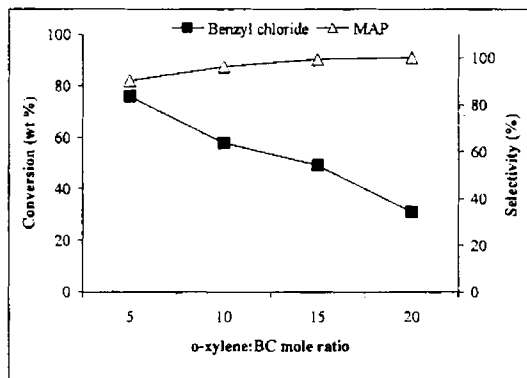
Reaction conditions:- Ni(8)CeZr-0.2g, Time-3h.,

Temperature-110°C.

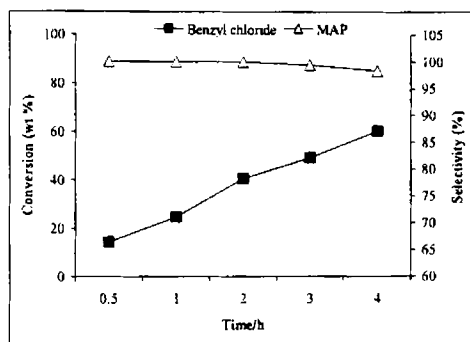**Figure 5.3 b** Effect of *o*-xylene:BC ratio on benzylation

5.2.4 Effect of Time

The reaction was carried out for 4h in order to study the effect of time on conversion and selectivity. Results are shown in Figures 5.4a and 5.4b. After half an hour, the conversion was only 6% for toluene. As the time increases, conversion gradually increases. Benzylation of *o*-xylene also follows the same path. At 4h, formations of side products were detected. The continued increase of percentage conversion with time for both toluene and *o*-xylene is indicative of the heterogeneous nature of the reaction.

Reaction conditions:- Ni(8)CeZr- 0.2g, Toluene:Benzyl chloride- 10:1, Temperature-110°C.

Figure 5.4 a Effect of time on benzylation of toluene

Reaction conditions:- Ni(8)CeZr- 0.2g, *o*-xylene: Benzyl
chloride- 10:1,Temperature- 110°C.

Figure 5.4 b Effect of time on benzylation of *o*-xylene

5.2.5 Leaching

To evaluate the heterogeneous nature of the reaction leaching studies were conducted. The catalyst was removed from the reaction mixture after 1h by hot filtration. The filtrate is again allowed to react for 2h at the same reaction conditions. The results are given in Table 5.1. The conversion is somewhat higher in the filtrate. Leaching of small quantity of metal ions may be take place.

Table 5.1 Effect of metal leaching in Benzylation of Toluene and *o*-xylene

Catalyst	Time/h	Benzyl chloride conversion (wt.%)	
		Toluene	*o*-xylene
Cr(5)Ce	1	12.3	15.3
Filtrate	3	14.3	17.3
Mn(5)Ce	1	11.2	13.2
Filtrate	3	12.1	14.3
Fe(5)Ce	1	9.7	13.6
Filtrate	3	12.3	15.7

Catalyst: 0.2g, Substrate: Benzyl chloride-10:1, Temperature: 110°C

5.2.6 Reusability

For checking reusability, the catalyst was removed from the reaction mixture by filtration. It was thoroughly washed with acetone until free of reaction mixture, dried in air oven for over night and activated at 500°C for 5h. The same catalyst was again used for carrying out another reaction under similar reaction conditions. Two catalysts were tested for reusability and the observations are listed in Table 5.2 A decrease in conversion is observed, even though it is negligible. The prepared catalysts can be effectively regenerated without loss of activity up to fourth cycle.

Table 5.2 Reusability of the catalysts

Catalyst	Cycle	Benzyl chloride Conversion (wt.%)	
		Toluene	o-xylene
Cr(5)Ce	1	46.3	47.6
	2	45.3	46.3
	3	42.1	44.9
	4	39.3	40.3
Mn(5)Ce	1	42.1	45
	2	40	44.8
	3	39.2	42.3
	4	32.1	38.3

Catalyst: 0.2g, Substrate: Benzyl chloride-10:1, Temperature: 110°C

5.3 Comparison of Catalysts

After studying the influence of reaction parameters on the benzylation of toluene and o-xylene, the reaction condition was selected to get high conversion and selectivity. Benzylation of toluene and o-xylene was done using all the prepared

catalysts with substrate to benzyl chloride molar ratio of 10:1, reaction temperature of 110°C and 0.2g catalyst and the results are given in Tables 5.3 and 5.4.

Table 5.3 Benzylation over transition metal modified ceria catalysts

Catalyst	Toluene		*o*-xylene	
	Benzyl chloride Conversion (wt.%)	MAP Selectivity (%)	Benzyl chloride Conversion (wt.%)	MAP Selectivity (%)
Ce	24	100	29	100
Cr(2)Ce	45.9	100	44.9	100
Cr(5)Ce	46.3	100	47.6	100
Cr(8)Ce	49.2	100	59.1	98.7
Mn(2)Ce	40.3	100	43.3	100
Mn(5)Ce	42.1	100	45.0	100
Mn(8)Ce	45.6	100	52.2	100
Fe(2)Ce	44.1	100	48.3	100
Fe(5)Ce	42.1	100	49.5	100
Fe(8)Ce	36.3	100	46.8	98.3
Co(2)Ce	27.3	100	40.3	100
Co(5)Ce	32.1	100	41.6	100
Co(8)Ce	28.9	100	38.9	100
Ni(2)Ce	34.9	100	39.9	100
Ni(5)Ce	35.3	100	42.3	100
Ni(8)Ce	39.3	100	46.3	100
Cu(2)Ce	33.6	100	43.7	100
Cu(5)Ce	35.7	100	48.6	100
Cu(8)Ce	37.2	100	46.5	100

Catalyst: 0.2g, Substrate: Benzyl chloride-10:1, Temperature: 110°C, Time-3h

Table 5.4 Benzylation over transition metal modified ceria-zirconia catalysts

Catalyst	Toluene		o-xylene	
	Benzyl chloride Conversion (wt.%)	MAP Selectivity (%)	Benzyl chloride Conversion (wt.%)	MAP Selectivity (%)
Zr	23.7	100	27.0	100
CeZr	26.3	100	31.6	100
Cr(2)CeZr	56.1	100	67.3	100
Cr(5)CeZr	54.2	100	65.8	100
Cr(8)CeZr	51.2	100	62.3	98.3
Mn(2)CeZr	41.9	100	47.3	100
Mn(5)CeZr	43.2	100	51.2	100
Mn(8)CeZr	41.3	100	49.3	100
Fe(2)CeZr	44.6	100	58.3	100
Fe(5)CeZr	43.2	100	57.3	98.1
Fe(8)CeZr	41.2	98.6	53.6	97.6
Co(2)CeZr	46.9	100	58.2	100
Co(5)CeZr	38.6	100	48.6	100
Co(8)CeZr	38.1	98.9	47.3	97.6
Ni(2)CeZr	44.3	100	55.7	100
Ni(5)CeZr	42.8	100	52.3	100
Ni(8)CeZr	38.5	100	49.3	100
Cu(2)CeZr	40.2	100	51.6	100
Cu(5)CeZr	39.2	100	53.0	100
Cu(8)CeZr	39.0	100	51.0	100

Catalyst: 0.2g, Substrate: Benzyl chloride-10:1, Temperature: 110°C, Time-3h

Pure metal oxides gave low conversions than the metal modified ones. Catalytic activity of various metal incorporated systems varies not much with variation in metal content. Cr, Mn and Fe incorporated systems gave comparatively good conversions. Transition metal modified ceria-zirconia systems show better conversion than corresponding transition metal loaded ceria systems. Mono alkylated product selectivity remains approximately 100% for almost all catalysts.

All prepared catalysts shows high selectivity to α-methyl styrene during cumene cracking reactions which indicates the availability of Lewis acid sites over the catalysts. The involvement of Lewis acid sites in carbocation generation is well established. Good correlation is obtained with benzyl chloride conversion in toluene benzylation and α-methyl styrene selectivity (Figure 5.5).
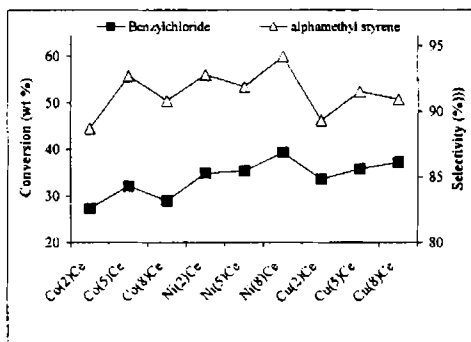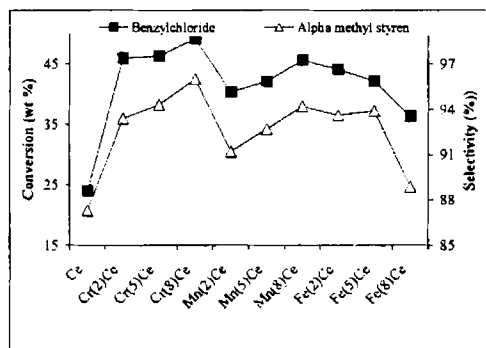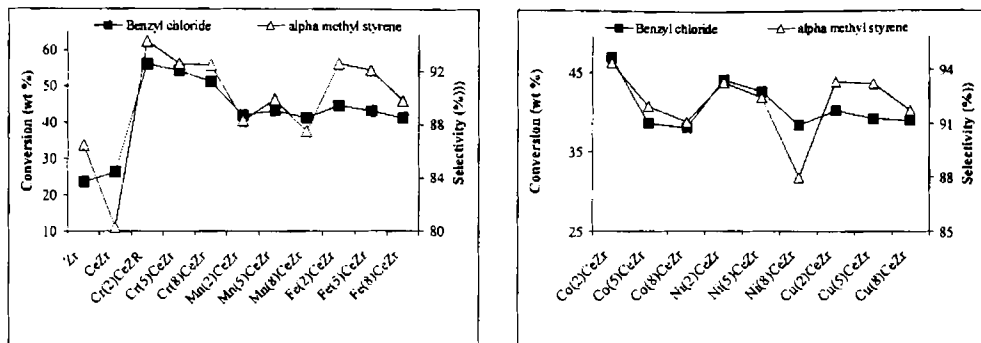
Figure 5.5 Alkylation vs α-methyl styrene selectivity

A Friedel-Crafts alkylation is an aromatic substitution reaction in which the carbocation is formed by complexation of alkyl halide with the catalyst. The carbocation generated attacks the aromatic species for alkylation. Formation of carbocation is thus an important step in the reaction mechanism. According to Ghorpade et al.[16] the lower conversion of individual metal oxides may be due to the higher activation energy and lower strength of Lewis acid sites. A possible mechanism for benzylation of aromatic substrates is given in Scheme 5.2.
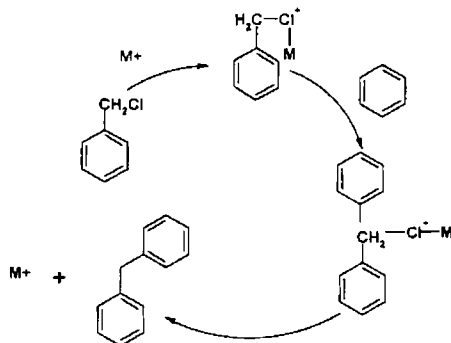
Scheme 5.2 Mechanism of benzylation of aromatics

5.4 Conclusions

The following conclusions can be drawn from the present study.

- ✓ Transition metal modification of ceria and ceria-zirconia could result in better catalysts for benzylation of toluene and *o*-xylene.
- ✓ Benzyl chloride conversion depends strongly on reaction variables like temperature, substrate to benzylchoride mole ratio, catalyst concentration and reaction time.
- ✓ The selectivity to monoalkylated products remains approximately 100% over all the catalysts.
- ✓ Generation of Lewis acid sites on metal modification leads to better catalytic activity. A possible mechanism involving Lewis acid site is proposed.

References

[1] G. A. Olah, "Friedel-Crafts Chemistry", Wiley-Interscience, New York, London, Sydney, Toronto (1973).

[2] R. Commandeur, N. Berger, P. Jay, J. Kervennal: EP 0442 (1991) 986.

[3] N. Narender, K. V. V. Krishna Mohan, S. J. Kulkarni, 1. A. K. Reddy, Catal. Commun. 7 (2006) 583.

[4] V. R. Choudhary, S. K. Jana, B. P. Kiran, Catal. Lett. 59 (1999) 217.

[5] H. Suja, C. S. Deepa, K. Sreejarani, S. Sugunan, React. Kinet. Catal. Lett. 79 (2003) 373.

[6] Y. Xia, W. Hua, Z. Gao, Catal. Lett. 55 (1998) 101.

[7] S. K. Bhaskaran, V. T. Bhat, React. Kinet. Catal. Lett. 75 (2002) 239.

[8] S. B. Bhaskaran, T. T. Venugopal, React. Kinet. Catal. Lett. 74 (2001) 99.

[9] F. J. Palathingal, S. Sugunan, React. Kinet. Catal. Lett. 84 (2005) 207.

[10] K. Bachari, O. Cherifi, Catal. Commun. 7 (2006) 926.

[11] P. Pushpaletha, S. Rugmini, M. Lalithambika, Appl. Clay Sci. 30 (2005) 141.

[12]   K. R. Sunajadevi, S. Sugunan, Catal. Commun. 5 (2004) 575.

[13]   A. P. Singh, B. Jacob, S. Sugunan, Appl. Catal. A 174 (1998) 51.

[14]   B. Coq, V. Gourves, F. Figueras, Appl. Catal. A 100 1 (1993) 69.

[15]   D. U. Singh, S. D. Samant, J. Mol. Catal. A Chem. 223 (2004) 111.

[16]   S. P. Ghorpade, V. S. Darshane, S. D. Dixit, Appl. Catal. A 166 (1998) 135.

[17]   B. M. Choudary, R. S. Mulukutla, K. J. Klabunde, J. Am. Chem. Soc. 125
   (2003) 2020.

METHYLATION OF PHENOL AND *o*-CRESOL

Abstract

The methylation of phenol and *o*-cresol was investigated over transition metal modified ceria and ceria-zirconia mixed oxide catalysts. Influence of various reaction parameters like reaction temperature, feed composition, flow rate and durability of the catalysts during methylation were investigated. *o*-cresol and 2,6-xylenol are formed as the main products for the methylation of phenol and 2,6-xylenol as the main product for the methylation of *o*-cresol. The catalytic activity is correlated with the acidic properties.

6.1 Introduction

Alkylation of phenol with methanol is an industrially important reaction. Products such as *o*-cresol and 2,6-xylenols are used as chemical intermediates for the synthesis of a variety of fine chemicals, pharmaceuticals, peptides and plastics[1,2]. The stringent specifications and demand for high purity to use them in drugs and pharmaceuticals necessitate the synthesis of these compounds selectively. In recent times, the vapor phase alkylation of phenol with methanol over various solid catalysts, without causing any environmental impact, is considered to be a promising route for the synthesis of these compounds selectively. Cresols, xylenols, ring-methylated products and anisole, oxygen methylated products, are produced by alkylation of phenol with methanol. The formation of products is given in Scheme 6.1. The products formed in the direct methylation of *o*-cresol are given Scheme 6.2.
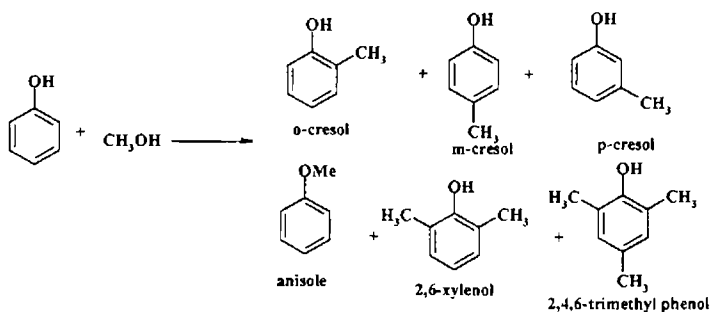
Scheme 6.1 Methylation of phenol
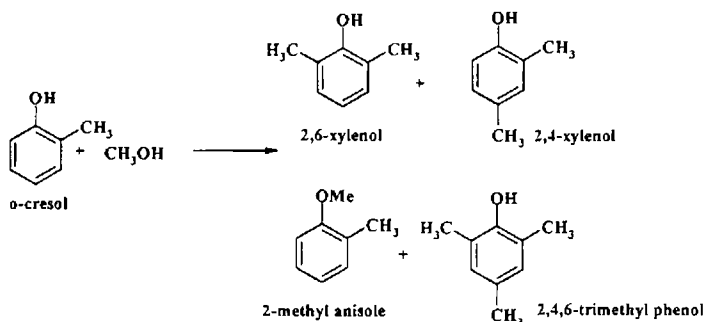
Scheme 6.2 Methylation of *o*-cresol

A variety heterogeneous catalyst has been investigated for the methylation of phenol. Malshe et al[3]. carried out selective C-methylation of phenol to o-cresol and 2, 6-xylenol over borate zirconia solid acid catalyst. The large number of weak and medium acid sites favored C-alkylation and the preferential o-alkylation is attributed to the perpendicular orientation of phenol aromatic ring on catalyst surface. Effect of substitution of Fe^{3+} /Cr^{3+} on the alkylation of phenol with methanol over magnesium-aluminium hydrotalcite was studied by Velu et al[4]. The alkylation reaction was found to proceed exclusively at C-centres to give *o*-cresol as the major product. Alkali supported SiO_2 samples are employed as good catalyst for the O-alkylation of phenol and it is observed that the deactivation rate decreases with increase in basicity of the catalyst[5]. Reddy et al.[6] evaluated phenol alkylation activity of molybdenum oxide supported on NaY zeolite and observed that the acid sites are playing an important role in determination of the activity of the catalysts and selectivity for the formation of C- or O- alkylated products.

Co and Ni based ferrospinels were effectively used as catalyst for methylation of phenol[7]. The catalytic activity and product selectivity depend on the Co^{2+}/Ni^{2+} ratio in the spinel matrix and also on the surface acid-base properties of the system. The strong acid sites are required for secondary alkylation to yield 2,6-xylenol, whereas

only weaker acid sites are needed for the formation of primary alkylation to yield *o*-cresol. Choi et al.[8] investigated alkylation of phenol over magnesium oxide catalyst modified with the addition of small amount of vanadium, manganese and sodium. They observed that addition of small amount of dopants into the magnesium oxide gave better activity and selectivity to 2,6-xylenol than the pure MgO catalyst. Rare earth promoted sulfated tin oxide catalyst has been used for alkylation of phenol and it is noted that sulfate modification resulted in a large variation in product selectivity and reaction pathway due to the creation strong acid sites, which alters the nature of adsorption of phenol on the catalyst surface[9]. Gandhe et al[10]. investigated alkylation of phenol over an active rutile titania catalyst and the high ortho-selectivity of the synthesized rutile sample is attributed to the unique presence of weak basic sites. Al-MCM-41 was shown to be a promising catalyst for the methylation of phenol[11]. O-alkylation of phenol was favored in presence of alkali metal loaded zeolites and is observed that reactivity of the catalyst increased with the basicity of loaded metal[12]. Selective O-alkylation of cresol with methanol by Cs loaded silica which is a base catalyst was reported by Rajaram et al.[13]. Jyothi et al[14]. reported the formation of 2,6-xylenol by the selective methylation of anisole over rare earth promoted SnO_2 catalysts. The higher selectivity was ascribed to the weak acid sites and comparitively strong basic sites. Vapour phase isopropylation of *o*-, *m*- and *p*-cresol over alumina catalysts was also reported[15].

Sato et al. from their examination for alkylation of phenol with methanol over various oxides of rare earth metals found that only ceria has sufficient activity and selectivity for the reaction[16]. Selective ortho methylation of phenol with methanol over CeO_2-MgO catalysts was reported. The mechanism speculated is that the ortho position of phenol adsorbed perpendicularly on the basic site on CeO_2 species is selectively alkylated by methanol which is possibly activated in the form of formyl/

hydroxy methyl group rather than methyl cation[17]. Klimkiewicz et al. used Sn-Ce-Rh-O monophase system as ortho-selective catalyst for phenol alkylation[18].

Methylation was carried out in a vertical down flow glass reactor. All the reactions were carried out using 0.5 g charge of the catalyst. Prior to the reaction the catalysts were activated in the muffle furnace for 1h at 500°C. The catalyst was packed between the layers of quartz wool, and the upper portion of the reactor was filled with glass beads, which served as pre-heaters for the reactants. The reactor was placed inside a temperature-controlled furnace with a thermocouple placed at the centre of the catalyst bed for measuring the reaction temperature. In a typical reaction, a mixture of phenol or cresol and methanol in required molar ratio was fed into the reactor at pre-determined flow rate through a syringe pump at a particular reaction temperature. The products were condensed and collected in an ice trap. The products were identified by GC-MS and were analyzed by a Chemito 8610 GC using a FID detector and an OV-17 column. The conversion was expressed in terms of phenol/*o*-cresol reacted and the product selectivity was obtained as the amount of the particular product divided by the total amount of products multiplied by 100.

6.2 Influence of Reaction conditions
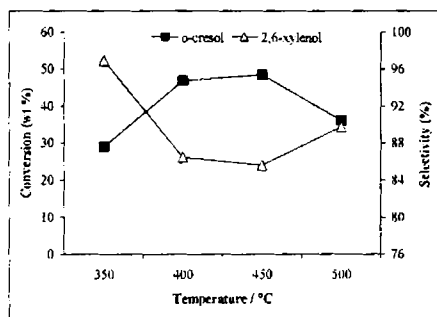
6.2.1 Effect of Temperature

Studies on the effect of temperature of methylation of phenol were carried out over Ni(2)Ce catalyst in the temperature range 450-500°C. The conversion of phenol and selectivities to o-cresol, 2,6-xylenol and anisole are shown in Figure 6.1a. Conversion of phenol and selectivity to 2,6-xylenol increased with increase in temperature while selectivity to *o*-cresol decreased. Anisole selectivity remained almost constant independent of the reaction temperature.
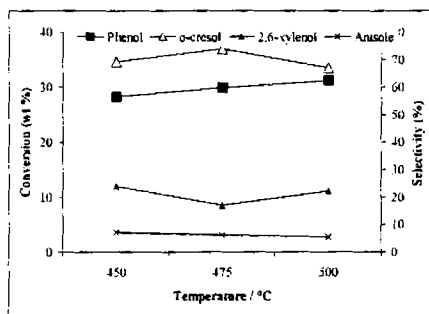
Reaction conditions:- Ni(2)Ce-0.5g, Flow rate-4mLh[-1],

Phenol:methanol-1:4, TOS-2h.

Figure 6.1a Effect of temperature on methylation of phenol

The effect of temperature on cresol conversion is depicted in Figure 6.1b. The increase in reaction temperature increases o-cresol conversion, then attains a steady state and then decreases in agreement with the general trend for alkylation[11]. The less conversion at low temperature can be attributed to the molecular association that reduces adsorption and dissociation on the actives sits[19]. 2, 6-xylenol selectivity decreased with increase in temperature due to the possible formation of higher alkylated product at high temperature. The decrease in conversion at high temperature can be attributed to the coke formation at active sites.


Reaction conditions:- Ni(5)CeZr-0.5g, Flow rate-4mLh[-1],

o-cresol:methanol-1:4, TOS-2h.

Figure 6.1b Effect of temperature on cresol conversion

6.2.2 Effect of Flow Rate

The influence of flow rate on reaction was investigated by varying the flow rate at 500°C. The conversion of phenol and selectivities varied as shown in the figure 6.2a. Phenol conversion and 2, 6-xylenol selectivity decreased with increase in flow rate while o-cresol selectivity increased. At higher flow rate, the conversion is less, suggesting attainment of high rate of diffusion reducing the chemisorption[20]. o-cresol is the primary product and 2,6-xylenol is the secondary product of the alkylation reaction. Hence increase in flow rate results in more o-cresol selectivity[8]. Flow rate did not show any marked influence on O-alkylation and anisole concentration remains unchanged.
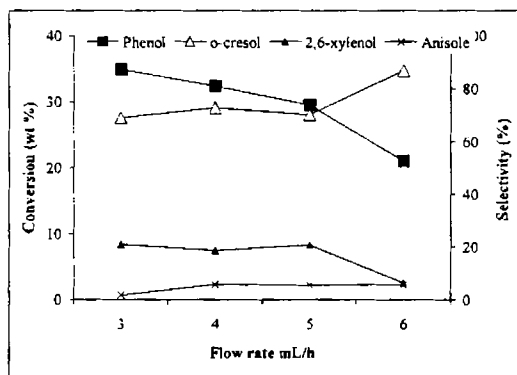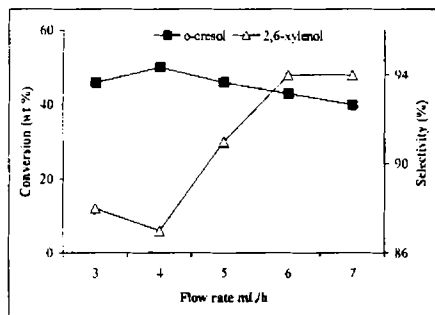

Reaction conditions:- Ni(2)Ce-0.5g, Temperature- 500°C

Phenol:methanol-1:4, TOS-2h.

Figure 6.2a Effect of flow rate on methylation of phenol

The influence of flow rate on *o*-cresol conversion is evident from Figure 6.2b. When the flow rate is increased from 3 to 4mLh[-1], the conversion of o-cresol increases first and then decreases at higher flow rates. Less conversion at low flow rate (3mLh[-1]) could be attributed to the coke formation at lower contact times. At higher flow rate diffusion of reactant molecules is high which results in low conversion of phenol[19].

Selectivity towards 2, 6-xylenol is found to be increased with increase in flow rate as the probability for consecutive methylation is less.
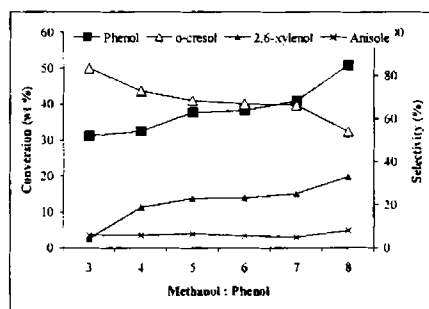

Reaction conditions:- Ni(5)CeZr-0.5g, o-cresol : methanol – 1:4,

Temperature-400°C, TOS-2h.

Figure 6.2b Effect of flow rate on *o*-cresol conversion

6.2.3 Effect of Methanol to Substrate mole ratio

Figure 6.3a shows the effect of feed composition on phenol conversion and selectivities. The total conversion of phenol increased with an increase in amount of methanol in the feed. The selectivity of 2,6-xylenol shows identical trend. *o*-cresol selectivity decreased with increase in methanol content.
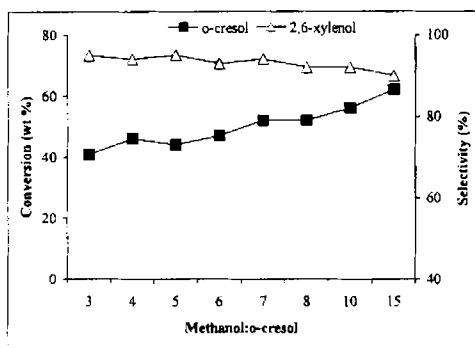

Reaction conditions:- Ni(2)Ce-0.5g, Temperature- 500°C

Flow rate-5mLh^{-1}, TOS-2h.

Figure 6.3a Effect of methanol: phenol mole ratio methylation

Effect of change in methanol: *o*-cresol mole ratio on conversion and selectivity is shown in Figure 6.3b. The conversion of o-cresol is increased form 3 to 15 due to the availability of additional methyl groups for the reaction[3]. Decrease in 2,6-xylenol selectivity at higher mole ratio is due to the possibility for consecutive methylation.


Reaction conditions:- Ni(5)CeZr-0.5g, Flow rate-5mLh[-1],

Temperature-400°C, TOS-2h.

Figure 6.3b Effect of methanol:*o*-cresol mole ratio on methylation

6.2.4 Effect of Time-Deactivation

The time on stream studies using representative catalysts for methylation of phenol and *o*-cresol was done by carrying out the reaction continuously for 8h. Results are shown in Figures 6.4a, 6.4b, 6.5a and 6.5b. Rate of deactivation for pure Ce is more compared to CeZr. Copper systems show very fast deactivation. The principal cause of deactivation has mostly been the build up of a layer of pseudographitic carbon referred to as coke or carbonaceous residues[16].
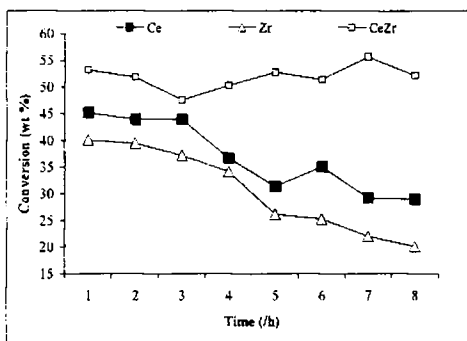
Reaction conditions:- Temperature-500°C, Phenol:

methanol- 1:5, Flow rate-4mLh^{-1}

Figure 6.4.a Effect of time on methylation of phenol
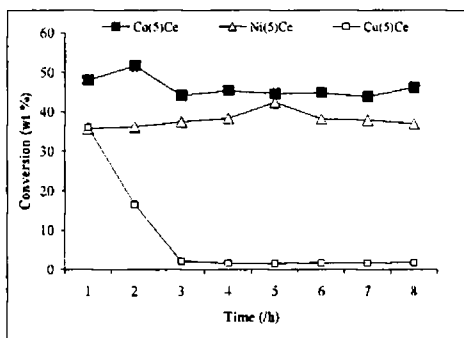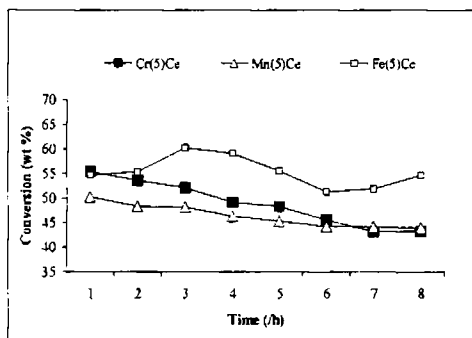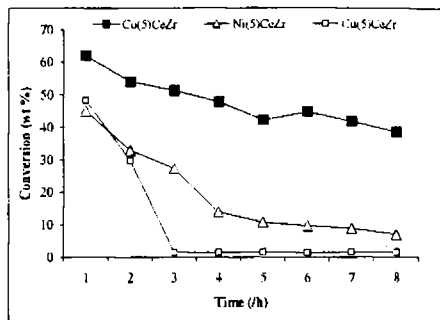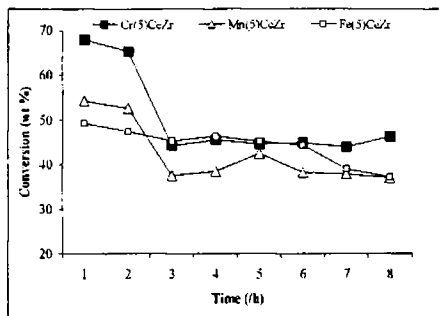
Reaction conditions:- Temperature-500°C, Phenol: methanol- 1:5, Flow rate-4mLh^{-1}.

Figure 6.4b Effect of time over representative catalysts for methylation of phenol
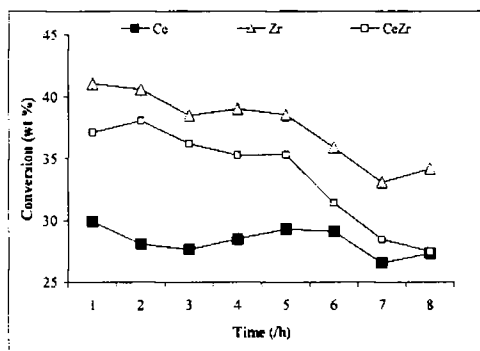
Reaction conditions:- Temperature-400°C, o-cresol :

methanol- 1:5, Flow rate-4mLh^{-1}.

Figure 6.5a Effect of time over Ce, Zr and CeZr for

methylation of *o*-cresol
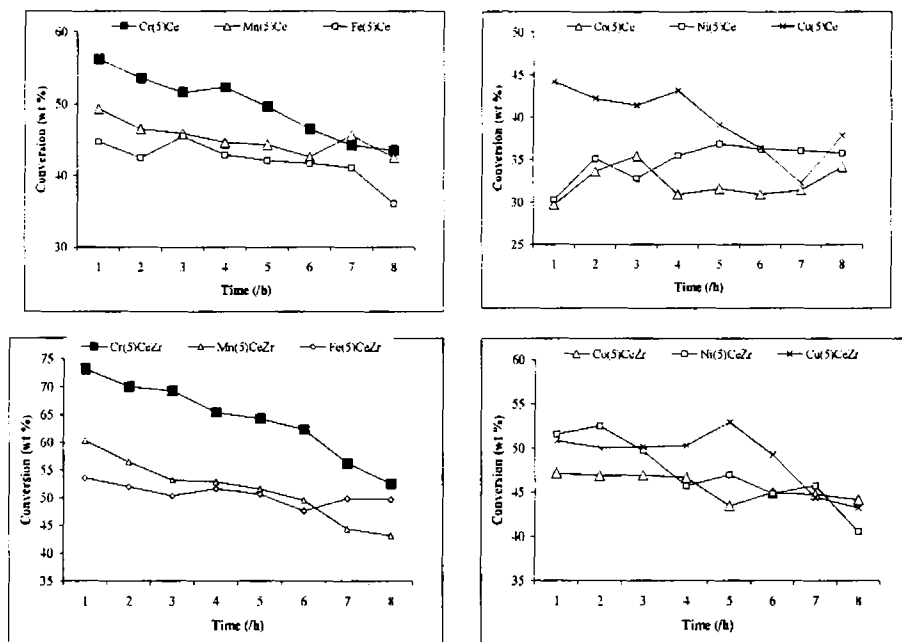
Reaction conditions:- Temperature-400°C, o-cresol : methanol- 1:5, Flow rate-4mLh^{-1}

Figure 6.5b Effect of time over representative catalysts for methylation of *o*-cresol

6.3 Comparison of Catalysts

Table 6.1 summarizes the catalytic results towards methylation of phenol over transition metal modified ceria catalysts. Pure ceria catalyst gave 44% phenol conversion and 90% o-selectivity. Among metal doped ceria catalysts chromium and manganese modified catalyst gave comparatively good conversion and ortho-selectivity. Selectivity to anisole remained <6% over ceria catalysts. About 55% phenol conversion is obtained over iron modified systems, but ortho selectivity is <50%. Cu modified systems gave comparatively less conversion with about 80% ortho selectivity.

Table 6.1 Methylation of phenol over ceria based catalysts

Catalyst	Conversion (wt.%)	Selectivity (%)				Ortho selectivity
		o-cresol	2,6-xylenol	Anisole	Others[a]	
Ce	34.0	65.6	24.0	5.6	4.8	89.6
Cr(2)Ce	47.0	62.2	26.8	4.0	7.0	89.0
Cr(5)Ce	53.6	59.2	32.2	3.2	5.4	91.4
Cr(8)Ce	56.2	51.2	38.6	3.4	6.8	89.8
Mn(2)Ce	45.2	68.2	21.8	2.9	7.1	90.0
Mn(5)Ce	48.3	62.7	26.9	2.1	8.3	89.6
Mn(8)Ce	49.5	48.2	38.2	1.9	11.7	86.4
Fe(2)Ce	55.8	36.6	12.9	4.2	46.3	49.5
Fe(5)Ce	55.4	29.0	8.7	4.0	58.3	37.7
Fe(8)Ce	54.1	33.5	9.6	2.2	54.7	43.1
Co(2)Ce	42.1	63.9	22.9	3.6	9.6	86.8
Co(5)Ce	51.7	49.8	26.1	4.3	19.8	75.9
Co(8)Ce	53.1	54.6	29.2	2.7	13.5	83.8
Ni(2)Ce	37.7	68.3	23.0	6.4	2.3	91.3
Ni(5)Ce	36.2	68.6	23.2	3.1	5.1	91.8
Ni(8)Ce	46.4	59.2	24.2	4.1	12.5	83.4
Cu(2)Ce	24.8	71.5	22.4	3.7	2.4	93.9
Cu(5)Ce	32.9	65.0	22.6	4.2	8.2	87.6
Cu(8)Ce	35.4	67.8	26.5	3.4	2.3	94.3

[a] Other products are *p*-cresol, 2,4-xylenol, 2,4,6-trimethyl phenol and benzene.

Reaction conditions:- Catalyst-0.5 g, Temperature-500°C, Flow rate-4 mlh[-1], phenol:methanol- 1:5, Time- 2h.

Phenol conversion and product distribution of transition metal modified ceria-zirconia catalysts are tabulated in Table 6.2. Cr and Mn modified catalysts gave high

conversions and about 90% *o*-selectivity. 63% phenol conversion is obtained over iron modified ceria-zirconia catalyst with 54% o-selectivity.

Table 6.2 Methylation of phenol over ceria-zirconia based catalysts

Catalyst	Conversion (wt.%)	Selectivity (%)				
		o-cresol	2,6-xylenol	Anisole	Others[a]	Ortho selectivity
Zr	36.3	58.2	29.1	3.1	9.6	87.3
CeZr	43.2	59.2	26.9	7.9	6.0	86.1
Cr(2)CeZr	52.5	69.8	22.2	2.9	5.1	92.0
Cr(5)CeZr	55.3	66.2	24.1	2.7	7.0	90.3
Cr(8)CeZr	59.0	59.1	30.2	3.2	7.5	89.3
Mn(2)CeZr	48.3	70.3	24.2	1.8	3.7	94.5
Mn(5)CeZr	52.6	63.9	29.1	2.1	4.9	93.0
Mn(8)CeZr	57.3	59.8	33.2	3.1	3.9	93.0
Fe(2)CeZr	64.2	36.7	18.0	3.2	42.1	54.7
Fe(5)CeZr	47.4	44.4	12.5	2.9	40.2	56.9
Fe(8)CeZr	52.0	48.0	16.6	1.8	33.6	64.6
Co(2)CeZr	59.3	46.9	31.7	3.6	17.8	78.6
Co(5)CeZr	54.1	44.3	28.5	3.4	23.8	72.8
Co(8)CeZr	53.0	49.9	37.5	2.9	9.7	87.4
Ni(2)CeZr	34.8	61.6	15.6	2.7	20.1	77.2
Ni(5)CeZr	32.9	67.0	25.9	2.4	4.7	92.9
Ni(8)CeZr	46.2	56.3	18.8	2.4	22.5	75.1
Cu(2)CeZr	46.8	60.8	18.5	2.9	17.8	79.3
Cu(5)CeZr	29.8	65.2	15.1	3.4	16.3	80.3
Cu(8)CeZr	31.5	66.0	26.0	3.9	8.1	88.0

[a] Other products are p-cresol, 2,4-xylenol, 2,4,6-trimethyl phenol, benzene

Reaction conditions:- Catalyst-0.5 g, Temperature-500°C, Flow rate-4 mlh[-1],

phenol:methanol- 1:5, Time- 2h.

The results of alkylation using o-cresol as the reactant instead of phenol are shown in table 6.3 and 6.4. All the catalysts found to give 2,6-xylenol as the major product with about 90% selectivity. Unlike in the case of methylation of phenol, *o*-cresol methylation over iron catalysts show good *o*-cresol selectivity.

Table 6.3 Methylation of *o*-cresol over ceria based catalysts

Catalyst	Conversion (wt%)	Selectivity (%)	
		2,6-xylenol	2,4-xylenol and 2,4,6-trimethylphenol
Ce	28.1	95.4	4.6
Cr(2)Ce	42.9	92.0	8.0
Cr(5)Ce	44.6	93.0	7.0
Cr(8)Ce	48.3	98.6	1.4
Mn(2)Ce	36.2	97.6	2.4
Mn(5)Ce	39.1	93.2	6.8
Mn(8)Ce	43.2	90.1	9.9
Fe(2)Ce	47.1	95.5	4.5
Fe(5)Ce	44.8	91.3	8.7
Fe(8)Ce	34.5	98.8	1.2
Co(2)Ce	32.0	98.2	1.8
Co(5)Ce	33.6	97.8	2.2
Co(8)Ce	40.5	96.2	3.8
Ni(2)Ce	35.9	97.3	2.7
Ni(5)Ce	35.1	95.1	4.9
Ni(8)Ce	46.4	93.0	7.0
Cu(2)Ce	42.4	97.8	2.2
Cu(5)Ce	42.2	91.8	8.2
Cu(8)Ce	33.6	98.2	1.8

Reaction conditions:- Catalyst-0.5 g, Temperature-400°C, Flow rate-5 mlh^{-1}, *o*-cresol:Methanol- 1:7, Time- 2h.

Table 6.4 Methylation of *o*-cresol over ceria-zirconia based catalysts

| Catalyst	Conversion (wt.%)	Selectivity (%)	
		2,6-xylenol	2,4-xylenol and 2,4,6-trimethylphenol
Zr	40.6	82.9	17.1
CeZr	46.6	89.0	10.2
Cr(2)CeZr	56.0	92.6	7.4
Cr(5)CeZr	60.0	94.3	5.7
Cr(8)CeZr	63.5	93.9	6.1
Mn(2)CeZr	53.0	89.4	10.6
Mn(5)CeZr	56.5	91.2	8.6
Mn(8)CeZr	59.3	94.1	5.9
Fe(2)CeZr	42.2	96.8	3.2
Fe(5)CeZr	52.2	89.4	10.6
Fe(8)CeZr	47.9	92.1	7.9
Co(2)CeZr	42.1	92.6	7.4
Co(5)CeZv	46.8	95.3	4.7
Co(8)CeZr	40.1	94.7	5.3
Ni(2)CeZr	46.2	93.3	6.7
Ni(5)CeZr	52.5	95.1	4.9
Ni(8)CeZr	37.2	83.2	16.9
Cu(2)CeZr	43.2	90.1	9.9
Cu(5)CeZr	50.1	87.8	12.2
Cu(8)CeZr	55.6	90.7	9.3

Reaction conditions:- Catalyst-0.5 g, Temperature-400°C, Flow rate-5 mlh^{-1},

o-cresol:methanol- 1:7, Time- 2h.

The alkylation phenol with methanol being and acid-base catalyzed reaction; the product selectivity depends on the acidity as well as the basicity of the catalyst.

Reddy et al.[21] correlated the catalytic activity of copper manganese mixed oxide spinels with structure, as well as with acid-base properties. When we consider metal oxide catalysts, the Lewis acidity can be attributed to metal ions, whereas the basicity can be attributed to the presence of oxide anions on the surface of the metal oxide. The distribution of metal and oxide ions depends on the composition of the catalysts. When transition metal ions incorporated into ceria or ceria-zirconia, more coordinatively unsaturated metal ions are produced on the surface which leads to the formation of more Lewis acid sites. According to Tanabe et al[22], in the adsorption of the phenol on the catalyst surface, geometric factors play a fundamental role in affecting selectivity. The reactant phenol gets adsorbed on the catalyst surface perpendicularly or horizontally depending on the acidity of the catalyst. Santacesaria et al.[23] studied the effect of acidity of various catalysts on the activity and selectivities in phenol alkylation. They proposed perpendicular orientation of phenol over γ-alumina containing strong Lewis acid sites. Over Nafion-H containing Bronsted acid sites, they proposed two mechanisms, 1) a dual mechanism, in which an acid sties strongly bound to the oxygen of methanol forms methyl carbocation, while another acid sties directly interacts with the aromatic ring; and 2) a Rideal mechanism according to which the reaction occurs between the molecules of the adsorbed alkylating agent and the aromatic molecules from the vapour phase. Sato et al.[17] speculated that in the methylation of phenol, the redox property of the CeO_2 species is concerned with methanol activation and methanol is activated on the CeO_2 species as a form of formyl or hydroxy methyl group rather than methyl cation of acidic sites.

From the ammonia TPD measurements, it is visible that the acidity is enhanced upon metal incorporation. More than 80% ∝-methyl styrene selectivity is observed during cumene cracking for all the catalysts. This indicates the presence of sufficient number of Lewis acid sites on the catalyst surface. These Lewis sites are constituted by the coordinatively unsaturated Ce^{4+}, Zr^{4+} and transition metal ions.

From different characterization techniques like EPR and UV- Vis DRS, it is clear that incorporated metal ions exists in different oxidation states, e.g., chromium in Cr(III), Cr(V) and Cr (VI) with different coordination environments imparting redox nature to the catalyst systems. On incorporating zirconium and other transition metals into ceria lattice, the generation of exposed O^{2-} results leading to enhancement in basic properties of the catalysts. It is observed that dehydration of cyclohexanol to cyclohexene occurs on the surface acid sites while dehydrogenation to cyclohexanone is facilitated by basic sites originating from the lattice oxygen ions[24]. The results of cyclohexanol decomposition reaction clearly indicate the formation of cyclohexanone over all catalysts. This indicates the availability of basic sites on the surface. The thermodesorption studies of 2,6-dimethyl pyridine adsorbed samples the presence of Bronsted acid sites. The density of the Bronsted acid sites is comparatively less as evident from the benzene selectivity in cumene cracking reaction. Thus different types of acid sites are observed over the prepared catalysts. Phenol can orient both vertically and horizontally on the catalyst surface. Perpendicular adsorption is more preferred since number of Bronsted acid sites is comparatively less which can also confirmed from the high ortho selectivity. The possible orientations of phenol over the catalyst surface are given in Schemes 6.3 and 6.4.
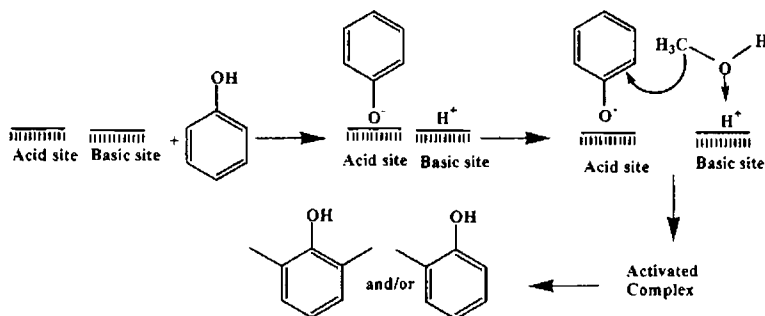

Scheme 6.3 Perpendicular orientation of aromatic ring on the
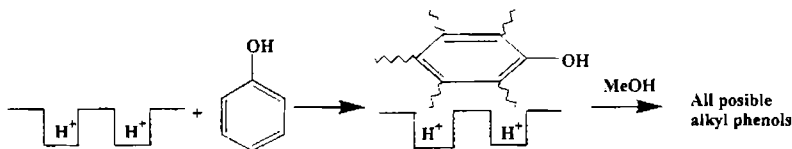
catalyst surface

Scheme 6.4 Parallel orientation of aromatic ring on the catalyst surface

Since methylation of phenols can be influenced by nature and strength of acid sites and basic sites and also by redox properties of the prepared systems, a one to one correlation of catalytic activity to any of these properties is rather impossible. However, a correlation between total acidity from ammonia TPD and conversion of phenol (o-cresol) is attempted. The profiles reveal the dependence of catalytic activity on acidity (Figures 6.6a and 6.6b).
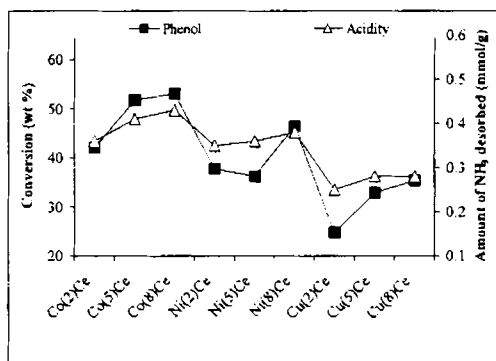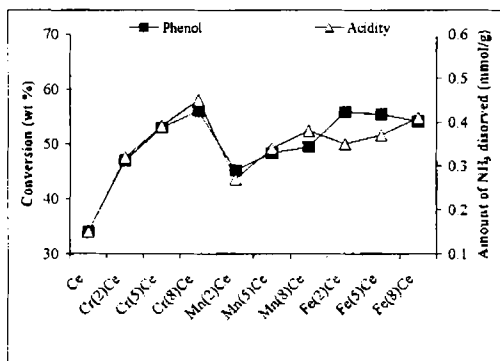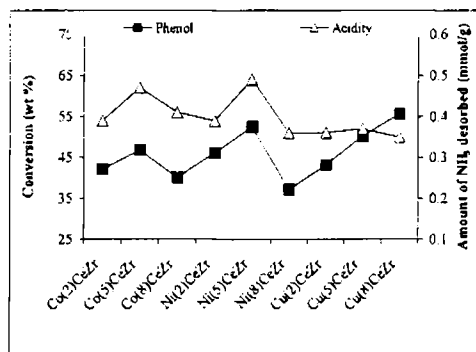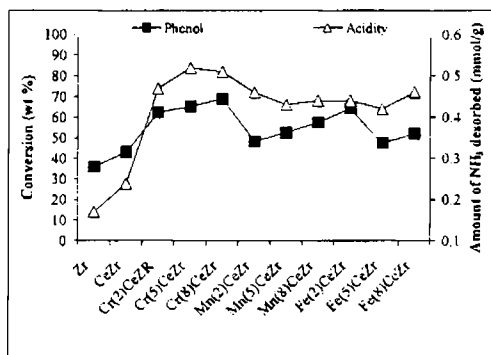
Figure 6.6a Phenol conversion Vs Acidity from NH₃-TPD
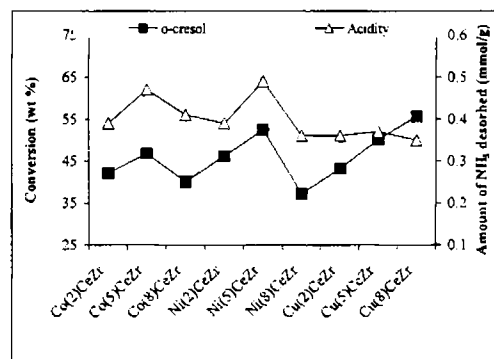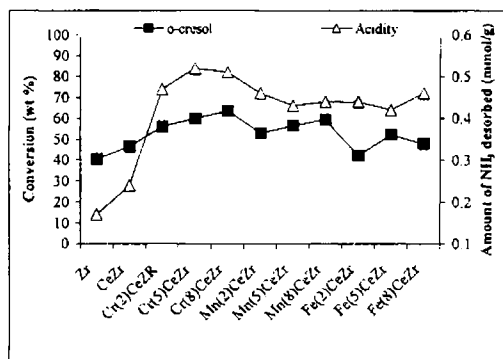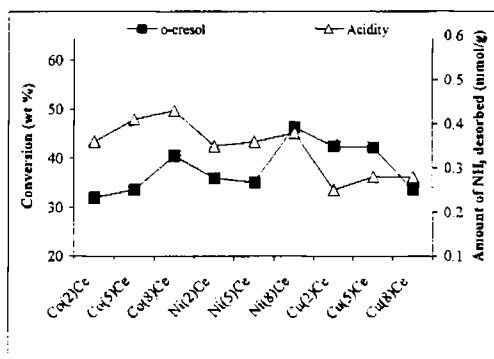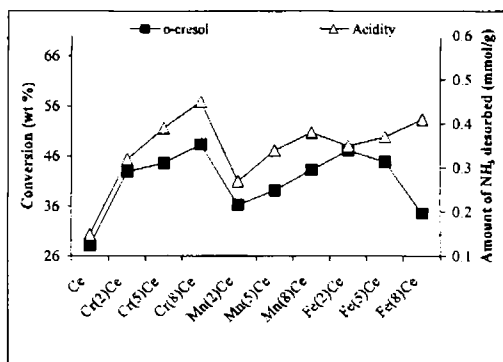
Figure 6.6b *o*-cresol conversion Vs Acidity from NH₃-TPD

6.4 Conclusions

The following conclusions can be drawn from the present study.

- ✓ Methylation of phenol and *o*-cresol over transition metal modified ceria and ceria-zirconia mixed oxides shows good catalytic activity and high ortho selectivity.

- ✓ The influence of various reaction parameters was studied and it is found that the product selectivity can be varied by selecting different reaction conditions.

- ✓ Catalytic activity of the catalysts strongly depends on the total acidity.

References

[1] H. Fiege, in: B. Elvers, S. Hawkins, G. Schultz (Eds.), Ullmann's Enclycopedia of Industrial Chemistry, vol. A19, 5th ed., VCH, Weinheim, 1999, p.313.

[2] R. Dowbenko, in: J. I. Kroschwit, Mary Houl-Grant (Eds.) , Kirk-Othmer Encyclopedia of Chemical Technology, 4th ed., vol. 2, 1992, p.106.

[3] K. M. Malshe, P. T. Patil, S. B. Umbarkar, M. K. Dongare, J. Mol. Catal. A: Chem., 212 (2004) 337.

[4] S. Velu, C. S. Swamy, Appl. Catal. A 162 (1997) 81.

[5] R. Bal, S. Sivasankar, Appl. Catal. A 246 (2003) 373.

[6] K. R. Reddy, K. Ramesh, K. K. Seela, V. V. Rao, K. V. R. Chary, Catal. Commun. 4 (2003) 112.

[7] K. Sreekumar, S. Sugunan, J. Mol. Catal. A: Chem. 185 (2002) 259.

[8] W. C. Choi, J. S. Kim, T. H. Lee, S. I. Woo, Catal. Today 63 (2000) 229.

[9] T. M. Jyothi, K. Sreekumar, B. S. Rao, S. Sugunan, React. Kinet. Catal. Lett. 69 (2000) 339.

[10] A. R. Gandhe, J. B. Fernandes, Catal. Commun. 5 (2004) 89.

[11] K. G. Bhattacharyya, A. K. Talukdar, P. Das, S. Sivasanker, J. Mol. Catal.

A: Chem., 197 (2003) 255.

[12]   S. C. Lee, S. W. Lee, K. S. Kim, T. J. Lee, D. H. Kim, J. C. Kim, Catal. Today 44 (1998) 253.

[13]   Rajaram Bal, S. Sivasankar, Green Chem. 2 (2000) 106.

[14]   T. M. Jyothi, S. Sugunan, B. S. Rao, Green Chem. 2 (2000) 269.

[15]   Hanna Grabowska, Ludwik Syper, Miroslaw Zawadzki, Appl. Catal. A: Gen. 277 (2004) 91.

[16]   S. Sato, K. Koizumi, F. Nozaki, Appl. Catal. A 133 (1995) L7.

[17]   S. Sato, K. Koizumi, F. Nozaki, J. Catal. 178 (1998) 264.

[18]   R. Klimkiewicz, H. Grabowska, H. Teterycz, Appl. Catal. A 246 (2003) 125

[19]   Ajayan Vinu, Mani Karthik, Masahiko Miyahara, Velaudam Murugesan, Katsuhiko Ariga, J. Mol. Catal. A: Chem. 230 (2005) 151.

[20]   K. Shanmugapriya, S. Saravanamurugan, M. Palanichamy, B. Arabindoo, V. Murugesan, J. Mol. Catal. A: Chem. 223 (2004) 177.

[21]   A. S. Reddy, C. S. Gopinath, S. Chilukuri, J. Catal. 243 (2006) 278.

[22]   K. Tanabe, T. Nishizaki, in F. C. Tompkins (Ed.), Proc. 6th Int. Congress on Catalysis, The Chemical Society London (1997).

[23]   E. Santacesaria, D. Grasso, D. Gelosa, S. Carra, Appl. Catal. 64 (1990) 83.

[24]   B. G. Mishra, R. Ranga Rao, J. Mol. Catal. A: Chem. 243 (2005) 204.

CHAPTER 7

SUMMARY AND CONCLUSIONS

Abstract

The aim of catalysis research is to apply the catalyst successfully in economically important reactions in an environmentally friendly way. The present work focuses on the modification of structural and surface properties of ceria and ceria-zirconia catalysts by the incorporation of transition metals. The applications of these catalysts in industrially important reactions like ethylbenzene oxidation, alkylation of aromatics are also investigated. This chapter reviews the summary of the work detailed in the preceding chapters. The important conclusions obtained from the studies are also presented.

7.1 Summary

Chapter 1 deals with a general introduction on catalysis and metal oxides. A brief literature review on catalysis by transition metal modified ceria and ceria-zirconia mixed oxides is also included. The chapter also includes a brief outline on the reactions selected for the catalytic activity studies.

Chapter 2 contains a detailed description about the materials used and preparation method employed for the present investigation. A brief description of various instrumental techniques used for characterization is also given.

Chapter 3 focuses on the physicochemical characterization of the prepared systems. The catalyst composition was found out from energy dispersive X-ray analysis. The structural characterization of transition metal modified ceria and ceria-zirconia catalysts were done by different techniques like X-Ray diffraction analysis, Surface area and pore volume measurements, Scanning electron microscopy, Infrared spectroscopy, Electron paramagnetic resonance spectroscopy and Thermogravimetric analysis. The surface acidity measurements were done by temperature programmed desorption of ammonia and thermodesorption of 2,6-dimethyl pyridine. Cyclohexanol decomposition and cumene cracking were employed as test reaction to evaluate surface properties.

Chapter 4 discusses the catalytic activity of the prepared systems towards ethylbenzene oxidation. Tertiary butyl hydroperoxide was used as the oxidant. The influence of reaction variables such as catalyst concentration, temperature, solvent, time on stream, solvent volume and substrate to oxidant mole ratio were studied. Leaching studies and reusability of the representative catalysts were done.

In chapter 5 the catalytic activity of the systems towards liquid-phase benzylation of toluene and *o*-xylene is discussed. The influence of reaction parameters

are studied in detail. A possible mechanism involving Lewis acid sites of the catalysts is suggested.

Chapter 6 deals with methylation of phenol and *o*-cresol using the prepared catalysts. The effect of temperature, flow rate, methanol:phenol/*o*-cresol mole ratio on conversion and product selectivity was examined. Deactivation profiles of representative catalysts were obtained by doing reaction for 8h.

Chapter 7 presents the summary, conclusion and future outlook for the present thesis work.

7.2 Conclusions

The general conclusions that can be drawn from the present investigations are the following.

Sol-gel method is effective for the preparation of transition metal modified ceria and ceria-zirconia mixed oxide since it produces catalyst with highly dispersed incorporated metal. Unlike that of impregnation method plugging of pores is not prominent for sol-gel derived catalyst materials. This prevents loss of surface area on metal modification as evident for BET surface area measurements.

The powder X-ray diffraction analysis confirms the cubic structure of transition metal modified ceria and ceria-zirconia catalysts. The thermal stability is evident from TGA/DTA analysis. DR UV-vis spectra provide information on the coordination environment of the incorporated metal. EPR analysis of Cr, Mn and Cu modified ceria and a ceria-zirconia catalyst reveals the presence of different oxidation states of incorporated metal.

Temperature programmed desorption of ammonia and thermogravimetric desorption of 2,6-dimethyl pyridine confirms the enhancement of acidity on metal

incorporation. High α-methyl styrene selectivity in cumene cracking reaction implies the presence of comparatively more number of Lewis acid sites with some amount of Bronsted acid sites. The formation of cyclohexanone during cyclohexanol decomposition confirms the presence of basic sites on the catalyst surface.

Mn and Cr modified catalysts show better activity towards ethylbenzene oxidation. A redox mechanism through oxometal pathway is suggested.

All the catalysts were found to be active towards benzylation of toluene and o-xylene. The selectivity towards monoalkylated products remains almost 100%. The catalytic activity is correlated with the Lewis acidity of the prepared systems.

The activity of the catalysts towards methylation of phenols depends on the strength acid sites as well as the redox properties of the catalysts. A strong dependence of methylation activity on the total acidity is illustrated.

7.3 Future Outlook

The present investigation clearly shows the improvement of structural and surface properties of ceria by the addition of transition metal. Cr and Mn modified catalysts can be further employed for the oxidation of different aromatic substrates. The application of the catalyst as three-way catalyst in environmental exhaust emission control can be also investigated.